

6-6-2014

Solution Processable Novel Organic Electronic Devices for New Generation Biomedical Applications

Munish Puri

University of South Florida, mpuri@mail.usf.edu

Follow this and additional works at: <https://scholarcommons.usf.edu/etd>

 Part of the [Electrical and Computer Engineering Commons](#)

Scholar Commons Citation

Puri, Munish, "Solution Processable Novel Organic Electronic Devices for New Generation Biomedical Applications" (2014).
Graduate Theses and Dissertations.
<https://scholarcommons.usf.edu/etd/5290>

This Dissertation is brought to you for free and open access by the Graduate School at Scholar Commons. It has been accepted for inclusion in Graduate Theses and Dissertations by an authorized administrator of Scholar Commons. For more information, please contact scholarcommons@usf.edu.

Solution Processable Novel Organic Electronic Devices for New Generation Biomedical
Applications

by

Munish Puri

A dissertation submitted in partial fulfillment
of the requirements for the degree of
Doctor of Philosophy in Electrical Engineering
Department of Electrical Engineering
College of Engineering
University of South Florida

Co-Major Professor: Wilfrido Moreno, Ph.D.
Co-Major Professor: Srinivas Tipparaju, Ph.D.
Paris Wiley, Ph.D.
Andrew Raij, Ph.D.
Andrés E. Tejada-Martínez, Ph.D.
Yashwant Pathak, Ph.D.

Date of Approval:
June 6, 2014

Keywords: VOFET, vertical transistor, low voltage bioelectronics, flexible cardiac sensor, wet electronics

Copyright © 2014, Munish Puri

DEDICATION

I want to dedicate this work to my family for their constant encouragement and support to make this happen. Without their sacrifice, it would have been impossible to achieve this major professional accomplishment.

ACKNOWLEDGMENTS

I would like to express my sincere gratitude and appreciation to everyone who contributed and made this work a reality. I want to express my gratitude and thank from the bottom of my heart to Dr. Wilfrido Moreno my Co-Major Professor for his guidance, encouragement, dedication and vision in helping me achieve the objective of this dissertation. It was an honor and privilege to work under his supervision. It would not have been possible without the help, support and patience of Dr. W. Moreno.

I also would like to express my gratitude and sincere thanks to Dr. Srinivas Tipparaju, my Co-Major Professor, without whose support and constant guidance it would have been impossible to achieve this objective. I feel honored to have him as my Co-Major Professor. I also want to say thank you to my committee members for their valuable suggestions, support and help in accomplishing this work.

I am very grateful to Prof. Thomas Weller, Department of Electrical Engineering Chair, for supporting me financially and morally throughout my Ph.D. journey. It was an honor and privilege to work under his able leadership.

I cannot forget to express my gratitude, thanks and respect to Dr. Paris Wiley for guiding and supporting me at every single step of my Ph.D., including funding support. I cannot express in words what I have learned from him while carrying out my teaching assistantship responsibilities under his guidance.

I want to thank Dr. Yashwant Pathak for his support, encouragement and envisioned approach in helping me achieve this objective. I learned a great deal under his mentorship in

terms of scientific leadership, higher aspects of planning and conducting projects and endeavors. Especially for his unselfishness kindness towards my family, I will forever be very grateful. I want to convey my sincere thanks to Dr. Sanjukta Bhanja for supporting me in the initial stages of my Ph.D.

I want to express my gratitude and sincere thanks to Dr. Marilyn Bui, Dr. Mark Lloyd and Dr. Amarjit Saini of H. Lee Moffitt Cancer Center for their help, support and valuable suggestions.

I would like to acknowledge the staff of the Electrical Engineering Department for their constant help and guidance. I am most grateful to Ms. Catherine Burton for her guidance and help in this dissertation formatting and writing. I want to convey my thanks to the NREC staff, College of Pharmacy and H. Lee Moffitt Cancer Center for providing their facilities, help and valuable suggestions.

Last, but by no means least, I would like to thank GND University and college back in India for morally supporting me to fulfill my dreams.

TABLE OF CONTENTS

LIST OF TABLES	iv
LIST OF FIGURES	v
ABSTRACT	ix
CHAPTER 1: INTRODUCTION.....	1
1.1 Organic Electronics.....	3
1.2 Low Cost Flexible Organic Devices.....	5
1.3 Organic Field Effect Transistor	6
1.4 Need for Speed	7
1.5 Translational Technologies into the Biomedical Area	8
1.5.1 Flexible Cardiac Sensors	8
1.5.2 OFET Imagers for Cancer Detection in Digital Pathology	9
1.5.3 Flexible Radiation Sensors	10
1.6 Objective and Dissertation Organization	11
CHAPTER 2: THEORY AND BACKGROUND	12
2.1 Conjugated Polymers	13
2.2 Molecular Orbital Theory	14
2.3 Organic Semiconductors	15
2.3.1 Solution-Processable Organic Devices.....	16
2.3.2 Solution-Processing Low Cost Techniques	16
2.4 Theory and Operation of Organic Field Effect Transistor	17
2.4.1 Types of Organic Field Effect Transistors.....	17
2.4.2 Lateral OFETs.....	18
2.4.3 Operation of Lateral OFET	20
2.4.4 Vertical Organic Field Effect Transistors.....	21
2.4.5 Operation of Vertical OFET	23
2.4.6 Important Terms Involved in VOFET Operation	23
2.4.6.1 Mobility.....	24
2.4.6.2 Linearity Effects	24
2.4.6.3 ON/OFF Ratio	24
2.4.6.4 Contact Resistance	25
2.4.7 Factors Affecting VOFET Operation	25
2.4.7.1 Short Channel Effect.....	25

2.4.7.2 Contact Effects	26
2.5 Literature Survey and Progress Review in Vertical OFET	26
CHAPTER 3: SOLUTION PROCESSABLE VOFET DEVICE FABRICATION	33
3.1 Solution Processable VOFET: Three Stage Process	34
3.1.1 Stage I Gate, Source Fabrication and Precursor Deposition.....	36
3.1.2 Stage II Pentacene Metrology Characterization.....	38
3.1.3 Stage III Final Device Fabrication	40
3.1.4 Precursor to Pentacene Conversion.....	41
3.2 Low Cost Fabrication.....	43
3.2.1 Low Cost Design Process	44
3.2.2 VOFET Device Processing Temperature	44
3.3 Spin Coating Method.....	45
3.4 Drop Casting Method.....	46
3.5 Precursor to Pentacene Conversion	46
3.5.1 Solution Preparation	47
3.5.2 Time Temperature Optimization.....	48
3.6 Masking and Geometry Optimization.....	49
3.6.1 Polyimide Masking for Electrode Protection.....	49
3.6.2 Polyimide Shadow Masking in Metal Deposition	50
CHAPTER 4: VOFET DEVICE CHARACTERIZATION	52
4.1 Electrical Characterization	52
4.1.1 Current-Voltage Characteristics.....	53
4.1.2 Capacitance-Voltage Characteristics.....	60
4.1.2.1 C-V Analysis	62
4.1.3 Transient Time Analysis.....	63
4.1.4 Resistivity Measurements	64
4.2 Surface Metrological Characterization	65
4.2.1 Transmission Electron Microscopy.....	66
4.2.2 Atomic Force Microscopy	67
4.2.3 Scanning Electron Microscopy	70
4.2.4 Raman Spectroscopy	70
4.2.5 X-Ray Diffraction	72
4.3 Radiation Sensor Test	73
4.4 Flexible Cardiac Sensor	74
4.4.1 Implantable Cardioverter Defibrillator.....	74
4.5 Imager for Digital Pathology in Breast Cancer Analysis.....	77
4.5.1 Nuclear Pleomorphism	79
4.5.2 Experiment Design for Classifier Optimization.....	81
CHAPTER 5: CONCLUSIONS, APPLICATIONS AND FUTURE WORK	85
5.1 Conclusions	85
5.1.1 Influence of SCLC Effect	86
5.1.2 Facts, Factors and Findings in Solution Processable VOFET	88
5.2 Applications.....	91

5.2.1 Novel Neuroprosthetics Using Flexible Organic Electronics	93
5.2.2 Flexible Stimulating Probes	94
5.3 Future Work	95
REFERENCES	97

LIST OF TABLES

Table 1.1 Comparison of silicon and organic electronics	4
Table 1.2 Estimated organic electronics industry and its respective market share growth.....	5
Table 2.1 Literature of VOFET in various vertical orientations and geometries	28
Table 2.2 OFET used for various biomedical applications	32
Table 4.1 Device parameters of two types of devices fabricated by spin coating and drop casting techniques.....	56

LIST OF FIGURES

Figure 1.1	Two architectures of OFETs (a) as an imager using an organic photo-diode and (b) as a pressure sensor to record a signal from a stretchable biological tissue	9
Figure 2.1	Conjugation in polymers (a) delocalized π bond formation (b) polyacetylene molecular chain of alternating single and double bonds.....	13
Figure 2.2	Energy levels of molecular orbital such as HOMO and LUMO for charge transfer	14
Figure 2.3	Various topologies of OFET device geometries	20
Figure 2.4	Circuit diagram of a p-type OFET device in lateral geometry	21
Figure 2.5	Vertical OFET geometry (a) charge carrier flow and biasing circuit (b) VOFET layout	22
Figure 3.1	VOFET device fabrication steps elicited the whole fabrication scheme from Stage I to Stage III.....	35
Figure 3.2	VOFET fabrication stage I starting from gate deposition (top left) to pentacene conversion.....	37
Figure 3.3	E-beam chamber for electrode deposition (a) gold metal evaporation (b) e-beam facility at NREC.....	38
Figure 3.4	VOFET fabrication Stage II for pentacene conversion and metrological testing.....	39
Figure 3.5	Stage III of fabrication elicited Au deposition and fabricated device picture	41
Figure 3.6	Soluble pentacene precursor and scheme adopted for conversion process	42
Figure 3.7	Molecular structure of pentacene, SU-8 and PMMA.....	42

Figure 3.8 Complete VOFET fabrication steps (a)-(b) process flow (c) sequence of stacking layers	43
Figure 3.9 Spin coating deposition method (a) diluted pentacene precursor suspension (b) spin coater.....	45
Figure 3.10 Drop casting deposition method where diluted pentacene precursor is dropped over patterned source	47
Figure 3.11 Time-temperature optimization curve for precursor to pentacene conversion process	48
Figure 3.12 Various shadow masking designs made out of polyimide Kapton tape.....	50
Figure 4.1 Current-voltage (I-V) output characteristic plots at various channel lengths	54
Figure 4.2 Output characteristic plots at three different channel lengths elicited short channel at L=265nm (green line)	55
Figure 4.3 Type I devices (a) device layout (b) picture (c) I-V plot at L=300nm and (d) transfer characteristic curve	57
Figure 4.4 Type II devices (a) device layout (b) perforated source electrode (c) I-V plot at L=2 μ m, and (d) drop casting process	58
Figure 4.5 Current density Vs V _{DS} plot for L=265nm channel length depicts SCLC effect at n>2	59
Figure 4.6 C-V plot of VOFET device (a) at frequencies ranging from 100Hz to 60 KHz (b) spectrum analyzer (c) Mott-Schottky plot i.e. 1/C ² -V	61
Figure 4.7 Quasi-static C-V plot of Type I device elicited the accumulation and depletion regions.....	62
Figure 4.8 Time of flight (TOF) experiment setup (a) circuit layout (b) applied input pulse (up) and recorded output (below) (c) pulse delay	63
Figure 4.9 Contact resistance (a)-(b) parasitic and channel resistance (c)-(d) four probe set up and circuit connections	65
Figure 4.10 TEM images reveal formation of pentacene crystal size and grain boundaries.....	67

Figure 4.11 AFM image (left) dendritic growth after precursor annealing (right) fully converted pentacene.....	68
Figure 4.12 AFM height (left) and phase (right) images of pentacene after thermal treatment	69
Figure 4.13 Mean (red) and average (black) grain size of pentacene recorded after conversion in AFM surface analysis	69
Figure 4.14 SEM image of deposited material layers elicited SU-8 insulating layer under the Au metal electrode	70
Figure 4.15 Raman spectroscopy measurement (left) and schematic representation of a Raman spectra (right)	71
Figure 4.16 X-RD measurement (left) X-RD plot (right) diffraction system facility.....	72
Figure 4.17 I-V plot of a VOFET resistive radiation sensor	73
Figure 4.18 Schematic representation of OFET flexible sensor integration	75
Figure 4.19 Proposed scheme of digital pathology for automated breast cancer scoring system	79
Figure 4.20 Breast cancer data classification results from MATLAB and NeuroSolutions classifier	82
Figure 4.21 Artificial Neural Network classifier result (a)-(c) data for 699 breast cancer patients	83
Figure 5.1 Short channel effects (a) the SCLC region formation and (b) the circuit operation	87
Figure 5.2 Facts and findings about solution processed VOFET device	89
Figure 5.3 Summary of research problems addressed and proposed	90
Figure 5.4 VOFET used in neuroprosthetics (a) sensor application (b) neural stimulation.....	94
Figure 5.5 VOFET integration into large area stimulation electrodes for novel neuroprosthetics applications	95

Figure 5.6 Integration of organic materials for new generation bio-electronic applications
using VOFET transistors.....96

ABSTRACT

The following dissertation addresses a novel low cost process developed to fabricate a Vertical Organic Field Effect Transistor (VOFET). The solution processable VOFET is designed, fabricated and tested in the context of bioengineering domains. The scope of distinct biomedical applications has also been explored.

Organic thin-film transistors are gathering industrial attention as a potential candidate for future electronics analogous to silicon technology. Low fabrication cost, structural miniaturization and low operational voltage are the challenges for fabricating an Organic Field Effect Transistor (OFET). To create these devices, OFETs require new design paradigms and wet processing routes. However, conventional lateral OFET geometry cannot satisfy these demands because of process complexities and the high cost to achieve sub-micron channel length. Despite these barriers, solvent sensitivity towards organic semiconductors, electrode patterning and masking make this process more challenging than are associated with current technologies. Therefore, the need for production of a low cost high efficiency OFET is of high importance. The soluble organic semiconductor exhibits promising device properties. The growing demand of organic electronics poses great difficulty in adapting standard photolithography patterning for fabrication. The main issue is incompatibility in handling organic materials. To circumvent these challenges, a novel fabrication process has been developed to build OFETs in vertical geometry. The novelty of this process allows for creation of sub-micron channel devices at very low cost.

Solution processed VOFET devices are fabricated using a 13,6-N-sulfinylacetamidopentacene (NSFAAP) precursor. Low cost fabrication techniques such as spin coating and drop casting are employed for achieving submicron channel length. Nanoscale devices, i.e. channel lengths, $L=265\text{nm}$, 300nm and 535nm , are respectively fabricated using the spin coating technique. Output characteristics are recorded at an operational voltage of 1volt. Short channel effects dominate the device performance, resulting in a linearity effect in I-V characteristics. Strategies, such as perforated source electrode design and drop casting techniques, are evolved and employed to minimize the short channel effects.

Space Charge Limited Current (SCLC) effects, better known as short channel effects, are observed during I-V characterizations at high longitudinal fields. The drop casting technique is used over Patterned Electrode (PE) for reducing these SCLC effects. Thick channel devices, i.e. $L=2\mu\text{m}$, are fabricated to minimize the SCLC effects. Low cost polyimide 3M kapton tape is used as masking material in between the stacked layers. Time-temperature balance is optimized during the precursor to pentacene growth process. Metrological characterizations such as TEM, SEM, AFM, Raman Spectroscopy and X-RD are performed to confirm the precursor to pentacene conversion. AFM scanning illustrates dendritic pentacene molecular growth at 170°C annealing. Consequently, the conversion temperature is optimized around 200°C .

In life sciences, there is always striving for translational technology development that can mimic, integrate and manipulate the biological system. Electrical signals enhance the capabilities of electronics to interact and understand the signaling pathways in a biological system. Keeping this in view, the potential applications into biomedical areas, such as flexible sensors and biomedical imagers, are proposed. VOFET has been proposed as a mainstay for flexible cardiac sensors and as imagers. OFET sensors could be designed to cover highly

stretchy and arbitrary cardiac tissue. Sensor web integration with pacemakers and Implantable Cardioverter Defibrillator (ICD) device systems has been proposed. The OFET imaging sensor holds potential for early detection of cancer by detecting nuclear level changes in breast cancer images. Nuclear pleomorphic (shape and size distortion of cancerous nuclei) feature detection and analysis could be a step forward in the direction of digital pathology. The conventional analysis approach is time-consuming and error prone as it depends on visual inspection by pathologists. The proposed approach is parallel in nature and supports the existing method of cancer detection.

CHAPTER 1: INTRODUCTION

Organic electronics have shown incredible expansion over the last decade driven by innovative products. Significant growth has been observed in key areas such as conformal large area sensors [1], chemical sensors [2], and e-skin [3]. A highly conductive polymer called polyacetylene, was discovered in 1977 by researchers Alan J. Heeger, G. MacDiarmid, and Hideki Shirakawa. Their discovery triggered a new era of organic electronics also known as polymer or plastic electronics. Organic semiconductors are widely accepted as active materials in manufacturing organic electronic devices because of their lighter weight and flexibilities. Their properties at the molecular level enable the manipulation and building of inexpensive and lighter weight electronic devices.

OFETs are the main switching elements and play an important role in building organic electronics. In general, organic semiconducting materials are used for fabricating OFETs. However, an organic FET's performance is inferior as compared to a silicon thin film transistor. This is because of the fact that organic materials are highly disordered at the molecular level. Thus, the required switching voltage to operate the OFET is very high. This is mainly because of the low mobility of charge carriers in organic material. To operate an OFET at low voltages around 2-5 volts, the device channel length has to be reduced. Reducing the channel length using standard photolithography is not only a costlier job but also invokes process complexities. By altering the geometry in the vertical direction, channel length reduction and low operational voltages can be achieved.

In vertical OFETs, the thickness of organic material defines the device channel length. Spin coating is extensively employed as a low cost deposition technique in vertical OFETs. The channel thickness can easily be controlled up to nanoscale during coating speed. Therefore, by reducing the channel length in vertical OFETs, a low voltage and high current density can be obtained [4]. Therefore, the main advantages of VOFET are its ease of fabrication, achieving short channel at low cost, low operational voltages, and high current density.

OFETs can be fabricated over a variety of substrates such as paper, plastic, silk and biocompatible rubbers. Ease of fabrication over a range of flexible substrates and inherent weak molecular bonding (van der Waals) within organic materials makes them malleable and flexible. Flexible OFETs are in high demand for various technology applications such as bendable large area displays and foldable monitors. With the advent of synthetic chemistry, there is an opportunity of functional chemical structures which can be designed for developing new technologies in large area electronics [5]. Organic materials are biocompatible and environmentally safe for disposal. Thus, OFET sensors have huge potential applications in the food industry, most notably to monitor freshness and quality of packaged food [6]. The biological and chemical sensing features of OFET have been extensively studied for the potential use in biomedical sensing applications [7]. Flexible OFETs are being applied to novel neuroprosthetics areas such as Brain-Computer Interface (BCI) and biomedical implants [8, 9]. OFETs are an excellent candidate for tissue-electronics interface because of their ability to conduct electrons and ions. In wireless sensing, potential technology applications are Organic Radio Frequency Identification (ORFID) tags [10], OFET sensors [11], and smart flexible displays. Also, OFETs have been studied for biomedical application in medicine [12], cancer [13], bioelectronics [14], flexible explosive sensors [15], smart textiles [16], electronic robotic

skin [17], and advanced flexible electronic assemblies for human skin [18]. In addition, for a new generation of implants, flexible organic electronics offers opportunities to integrate signal recording microelectrodes into the biological system.

1.1 Organic Electronics

Organic electronics is defined as the area of electronics which uses organic materials as the active medium for current conduction. Organic electronics are named by the use of materials for fabricating devices, such as polymer/plastic electronics, or by the fabrication process, such as printed electronics or soft electronics. Due to an organic material's solution processing capabilities at room temperature, organic electronics is advantageous over costlier technologies. Silicon devices are fabricated over thin, rigid silicon wafers in a highly mechanized and ultra-clean micro-fabrication facility. On the other hand, OFETs can be printable by inkjet printing machines over any substrate, ranging from glass, plastic, paper or silk, without requiring any ultra-clean room environment. In a standard micro-fabrication process, the steps involved in electronic device fabrication takes a longer time (a few weeks) than printing an electronic circuit over plastic sheets or paper. Also, organic electronic devices are lightweight, flexible, and stretchable [19].

Purity of silicon is an important material property considered while making electronic devices. To fabricate silicon devices, the cost involved is very high due to the requirement of the ultra-clean room environment. A clean room facility is of utmost priority, as even a small dust particle can ruin the whole integrated circuit. In the case of organic device fabrication, material purity is not required because the charge carriers are injected from outside. Normally, organic devices work on injection mode instead of material doping, i.e. charge carriers are not generated within the organic material, but injected from outside. In addition, organic devices have a low

performance due to their low mobility, which allows the silicon devices to gain an advantageous edge. The organic materials encourage the growth of the biological system over it, which is suitable for bioelectronics applications. An organic material's ability to conduct electrons, holes and ions makes it biocompatible and feasible to interface with a biological system. Table 1.1 summarizes the comparison of silicon and plastic electronics and its biocompatible properties.

Table 1.1 Comparison of silicon and organic electronics.

Parameters	Silicon Electronics	Organic Electronics
Flexibility	Brittle	Highly Flexible
Processing Temperature	High Temperature	Room Temperature
Fabrication Time	Few Weeks	Few Days
Purity	99.99%	Not Required
Performance	High	No High Expectations
Cost	High (\$Billions)	Low (\$Thousands)
Biocompatibility	No	Yes
Tissue Interface	Loose Interface	Excellent

There is a huge potential of market growth of plastic electronics in the next 5-12 years as surveyed by the market research company IDTechEx. In Table 1.2 , the market share of plastic

electronic spin offs like OLED displays, photovoltaic and logic memory has been predicted to have an estimated growth of \$330 billion by 2027.

Table 1.2 Estimated organic electronics industry and its respective market share growth. (Source: IDTechEx)

Industry	Market Share (%)
OLED Light	11%
Photovoltaic	14%
OLED Display	20%
Logic/Memory	38%
OLED Billboard Etc.	7%
Electrophoretic	6%
Others	4%

1.2 Low Cost Flexible Organic Devices

Organic electronics hold great potential for new generation flexible and printable low cost mobile devices [20]. In flexible electronics, polymeric materials are used for fabricating devices, as well as supporting substrates. Thus, materials such as papers, plastic, polyimide and silk have been used for fabricating organic devices for various technological applications. An organic electronic circuit can be printed on a flexible substrate using low cost printing technologies. The use of polymeric materials in organic electronics could be a choice for disposable and biodegradable green electronics. An important consideration in this direction to build organic electronic devices is the ease of fabrication at room temperature, no high resolution photolithography requirement, and low per unit area cost. Inkjet printers and material printers

are widely used for printing a range of organic semiconductors and metallic materials on a variety of flexible substrates. Printing the whole organic electronic circuit in a few days is a major factor towards cost reduction. The advancement of low voltage OFETs on transparent flexible substrates also has been reviewed [21].

1.3 Organic Field Effect Transistor

Organic transistors have been studied for the last few years and gathered significant attention of the research and industrial community toward its low cost manufacturing. The OFET's working principle is the same as that of the Metal Oxide Semiconductor Field Effect Transistor (MOSFET). In generic terms, OFETs can be fabricated into two topologies, in lateral and vertical configurations. In general terms, OFETs in the lateral geometry can be fabricated in top and bottom contact configurations. In the same geometry and configuration, scaling the channel length down to submicron levels makes the fabrication process more complex and costlier. Advanced patterning and standard lithography is the technique normally used to achieve submicron channel length in planar (lateral) OFETs. Lithography cannot be employed for fabricating organic devices because of two major reasons. First, the solvents used in photolithography are mostly unfriendly to organic materials. Second, every additional masking in photolithography makes the process more challenging and costly. Therefore, photolithography is incompatible for fabricating organic devices, particularly in vertical geometry.

Materials such as gold (Au) and aluminum (Al) are widely used in OFET fabrication for designing source, drain and gate electrodes. As an insulating medium between the gate electrode and organic semiconductor (in bottom gated devices), silicon dioxide (SiO_2) has been extensively adopted. The main role of organic semiconductors is to facilitate charge carrier

conduction. Charge carriers are injected from the source electrode flow through an active medium and are collected at drain electrodes, which finally constitute an output current. The OFET works in injection mode, i.e., charge carriers are injected from the source electrode and move through the channel to reach drain electrode. Channel width and length are the important physical device parameters related directly to output drain current. Channel width “W” is defined by the width of the source and the drain electrodes, whereas the semiconductor distance between the source and the drain is known as channel length “L”. Substrate materials vary from solid to flexible depending upon silicon or plastic/polyimide (in the case of flexible electronics).

1.4 Need for Speed

Organic electronics are gathering considerable attention of market giants like Samsung and Philips most notably in the area of flexible mobile phones and foldable monitors. In the majority of commercially used organic displays, an organic FET is used as a fundamental switching element. The low mobility of organic materials is the limitation involved in using an OFET, which results an inferior performance. Indeed, VOFET is a potential alternative available to compensate for the low speed of OFET. By lowering the channel length in vertical OFETs, the speed and current density could be enhanced.

Why a solution processable vertical organic FET?

- VOFET can be fabricated at room temperature.
- No clean room and high vacuum are required for VOFET fabrication.
- No high resolution photolithography is required.
- Can be printable using polymers for a 3D biological system.
- Integration on packaging (no extra packaging cost like in silicon technology).
- Printable on paper, plastic and silk substrates.

- Can be realized using low cost fabrication techniques like inkjet printing, spin coating, and drop casting.

1.5 Translational Technologies into the Biomedical Area

In the development of new therapeutic tools, it is primarily important to understand the signaling pathways in a biological system. Biomedical electronics utilizes the strength of electrical signals to understand and to interact with the biological system. In this direction of employing organic electronics into biomedical domains, OFET is a promising candidate for numerous technological applications in biomedical areas [22]. Two important applications in which OFETs could be employed for translational technologies are flexible sensors and biomedical imagers [23]. The main role of an OFET is to drive the transducer, such as a pressure sensitive resistor or photodiode. The array of such OFET elements could be designed to cover the tissue for sensing biologically important signals.

1.5.1 Flexible Cardiac Sensors

The flatness and rigidity of silicon based electronics restrict its use in covering the three-dimensional shape of the biological tissue surface. Whereas, the stretchability of an organic electronic device enables to cover the large conformal area of interest, and establishes a natural interface with the biological system. To overcome the barrier of mismatch between rigid electronics and soft stretchable biological tissue, flexible organic electronics is an important interface. The most pronounced challenge is to establish good electrical contact between tissue and electronics. The human heart is a very good example of a highly stretchable tissue to test the tissue-electronics interface. Cardiac sensors could be designed and integrated with the existing pacemaker/ICD devices. An array of OFET-based sensors could be able to cover the cardiac surface to detect the origin of arrhythmias.

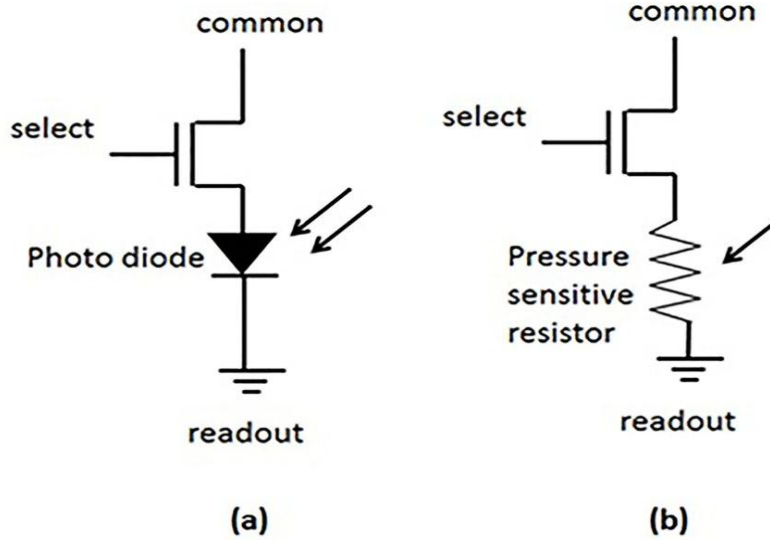


Figure 1.1 Two architectures of OFETs (a) as an imager using an organic photo-diode and (b) as a pressure sensor to record a signal from a stretchable biological tissue.

Polymer-based plastic electronics have been successfully demonstrated as a tactile sensor [24]. A flexible network of OFETs is capable of covering stretchy biological tissue for signal recordings [25]. Organs and tissues are stretchable and bendable in nature. Thus, an array of flexible OFET sensors can be used to record biologically important signals by establishing a proper electrical contact with flexible tissue in a wet environment [26]. The first reported flexible sensor application is demonstrated in robotic skin [2]. They demonstrated the possibility of creating a force map with the help of a flexible OFET back plane laminated in a stretchable conductive elastomer. Using the inkjet printing technique, soluble organic materials could be used to print an organic transistor for tactile transducers for use in artificial robotic skin [27].

1.5.2 OFET Imagers for Cancer Detection in Digital Pathology

Carbon nanotubes and organic materials are widely used in fabricating OFET devices for electro-optical lighting in optical communication system technologies [28]. A voltage or current-programmed OFET backplane offers great advantages in imaging applications. In a

novel architecture, an OFET and an organic photodiode per cell are incorporated to enable a fully adaptive photo sensing element on a flexible substrate [29]. Biomedical imaging and optogenetics are important application areas for flexible imagers to scan images deep inside a convoluted biological system. Optogenetics use light energy to control neuronal activities inside the brain in Parkinson's disease treatment. Flexibility constraints of currently available scanning tools make them unable to twist and bend, which restricts their use in scanning 3-D organs inside the human body. Flexible OFET imaging sensors hold potential for imaging abnormal cells in the early detection of cancer nuclei. Nuclear pleomorphic (shape and size distortion of cancerous nuclei) feature detection and analysis could be a step forward in the direction of digital pathology. Imaging cancer nuclei are supportive of the conventional approach, which is error prone as it depends on visual inspection by pathologists [30]. Low cost prototype devices are in high demand, especially for potential use in developing countries where the numbers of pathologists per patient are very few.

1.5.3 Flexible Radiation Sensors

Organic semiconductors have been explored for various sensing applications such as vapor sensing, biochemical sensing and ionizing radiation sensing. In radiation sensing, these materials have been studied as a potential candidate for detecting low dose ionizing radiations [31]. In principal, upon exposure to ionizing radiations, the conjugation length of organic semiconductor decreases, which enables the detection of a low dose radiation [32]. In an OFET detector, changes in I-V characteristics are recorded after exposing the devices under ionizing radiations. The change in electrical conductivity of organic material is measured as a function of ionizing radiations [33]. In radiation applications, an OFET is used as a two terminal resistor to measure the resistivity response of polymers towards ionizing radiations [34]. In radiation

sensing applications, solution processed OFETs have been studied as Infrared and Ultraviolet detector in military and security applications [35].

1.6 Objective and Dissertation Organization

The central objective of this research is to design, fabricate and test vertical OFETs. The novelty of research lies in a low cost solution processing technique and vertical design. The peripheral objective is to explore opportunities for biomedical translational technologies such as sensing and stimulating flexible electrodes. The organization of this dissertation is designed into five chapters.

- Chapter 1 covers the introduction into organic electronics, flexible electronics and the need for speed in organic semiconductor devices. The importance of vertical geometry is introduced and the need of vertical OFETs is discussed.
- Chapter 2 introduces the basic background of organic semiconductors, conjugated polymers, and molecular orbital theory. Organic FETs are discussed with types and the progress made so far on OFET development is reviewed.
- Chapter 3 presents and describes the solution processable fabrication techniques for a vertical OFET. Low cost techniques such as spin coating and drop casting are discussed. The precursor to the pentacene conversion process, masking methods for various source electrodes, is discussed in this chapter.
- Chapter 4 focuses on the main electrical and metrological device characterization techniques.
- Chapter 5 describes the application domain, especially the biomedical area for sensing biological signals. This chapter explores future applications of using a flexible VOFET array for detecting cardiac arrhythmia and localization.

CHAPTER 2: THEORY AND BACKGROUND

Organic semiconductors are the organic materials that exhibit semiconducting properties. The mobility of charge carriers is very slow in organic materials ($\sim 0.1 \text{ cm}^2/\text{Vsec}$ in pentacene) because of the disordered structure at the molecular level [36]. In organic semiconductors, the current conduction is possible only due to the movement of delocalized π electrons [37]. However, the charge generation center is not lying within the organic materials, rather charges are injected into the organic materials from outside. Organic materials are highly disordered in nature as compared to inorganic silicon. In organic materials, the movement of charge carriers follows the hopping mechanism because of the presence of multiple traps and defects. These defects and disordered molecular structure further create localized states. Thus, charge carriers hop and are trapped between localized states, which results in the low mobility. The multiple Trap and Release model (MTR) well describes this behavior of charge carrier movement in organic semiconductors [38].

Gate voltage dependent mobility is another aspect of predicting field effect mobility in polymers [39]. The hypothesis of this model is that as the gate field increases, the traps start filling up with the injected carriers and transport of charge carriers improves. The number of carriers injected, trapped and extracted can be measured in terms of displacement current. In a separate study, it has been found that the traps are more in Au contact devices than in Cu contacts [40]. The possibilities of charge conduction in polymers have been extensively explored. The conduction of charge carriers through organic semiconductors is possible because

of the presence of a conjugation system and delocalized π electrons. The charge conduction mechanism, thin film morphology, and its effect on OFET performance have been reviewed [41].

2.1 Conjugated Polymers

Conductive polymers are organic materials capable of conducting charge carriers. The conduction mechanism can be described in terms of a conjugation system. Conjugated organic molecules consist of repeating units of alternating single and double bonds. Delocalized π electrons lie above the sigma bond and participate in the conduction mechanism through p-orbitals. Polyacetylene is a good example of conjugated polymers having alternating single and double bonds.

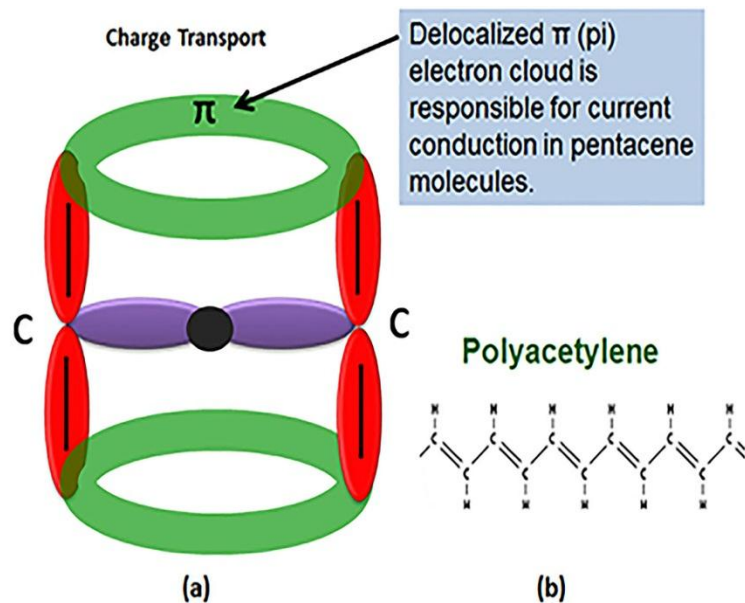


Figure 2.1 Conjugation in polymers (a) delocalized π bond formation (b) polyacetylene molecular chain of alternating single and double bonds.

Organic semiconductors are carbon based materials which have single and double bonds. Carbon forms one sigma and one π bond in its double bond configuration and only one sigma bond in single bond configuration. Figure 2.1 shows the formation of π bond and a sigma bond

in polymers. The Pi bond is a weak bond and a cloud of π electrons spreads over the region above the sigma bond plane; whereas, the sigma bond is a strong bond which is formed by Px orbitals while π bonds are formed by electrons in the Pz molecular orbitals.

2.2 Molecular Orbital Theory

The shape of organic molecular structures is determined by the delocalized π electrons. The shared electrons in the p-orbitals are responsible not only for current conduction, but also provide molecular stability. Figure 2.2 shows the orbital energy with reference to (w.r.t.) vacuum level as a reference line.

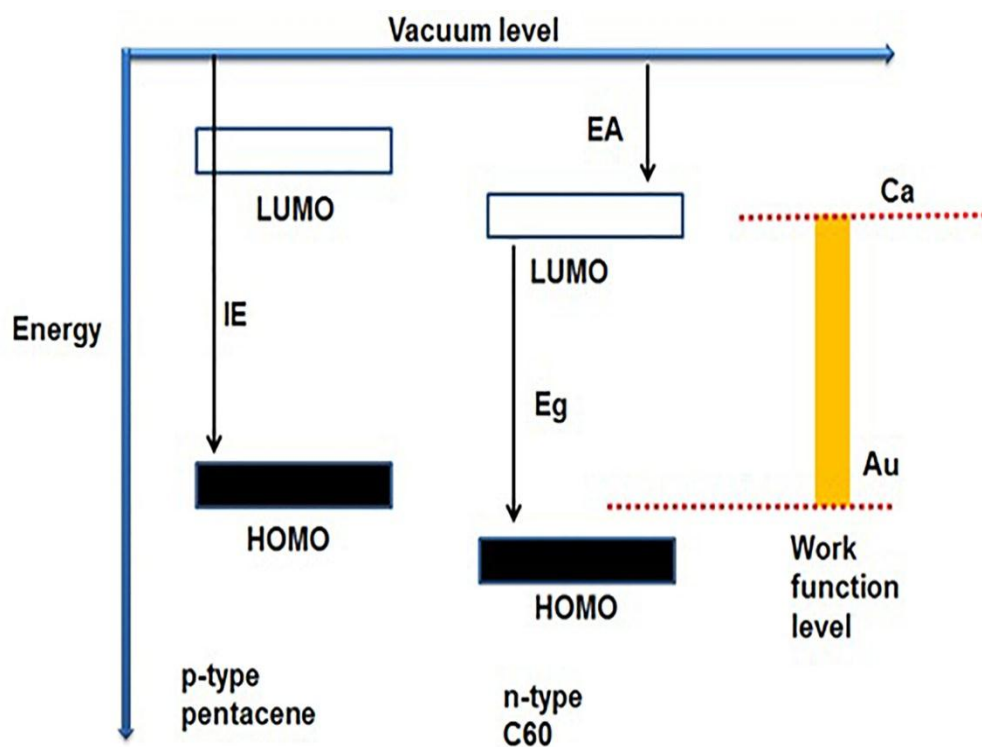


Figure 2.2 Energy levels of molecular orbital such as HOMO and LUMO for charge transfer.

Electron Affinity (EA) describes the position of Lowest Unoccupied Molecular Orbital (LUMO) band w.r.t. vacuum level, and Ionization Energy (IE) describes the position of the

Highest Occupied Molecular Orbital (HOMO) band from the same vacuum level. The HOMO band is analogous to the valance band in inorganic semiconductors, whereas LUMO can be understood as conduction band.

For fabricating hole (positive charge) transport devices, the energy level of a high work function metal like Au should be lined up with low IE or HOMO level materials. Similarly, low work function metals like Ca should be lined up with high IE or LUMO level materials for an efficient transport of charge carriers. With the advent of synthetic chemistry, for efficient charge migration it is now possible to move the position of molecular energies of HOMO or LUMO levels to match with the work function of metals.

2.3 Organic Semiconductors

Organic semiconductors are the family of electronic materials based on π conjugated carbon atoms. Organic semiconductors are broadly classified into two types, such as polymers and conjugated small molecules. The processing of polymers is a little easier (spin coating) than conjugated small molecules like pentacene (vacuum processed). Organic semiconductors have the tendency to trap electrons rather than holes [5]. Charge carriers such as holes and electrons further classify organic semiconductors as p-type or n-type, respectively. The p-channel or n-channel OFET is defined by the type of material used, either p-type or n-type. Usually p-type OFETs are more stable towards the environment and water than their counterparts. Pentacene is a p-type material which has been widely accepted to fabricate organic devices. Conjugation in organic semiconductors enables the charge carrier to move from one chain to the next by the sharing of electron clouds. Delocalized π electrons exhibit p type behavior which dominates the conduction mechanism in pentacene molecules. The five-ring structure of pentacene is supposed to be a highly stable chemical structure used for fabricating organic electronic devices.

2.3.1 Solution-Processable Organic Devices

Electronic devices can be made out of polymers using various fabrication techniques and deposition methods. Solution processable organic devices exhibit tremendous potential for a new generation of low cost electronics. Micron to nanoscale thin films of organic materials can be deposited using spin coating, drop casting and inkjet printing techniques. At the scale of sub micrometer, surface roughness is the main issue which should be considered to deposit a smooth thin film. Surface morphology and film thickness can be optimized in solution processable polymers to achieve the desired level of surface roughness. The best choice is polymer precursors, which exhibit promising trends in ease of deposition, quality of thin film, high performance and low cost fabrication. In large area displays, wet processing techniques offer huge opportunities in printing transparent electronics on foldable substrates for a variety of optoelectronic applications. Consequently, solution processable electronics are emerging fast and hold tremendous potential for flexible displays.

2.3.2 Solution-Processing Low Cost Techniques

Soluble materials and precursors are the building blocks of a solution processing technique. In fabricating low cost organic devices, organic materials are processed to form thin films for fabricating a variety of electronic devices using various low cost techniques such as:

- Spin Coating
- Drop Casting
- Dip Coating
- Doctor Blading
- Spray Coating
- Langmuir-Blodgett (LB)

Each of these above mentioned techniques has its own advantages and downsides. Spin coating could be advantageous for depositing uniform and pin-hole free thin films, but there is an issue of material wastage [42]. In atomic level deposition, the LB technique is an excellent option.

2.4 Theory and Operation of Organic Field Effect Transistor

In an organic field effect transistor, organic materials are treated as a charge transporting medium. The structure of OFET is almost similar to a MOSFET. In the device structure, source and drain are used for injecting and draining out charge carriers. An insulating layer is deposited to separate the gate electrode and semiconductor. The gate electrode is employed to provide a gate field, which is used to control the drain current. The charge-transporting channel forms at the interface of the insulator and the organic semiconducting layer, the width of which is controlled by the gate field. The main difference between an OFET and MOSFET, is the materials used and the mode of operation. Silicon is used as an active charge transporting material in a MOSFET, whereas an OFET uses organic materials and works in injection mode. Currently available OFETs operate at high voltage because of the low mobility of charge carriers. Normally OFET operates around 20-40 volts, which is a great concern towards fabricating low voltage organic devices.

2.4.1 Types of Organic Field Effect Transistors

Broadly speaking, organic field effect transistors can be differentiated into two types as

- Lateral (planar) OFET
- Vertical OFET

The movement of charge carriers from source to drain terminal defines the type of OFET as either lateral or vertical. In the lateral type, charge carriers move horizontally between the

source and the drain electrode; that is, the channel is parallel to the gate electrode. Whereas, the charge carrier moves vertically in vertical OFETs and the channel plane is normal to the gate electrode. The position of the gate w.r.t. the source and drain is another way to define lateral and vertical OFETs. The position of the gate electrode is symmetric in the lateral type while it is asymmetrical in vertical OFETs. In addition, the position of the gate is equidistant w.r.t. the source and drain in lateral devices. Whereas, in vertical OFETs, the gate electrode is placed near to a source terminal as compared to the drain. The thickness of the organic material describes the channel length in vertical OFETs. Thus, the organic semiconductor layer is sandwiched between the source and drain to define the channel in a vertical OFET. Another important parameter is the electric field profiles of the drain and gate. The electric field directions of both V_{DS} and V_{GS} differentiate between lateral and vertical OFET. The details of lateral and vertical OFETs, their structures and the corresponding effect of the geometry on the device performance will be discussed in the following chapters.

2.4.2 Lateral OFETs

As the name suggests, the lateral OFETs are known by the horizontal charge movement. In lateral OFETs, the drain source (V_{DS}) and gate source (V_{GS}) fields act normal to each other. Figure 2.3 shows the basic lateral OFET topologies and configurations. The lateral structure can further be divided into four sub-types. By changing gate position (top and bottom contact) and/or by changing the source drain placement within an organic semiconductor material defines new configurations, i.e. planar structure or staggered structure. Each design configuration has its own advantages and downsides. The charge carrier path, gate field effect and fabrication process complexities make each configuration a unique OFET design. For example, in the bottom gated co-planar configuration, the charge carrier movement lies in one plane and has greater gate field

control. Whereas in the bottom gated staggered structure, charge carriers follow a non-linear path to constitute the drain current. Similarly, changing the position of gate from bottom to top, a drop in the control of gate field is observed. In normal practice, bottom gated lateral geometries are widely used in the range of $0.5\mu\text{m}$ - $5\mu\text{m}$ channel length OFET devices. Fabrication of OFET beyond a $5\mu\text{m}$ channel length invokes process complexities and increased cost. In a standard photolithographic processing environment, achieving submicron channel length OFETs is a challenging task. Vertical geometry is an alternative available for achieving nanoscale OFETs without compromising the cost, with less process complexity.

Generally, lateral OFET is designed by placing a gate electrode at the bottom, called as bottom-gated or at the top, called a top-gated OFET. Further, the position of the source and the drain electrodes categorize lateral OFETs into coplanar or staggered types. Coplanar OFETs have the source and the drain in the same plane, whereas staggered OFETs have the source and the drain placed differently [43]. Each configuration introduces a series contact resistance depending on the interfaces formed in the material layers. Surface engineering and other techniques are used to reduce the series contact resistance. The contact resistance between metal and organic semiconductors can be either Ohmic or Schottky type. In staggered top-gated OFET geometry, contact resistance has been modeled and observed to be Ohmic [44]. In Ohmic contacts, the charge transport is bulk-limited, whereas in Schottky contacts, the transport is contact-limited. This implies that in short channel OFETs, the contact effects are more pronounced, as the charges are injected from outside. Charge carriers injected from source terminals create an electric field within the organic semiconductor. The excess charges accumulated within the semiconductor generate a space charge region and thus a resultant current known as SCLC current. Thus, the Schottky contacts exhibit non-linearity in OFET

characteristics. Whereas in Ohmic devices, the overall resistance is introduced mainly by the bulk of semiconductors and there is a very limited effect of parasitic contact resistance.

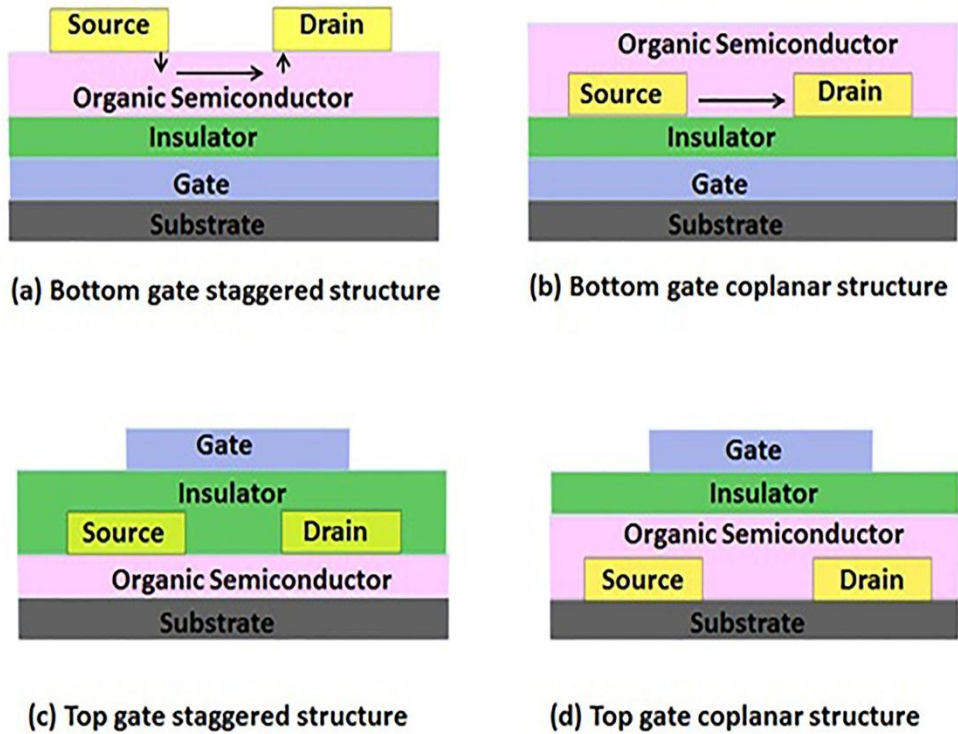


Figure 2.3 Various topologies of OFET device geometries. (a)-(b) bottom gated and (c)-(d) top gated.

Space charge limited current dominates in the region near the injection electrode due to poor mobility of organic materials. It's always challenging to minimize the contact effects while fabricating organic devices. Figure 2.3 (c) and (d) shows the lateral OFETs in top gate and bottom gate with respective staggered and coplanar configurations.

2.4.3 Operation of Lateral OFET

The geometry of OFET has improved over time. In terms of device parameters such as ON/OFF ratio, field effect mobility and threshold voltage, the effect of geometry on the performance of OFETs has been reviewed [45]. The working of lateral OFETs can be

understood by the circuit operation, as shown in Figure 2.4. A bottom gated p-type OFET is wired up for the measurement of I-V characteristics. By using this circuit configuration the output and transfer characteristics are measured and recorded.

Output characteristics are measured by supplying V_{DS} biasing between source and drain terminals and output current I_{DS} is measured across a load at a fixed value of V_{GS} biasing. Gate source voltage V_{GS} is gradually increased in steps and the corresponding change in output drain current is recorded. Transfer characteristics are measured by varying V_{GS} and measuring I_{DS} , keeping V_{DS} at constant. Transfer characteristics provide the threshold voltage and ON/OFF ratio, which are important switching parameters.

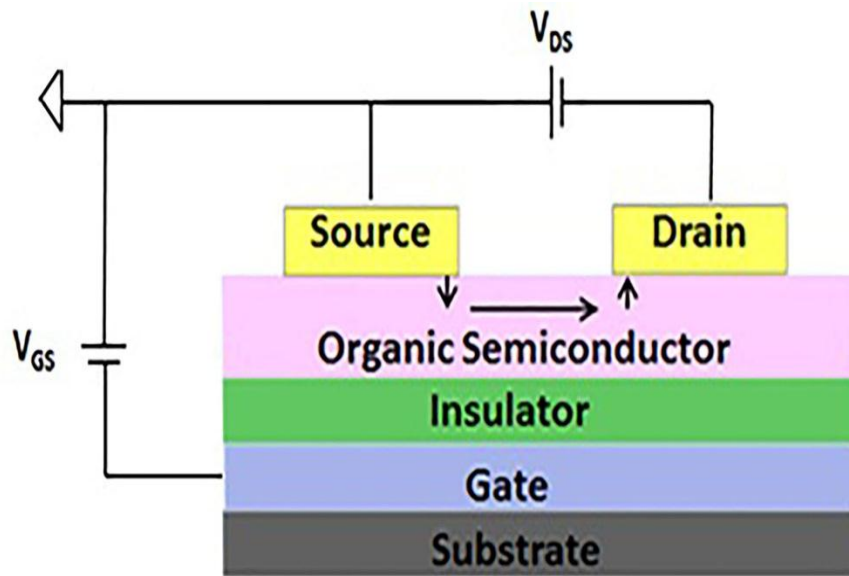


Figure 2.4 Circuit diagram of a p-type OFET device in lateral geometry.

2.4.4 Vertical Organic Field Effect Transistors

Channel length in vertical transistors is defined by the thickness of organic layers between metal electrodes. The main challenges involved in scaling down the silicon transistor are the cost and process complexities, which can be easily fixed in solution processed VOFET.

Channel length reduction is much easier in vertical geometries than can be controlled during spin coating. To achieve micron to nanoscale channel length, speed of coating and the thickness of a properly diluted organic material plays an important role.

Short channel OFETs are good in achieving low operating voltage and high current density. Reduction in channel length can control the maximum switching frequency as $f \propto \mu/L^2$, integration density $N \propto 1/L^2$, and drain current $I_D \propto \mu/L$ [46]. Short channel organic devices hold the potential for achieving a high output current, high circuit density in a small area and high switching frequency.

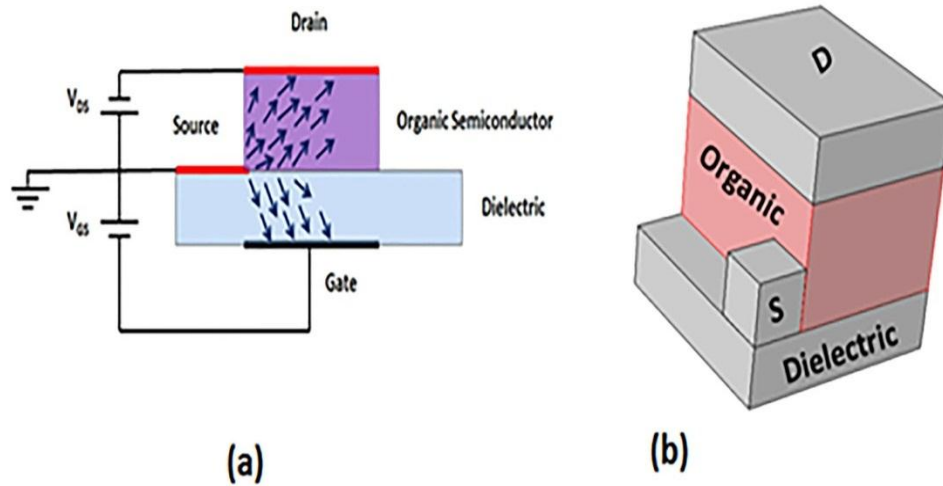


Figure 2.5 Vertical OFET geometry (a) charge carrier flow and biasing circuit (b) VOFET layout.

Achieving short channel up to certain limits, i.e., $L=10\text{nm}$ is possible in vertical OFETs. Quantum mechanical effects start playing a role while approaching the submicron regime. Consequently, unconventional output characteristics and decrease in ON/OFF ratio can be observed. Solution processed vertical OFETs have the advantage over conventional OFETs because of their high current handling capabilities at low operation voltage [47]. The device

performance of solution processed OFET depends on the surface interfacing, which has been explored in recent years [48].

2.4.5 Operation of Vertical OFET

The geometrical structure and operation of a vertical OFET is not exactly similar to that of a lateral OFET. Figure 2.5 shows the p-type VOFET in circuit operation and the arrows represent the flow of charge carriers inside the organic semiconductor. Drain and gate terminals are negatively biased through V_{DS} and V_{GS} supply voltages. The source terminal is kept grounded w.r.t. drain and gate terminals. Negative V_{DS} allows pulling the holes from the source towards the drain, which causes the current to flow through an active organic layer. The bottom gate field is increased in steps to allow a complete channel formation into the semiconductor layer. The concept of channel formation in VOFET is different from that of a lateral OFET. The location of the channel in VOFET is not at the interface of the insulator-organic layer, but it lies in between the 3D organic layer [49]. The influence of the SCLC effect in the channel drives the device operation into an entirely different mode; whereas in the case of lateral OFET, the channel is uniformly built at the insulator / semiconductor interface. The nanoscale channel in the vertical OFET will be explained in detail in chapter 4.

2.4.6 Important Terms Involved in VOFET Operation

For fabricating VOFET devices, the important terms involved are as follows:

- Mobility
- Linearity Effects
- ON/OFF Ratio
- Contact Resistance

2.4.6.1 Mobility

Charge carrier mobility is the term used to demonstrate the ability of carriers to move quickly into organic material. When an electric field is applied across the material, the charge carriers try to move with a velocity, known as drift velocity, which is proportional to the applied field. The drift velocity $v = \mu \cdot E$, where μ is the mobility of charge carriers and E is the applied field. The mobility of carriers in organic materials is very low compared to silicon. To meet the optimal performance of an OFET, the required biasing voltage is very high, up to 30-40 volts, because of the low mobility of organic materials. To circumvent the low mobility issue, a high current in a small region can be achieved at a very low voltage of around 1-2 volts in vertical OFETs. So, low mobility of organics can be compensated in vertical devices.

2.4.6.2 Linearity Effects

In vertical OFET characteristic curves, super linearity is normally observed due to short channel effects [50]. The device works in the linear region and is unable to attain saturation due to the presence of the SCLC effect. These types of devices are normally ON state devices and need biasing to switch it OFF or normally OFF and a required gate voltage to turn it ON. Other factors responsible for linearity are contact effects, such as the Schottky effect.

2.4.6.3 ON/OFF Ratio

The important term involved in OFET is the ON/OFF ratio, which determines the switching action of a transistor. It is defined as the ratio of maximum ON current (I_{ON}) and minimum leakage current (I_{OFF}). To achieve a good ON/OFF ratio, there should be a clear cut region of linear and saturation regimes of OFET. Normally in solution processed VOFET, poor ON/OFF ratio is observed and reported [57] because of the unsaturated behavior of VOFET devices.

2.4.6.4 Contact Resistance

In OFETs, the disordered organic material layer establishes uneven contacts with metals and dielectric layers. These non-uniform contacts and interfaces contribute series resistance. The change in resistance is observed when charge carriers move from metallic electrodes to organic semiconductors. These contacts play a crucial role in deciding device operation and characteristics. There is a capacitance associated with the device due to overlapping layers that frequently experience charging and discharging during device operation. The variation of capacitance restricts the device operation into a linear regime. In addition, the effect of contacts dominates and the channel resistance increases.

2.4.7 Factors Affecting VOFET Operation

There are numerous factors involved which affect the device performance and operation of VOFET. The operation of VOFET is different from its lateral counterpart due to its geometrical design. Two main factors which can commonly be observed in vertical OFET are:

- Short Channel Effect
- Contact Effects

2.4.7.1 Short Channel Effect

Short channel in a vertical OFET results in an undesired effect in device operation, which is known as a short channel effect. The main reason behind these unintended effects is the low mobility of charge carriers in organic materials. The rate of injection of carriers from outer electrodes is more than the rate of diffusion of carriers into the organic material. The injected charges try to accumulate around the injecting electrode and create a space charge region next to the depleted region. This accumulated charge drives the current into the unsaturated region and

creates more linearity in the I-V characteristic curve. Thus, this creates super linearity in characteristic curves and the device current is influenced under SCLC effects.

2.4.7.2 Contact Effects

In fabricating vertical OFETs, parasitic and contact resistances play a more dominant role in device performance. These effects are more prevalent in vertical organic devices where short channel effects are dominating. While stacking the layers vertically, the interfaces - namely metal/organic, organic/insulator and metal/insulator-are supposed to contribute towards respective contact resistances. Each interface resistance, parasitic resistance and bulk resistance contributes towards overall series resistance. To minimize the contact effects, surface engineering and sacrificial layers are to be employed.

2.5 Literature Survey and Progress Review in Vertical OFET

The structure optimization, interfacial and surface engineering, advanced functional materials, fabrication techniques and many more factors are involved, which need to be studied for improvement in performance of VOFET devices. So far, vertical organic transistors have been fabricated using polymeric materials in different configurations and geometries. The main fabrication process adopted for depositing thin films of organic material are thermal evaporation and spin coating. Thermal evaporation can be used for deposition of metals, organic semiconductors and oxides. In solution processed OFETs, thermal and e-beam evaporation techniques are used for source and drain electrode metallization. In a standard micro fabrication environment, photolithography is a promising and standard process available for high resolution patterning. Although, photolithography is a costlier process and involves the use of solvents like hydrofluoric (HF) acids, which are not friendly with organic materials. However, as an

alternative, low cost thin film deposition technique such as spin coating, drop casting, and dip coating, etc. are available.

Very limited literature is available on vertical OFETs since the area has recently emerged in the last 7-8 years and is still in its state of infancy. The solution-processed method is even younger than the photolithography process in vertical OFET fabrication. Therefore, efforts have been made to collect literature over organic FETs published in recent years in vertical geometries, materials used, deposition process adopted, and advantages of the fabrication process. In Table 2.1 and Table 2.2 literature related to vertical geometries, with their respective I-V characteristic curves in biomedical applications, is collected.

Table 2.1 Literature of VOFET in various vertical orientations and geometries. I-V characteristic curves, organic materials used, and fabrication process adopted.

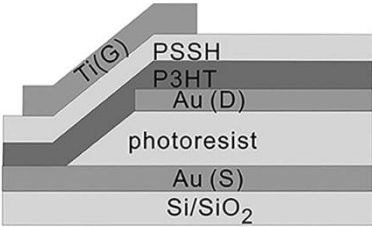
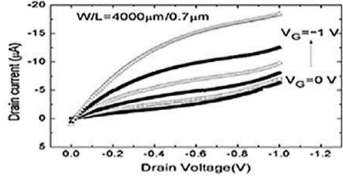
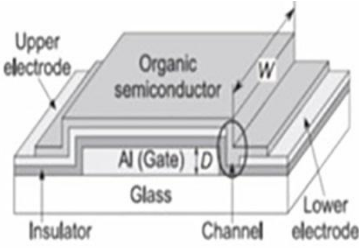
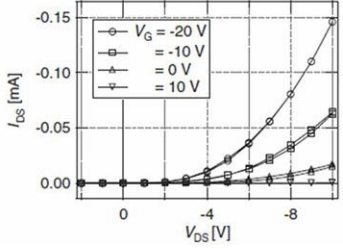
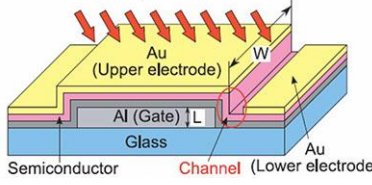
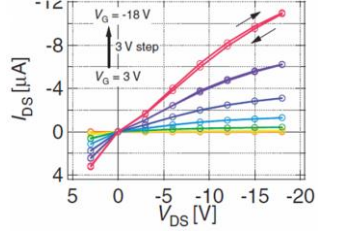
Vertical Device Structure	I-V Characteristics Curve	Material Used, Process Adopted	Reference
		<p>Poly-electrolyte gated, mask free photolithography</p>	<p>[50]</p>
		<p>6,13-Bis(trisopropyl-silylethynyl) Pentacene, step edge structure, photolithography</p>	<p>[51]</p>
		<p>Pentacene, photolithography advantage of reducing parasitic capacitance</p>	<p>[52]</p>

Table 2.1 (Continued)

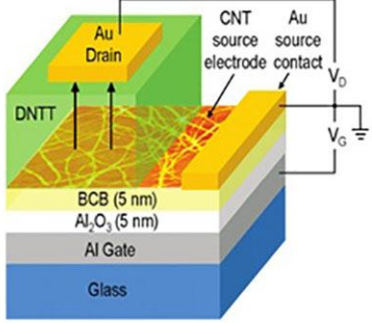
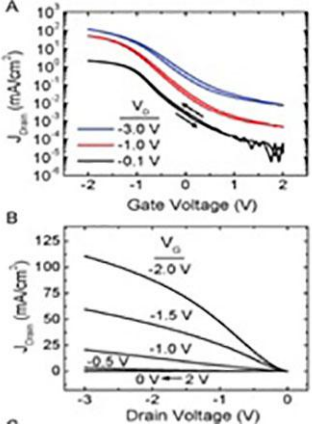
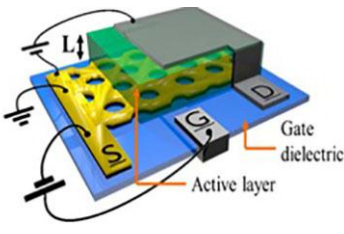
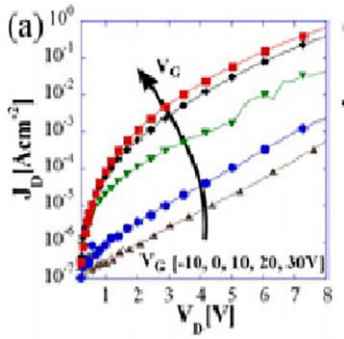
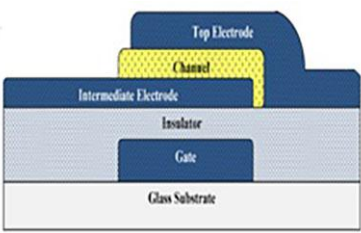
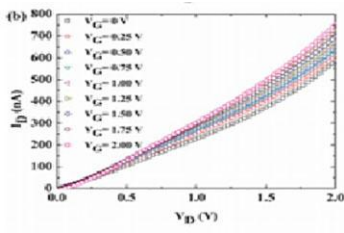
		<p>Carbon nanotubes, high resolution patterning, high current density</p>	<p>[53]</p>
		<p>P(NDI2OD-T2) polymer, solution-processed</p>	<p>[54]</p>
		<p>Polyvinyl alcohol and C60 fullerene, spin coating</p>	<p>[55]</p>

Table 2.1 (Continued)

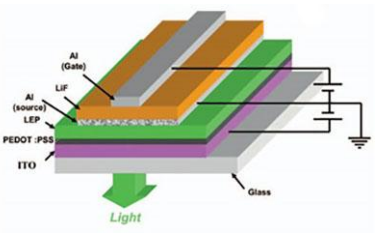
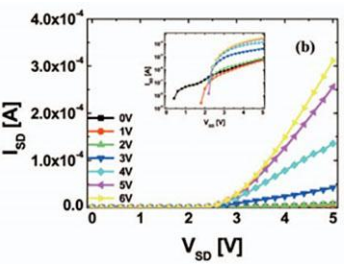
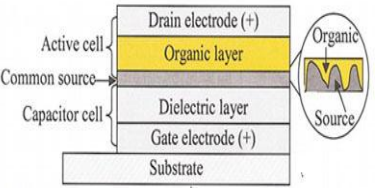
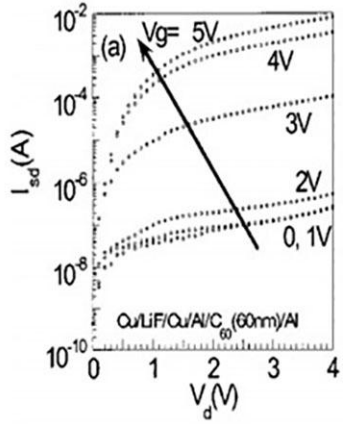
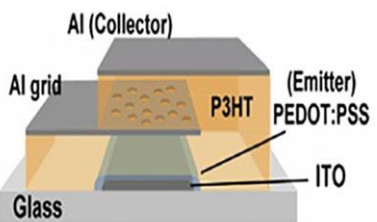
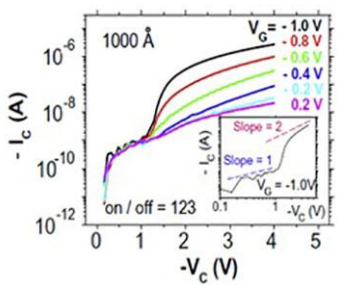
		<p>PEDOT:PSS, stacked OLET with capacitor structure, spin coating and thermal evaporation</p>	<p>[56]</p>
		<p>Vertically stacked super capacitor cell, C60, thermal</p>	<p>[57]</p>
		<p>PEDOT:PSS, non-photolithography</p>	<p>[58]</p>

Table 2.1 (Continued)

		<p>CuPc, organic SIT, nanoholes with thermal, photolithography</p>	<p>[59]</p>
		<p>DNTT, graphene source electrode, spin coating</p>	<p>[60]</p>
		<p>SPAN/Al bilayer as drain, C60 fullerene, vertical structure, thermal</p>	<p>[61]</p>

Table 2.2 OFET used for various biomedical applications.

Organic Field Effect Transistors	Biomedical Application Areas	Reference
Organic bioelectronics	OFET sensor, ability to conduct, charge carriers and ions	[62]
Organic bioelectronics in nanomedicine	Organic electrochemical transistor (OECT) for medicine	[63]
OFET stimulating electrode	Matrix-addressable high density stimulating electrodes	[64]
OECT in delivery of neurotransmitter in vivo	Device mimics nerve synapse	[12]
OFET recording probes	In vivo brain activity recording	[65]
OECT high trans conductance	High gain OFET for sensor application	[66]
OECT barrier tissue integration	Bioelectronics, organic device interface with barrier tissue	[67]
VOFET vertical OFET	High current, low voltage operation	[53]
VOFET low voltage	One volt operating voltage VOFET	[68]
Vertical organic light emitting transistor (VOLET)	Dual function of OLED and switching current transistor	[56]
VOFET low cost fabrication	Low cost fabrication of inkjet printing, spin coating, dip coating	[42, 69, 70]
OFET high speed	High speed flexible OFET in 3D structure	[71]
Solution-processed organic transistor	Solution processed organic transistor by nano imprint lithography	[72]

CHAPTER 3: SOLUTION PROCESSABLE VOFET DEVICE FABRICATION

Solution processable organic materials are emerging as a new choice of materials for making low cost OFET devices. Solution based electronics is widely accepted as a new class of fabricating technology for developing low cost flexible OFETs using conventional methods such as inkjet printing, spin coating, dip coating, and drop casting techniques [73]. Room temperature processability of organic materials and ease of deposition using a range of polymeric materials is paving ways for exploring possibilities for a new generation of flexible, disposable and environmental friendly green technology. As discussed in the previous chapter, the low mobility of organic materials limits its uses in fabricating devices; whereas, solution-processed devices are demonstrating improved performance and reliability for use in low cost flexible and disposable electronics. Impressive improvement in device performance has been demonstrated by the new design of functional materials in synthetic chemistry. Novel device structures have been fabricated using solution processable methods using wet chemistry routes.

Organic thin-film transistors are making inroads as potential electronic elements in the various flexible device application areas. Fabrication cost, structural miniaturization and low operational voltage are three important parameters that need to be addressed for fabricating the next generation OFETs. To realize these devices, OFETs require new design paradigms and wet-processing routes. However, the conventional lateral OFET geometry cannot satisfy these demands due to process complexities and high fabrication cost.

For developing organic devices using a standard photolithography technique, solvent sensitivity towards organic semiconductors, electrode patterning, and masking are major challenges. Therefore, the solution route and novel device geometry are the key factors that need to be integrated to achieve nanoscale organic transistors. Vertical OFETs have the potential to achieve sub-micron channel devices which can be achieved by stacking material layers in a vertical direction [74, 75]. Miniaturized device geometry in the vertical direction can be realized by applying low cost techniques such as spin coating [76], drop casting [77], dip coating [78], and ink jet printing etc. Precursors of soluble organic semiconductor exhibit promising properties for device fabrication [79]. To realize nanoscale film thickness, the spin coating technique is frequently used as a low cost deposition method. Concentration of material in solution, coating speed and ramping recipes decides the thickness of organic material.

3.1 Solution Processable VOFET: Three Stage Process

In this study, a soluble pentacene precursor is selected as the active organic semiconducting material. In normal routines, pentacene is deposited using thermal evaporation methods. However, a low cost solution route is adopted to deposit pentacene. For this purpose, the precursor is converted to pentacene molecules by a series of processes and treatments. The precursor 13,6-N-sulfinylacetamidopentacene based novel fabrication process is proposed to achieve a vertical OFET. The low cost device fabrication processing technique involves deposition of organic material without the use of high resolution photolithography and vacuum conditions. Sub-micron device features are optimized by controlling the thickness of the spin coated pentacene precursor. The VOFET device fabrication process is divided into three stages as follows and is depicted in Figure 3.1.

- Stage I Gate, Source Fabrication Steps, Pentacene Deposition, and Masking

In this stage the bottom gate electrode, insulating layer, source electrode and precursor thin film are deposited. The precursor is annealed at 200°C to convert it into pentacene.

Polyimide masking is adopted and applied for material separation.

- Stage II Pentacene Metrology Characterization to Confirm Conversion

In this stage the metrology characterization is performed to test and confirm the precursor to pentacene conversion process.

- Stage III Drain Deposition and Final Device Fabrication

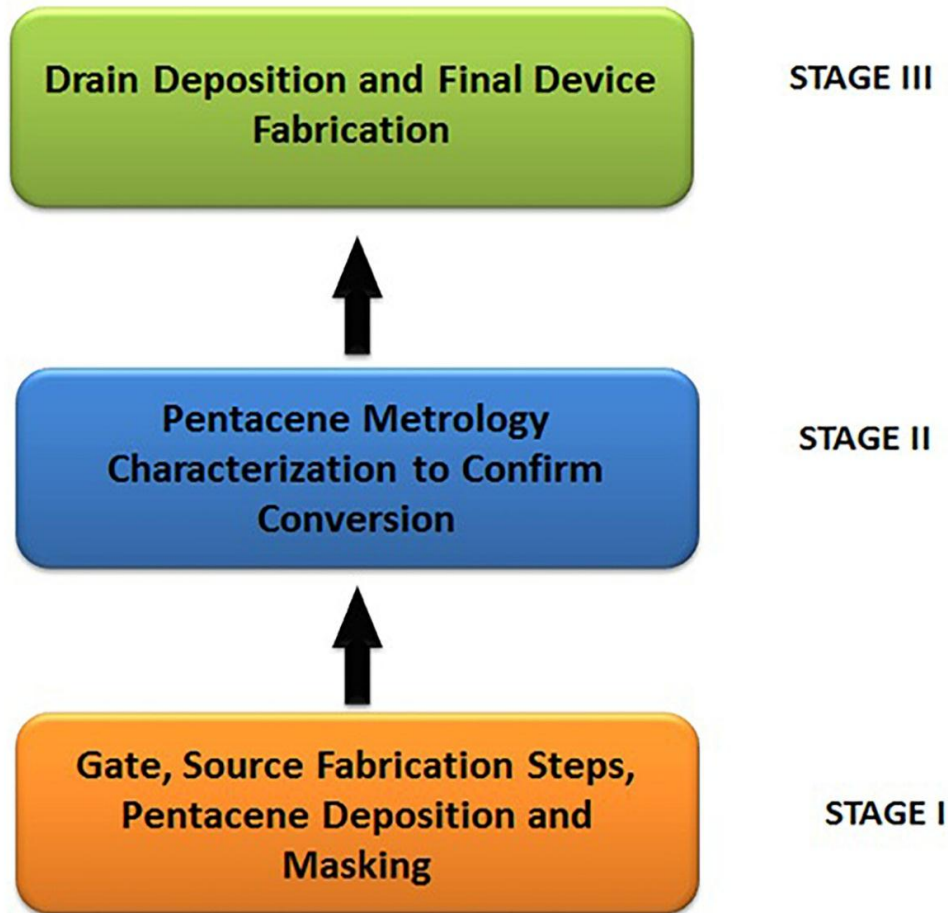


Figure 3.1 VOFET device fabrication steps elicited the whole fabrication scheme from Stage I to Stage III.

This is the final stage of device fabrication. This stage involves multiple sub steps, depositing the drain electrode in the first part, and then all necessary masking is partially peeled off for exposing electrodes open for device testing.

3.1.1 Stage I Gate, Source Fabrication and Precursor Deposition

This is the first stage of device fabrication. A highly-doped Si wafer is cleaned in the first step through the standard cleaning process in a clean room environment. An Al gate layer of 200nm is deposited using a shadow mask into an e-beam evaporator chamber at the rate of 1Å/sec at a base pressure of 10^{-6} Torr. Polyimide masking is made by hand in the lab and applied over the wafer so that it can cover and protect the gate terminal upon exposure into the e-beam vacuum chamber. The Al gate terminal is partially covered with kapton polyimide masking, keeping the rest of patterned Al open for the next layer of dielectric coating over it. Two types of devices are made for the study. Devices which represent for unpatterned source electrode into step geometry where SU-8 is taken as dielectric, are called Type I. Devices of the Type II category have polymethyl methacrylate (PMMA) used as the dielectric with the patterned electrode. SU-8 is selected as the gate dielectric in Type I devices due to its high thermal stability ($T_g > 200^{\circ}C$), to support the precursor to pentacene conversion process without any material degradation. After SU-8 coating, an Au electrode (100nm thick) is deposited over the SU-8 layer using a designed metallic shadow mask into an e-beam evaporator. Half of the Au electrode is masked partially with 3M Kapton polyimide tape (for connection openings later) to protect the source terminal during the precursor spin coating (shown in process flow steps). The inner edges of polyimide masking tape are cleaned carefully to remove the dust particles before applied for masking. The complete process flow in Stage I and steps involved are shown in Figure 3.2.

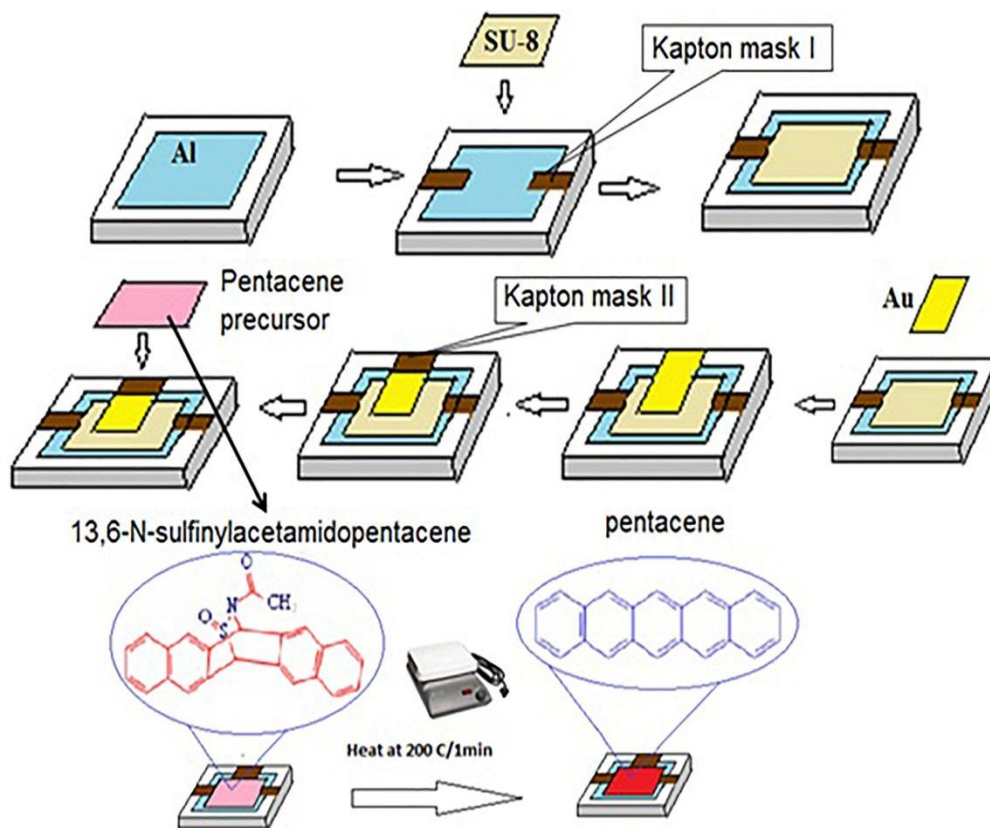
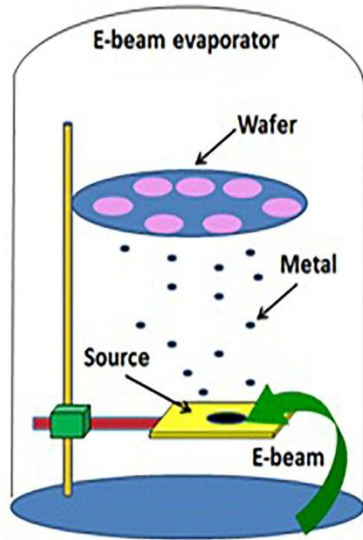


Figure 3.2 VOFET fabrication stage I starting from gate deposition (top left) to pentacene conversion.

The soluble pentacene precursor 13,6-Nsulfinylacetamidopentacene 97% (NSFAAP), is directly purchased from Sigma-Aldrich, a commercial supplier. It can be dissolved either in chloroform or dichlorobenzene organic solvents to make a uniform solution. In this case, it is dissolved in dichlorobenzene (15mg/ml) and stirred properly overnight to make uniform solution. The next step is to attach a 0.2 micron filter in front of a syringe filled with a precursor solution to be suspended over the wafer held over spin coating chuck. A few drops of precursor solution are suspended over the wafer so as to cover two-thirds of the wafer area consisting of gate and SU-8 layers. After spin coating at 3000 rpm for 1 minute (600 rpm in the first 5 sec and then ramp up), a uniform thin film free from holes and of submicron thickness is deposited. The thin film thickness is measured using a Filmetrics F20 Reflectometer.



(a)



(b)

Figure 3.3 E-beam chamber for electrode deposition (a) gold metal evaporation (b) e-beam facility at NREC.

The e-beam evaporator and the steps involved in the metallization process are shown in Figure 3.3. After thin film deposition, the wafer is removed from the spin coater chuck. Wafers are kept for two minutes in the hood to settle down the thin film morphology at the microstructural level before moving them for the annealing process. Thermal treatment is applied to convert the thin film of the precursor into pentacene over a preheated hot plate at 200°C for one minute. This conversion process is known as the reverse Diels-Alder process [79, 80].

3.1.2 Stage II Pentacene Metrology Characterization

In Stage II of device fabrication, the thermally treated thin film of soluble pentacene precursor 13,6-Nsulfanylacetamidopentacene 97% (NSFAAP) is tested to confirm the desired pentacene material. Surface morphological inspection, spectroscopy analysis, and electron microscopy metrology techniques are performed to validate the conversion process without

physically disturbing the thin film. Besides surface analysis, validation at molecular and atomic levels is also performed to make confirmation about a pentacene molecule. The following tests are performed and are demonstrated in Figure 3.4.

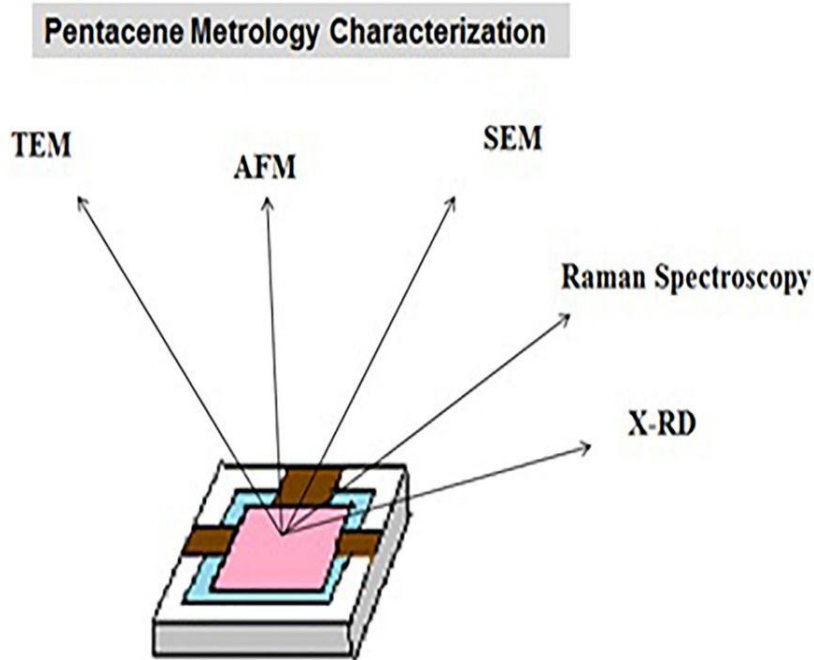


Figure 3.4 VOFET fabrication Stage II for pentacene conversion and metrological testing.

- Transmission Electron Microscopy (TEM): A TEM scan of the thin film sample is performed to confirm the crystal size of pentacene grains after annealing on a preheated hot plate for 1 minute at 200°C.
- Scanning Electron Microscopy (SEM): A cross sectional view of the SEM scan is recorded to confirm the stacked material layers in the vertical device structure.
- Atomic Force Microscopy (AFM): An AFM scan is performed over the surface of the organic layer to confirm the molecule and grain size of the pentacene molecule.

- Raman Spectroscopy: Raman Spectroscopy is performed to test and confirm the peaks of disordered pentacene in order to get the initial signature at molecular level.
- X-RD: X-ray diffraction techniques are employed for confirmation of pentacene at the atomic level, while matching the characteristic peaks with literature. The detail of their images and analysis is discussed in Chapter 4 under the characterization section. This stage of confirmation is very important before proceeding to the next level of VOFET device fabrication, in order to make sure that the converted material is actually the pentacene.

3.1.3 Stage III Final Device Fabrication

After the confirmation about the pentacene, the next and final step is to deposit the drain electrode. The device is shifted into the e-beam evaporator vacuum chamber for depositing a final layer of gold (Au) (100nm thick) over the pentacene material layer. The polyimide masking is applied (as shadow mask) to selectively protect the stacked bottom layers of the device. The organic layer is exposed for gold deposition.

There are chances of Au particles penetrating the organic layer and making a short circuit. Extra care has to be taken to avoid this problem. Three selective rates of Au deposition are selected, i.e., $0.5 \text{ \AA}/\text{sec}$, $1 \text{ \AA}/\text{sec}$, and $1.5 \text{ \AA}/\text{sec}$ to avoid the Au penetration into pentacene [81]. After gold deposition, the wafers are removed from the e-beam chamber to proceed to the next step. The novel device structure is designed in such a way that the upper layer should fully cover the organic layer to avoid any contamination. As shown in Figure 3.5, the final gold layer is not only to act as a drain electrode but also to protect the organic layer from the outer environment. Thus, the bottom pentacene layer is protected from oxide formation and other contaminants.

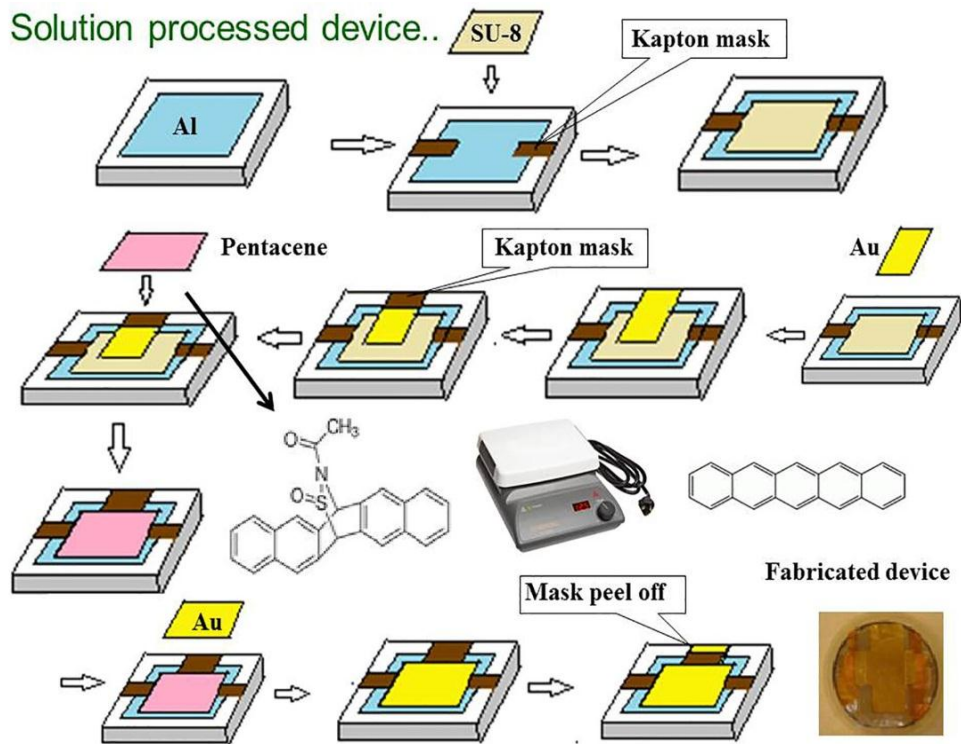


Figure 3.5 Stage III of fabrication elicited Au deposition and fabricated device picture.

3.1.4 Precursor to Pentacene Conversion

The soluble pentacene precursor is dissolved in dichlorobenzene to make a uniform solution. After spin coating at 3000 rpm, a 1 minute thermal treatment is performed for conversion over a preheated hot plate at 200°C by the process known as the reverse Diels-Alder process [80]. A final layer of Au (100nm) is deposited over pentacene at three selective rates of 0.5 Å/sec, 1 Å/sec, and 1.5 Å/sec to avoid the Au penetration into pentacene [81].

At the next level, masked electrodes are made open partially by peeling off the Kapton tape for establishing electrical connections and electrical characterizations. For Type II devices, the drop casting technique is employed on a patterned source electrode to avoid the problem of short channel effects.

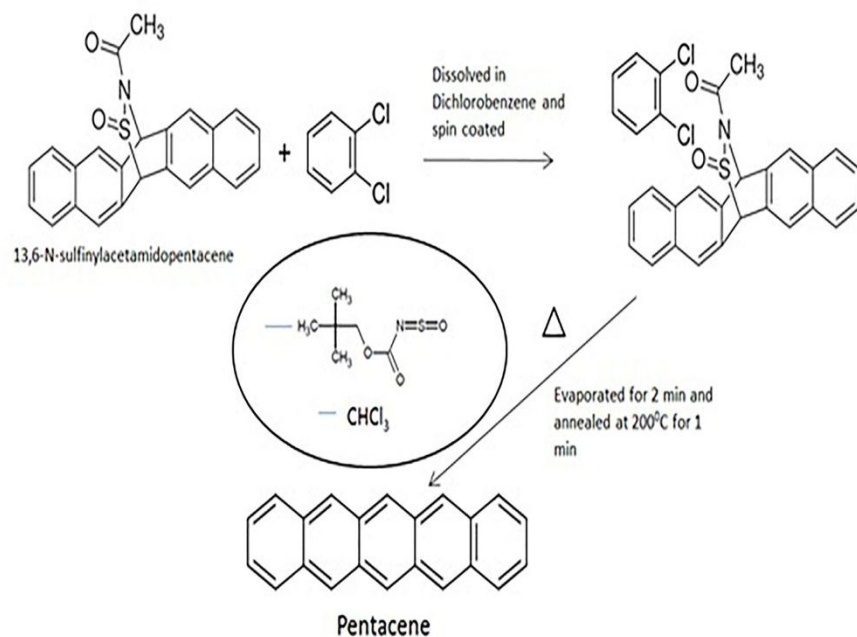
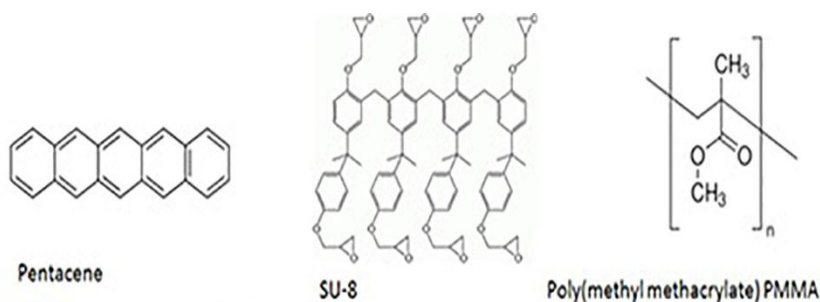


Figure 3.6 Soluble pentacene precursor and scheme adopted for conversion process.



	Material Properties	
SU-8	Glass temperature, T_g (fully cross-linked)	$>200^\circ\text{C}$
	Glass temperature, T_g (unexposed)	$\sim 50^\circ\text{C}$
	Degradation temperature (fully cross-linked)	$\sim 380^\circ\text{C}$
	Breakdown Voltage	$4.43 \pm 0.16 \cdot 10^8 \text{ V/m}$
	relative dielectric constant: ϵ_r	4

Figure 3.7 Molecular structure of pentacene, SU-8 and PMMA.

The drop casting method is basically applied for depositing thick films. The chemical reactions to complete the conversion process have been shown in Figure 3.6. The chemical structures of materials used such as pentacene, SU-8 and PMMA are shown in Figure 3.7. The material properties of SU-8 are also discussed.

3.2 Low Cost Fabrication

The complete device fabrication process flow is shown in Figure 3.8. The whole low cost device fabrication process is evolved around two central point, namely *novel device geometry* and *low operational power*.

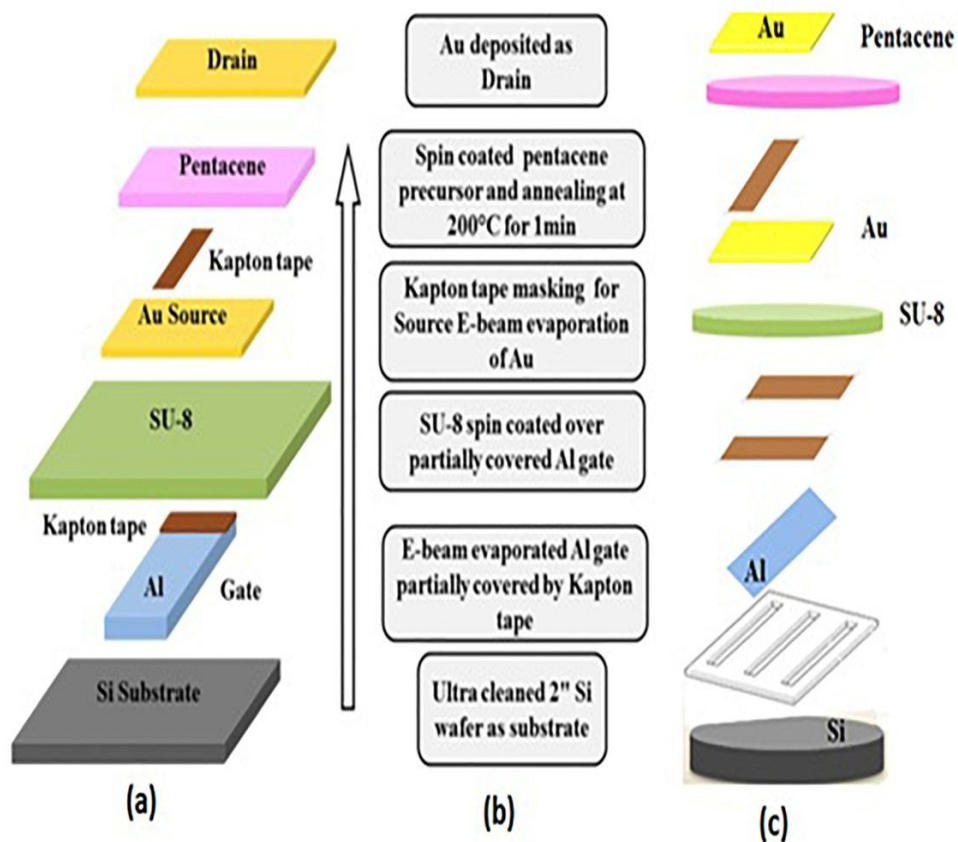


Figure 3.8 Complete VOFET fabrication steps (a)-(b) process flow (c) sequence of stacking layers.

The electrical parameters of low voltage around which the design of this experiment evolved, will be discussed in Chapter 4 in the electrical characterization section. The two major issues related to the physical device structure are listed below.

- Low Cost
- Processing Temperature

3.2.1 Low Cost Design Process

The device fabrication and design of experiments are planned to keep the novelty of process at a low cost. Keeping this novel feature of low cost in view, polyimide masking and spin coating deposition techniques are adapted. As known, standard micro fabrication processing involves a heavy cost, ultraclean room environment, photolithographic patterning, and high vacuum chambers. Masking the stacked layer is another challenge involved in fabricating nanoscale electronic devices. To mask the increased number of stacked layers not only raises the cost, but also raises the process complexities. In addition, the solvents used in standard photolithography masking are not organic friendly. Therefore, keeping all these challenges in view, the low cost novel process is evolved.

3.2.2 VOFET Device Processing Temperature

The fabrication process is evolved to maintain the glass transition temperature of materials between 200°C - 300°C . The selection of fabrication materials is planned to complement processing and glass transition temperature. The processing temperature of soluble pentacene precursor 13, 6-Nsulfanylacetamidopentacene 97 % (NSFAAP) is around 200°C and glass transition temperature (T_g) of SU-8 is $\sim 230^{\circ}\text{C}$. The device structure is intentionally designed as bottom gated so that no further thermal treatment should be performed after pentacene conversion. The final gold layer in VOFET is deposited at room temperature. The organic layer

is fully encapsulated by a gold layer for its protection from the outer environment. The complete fabrication process is explained in the previously published work [82].

3.3 Spin Coating Method

Spin coating method is emerging as a quick and low cost technique for depositing thin and uniform film of organic material on a flat surface [83]. In the first step, organic material is dissolved in solvents to make a homogeneous solution. A Few drops are dispensed over the surface of the substrate with the help of a dropper. The experiment is designed with a recipe to achieve the desired film thickness. A high speed rotation of the fluid centrifuges the excess material out of the surface and a nice uniform thin film is left. This method is so quick and fast, it achieves nanoscale film thickness within minutes.

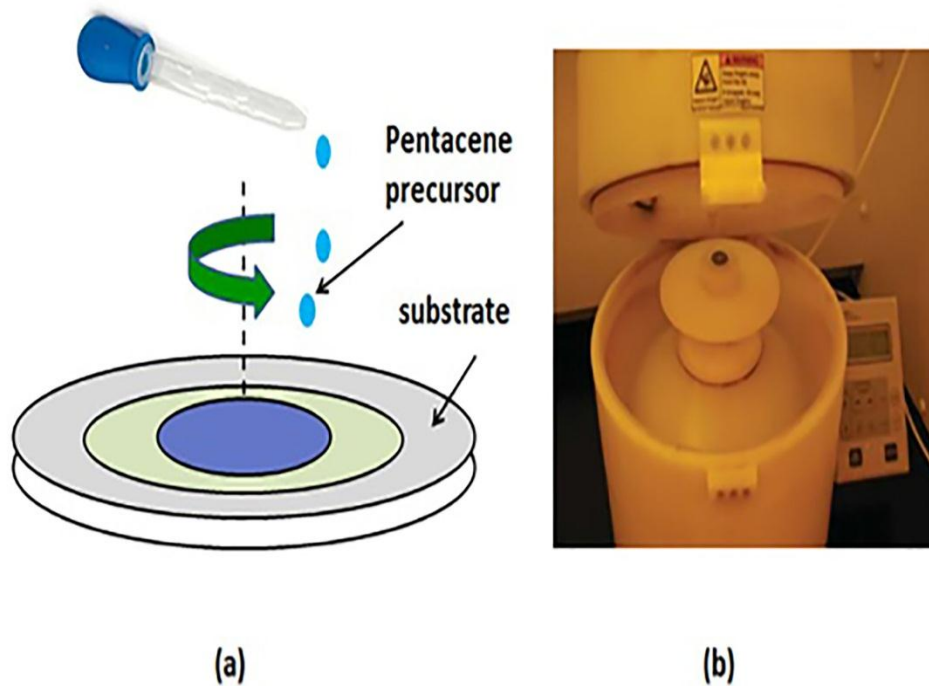


Figure 3.9 Spin coating deposition method (a) diluted pentacene precursor suspension (b) spin coater.

Figure 3.9 shows a sketch of a spin coater used for depositing pentacene precursor at the Nanotechnology Education and Research Center (NERC) facility at USF. Figure 3.9(a) shows the spin coating method, in which a diluted pentacene precursor is dropped over an insulating layer of a VOFET device.

3.4 Drop Casting Method

Drop casting is another low cost and quick method for thin film deposition in fabricating organic FETs [84]. It is the easiest way to get thin film. By dropping the solution on a substrate, the spontaneous evaporation of solvent leaves behind the desired material.

The film thickness is the function of solution concentration. This technique is advantageous over spin coating as there is no wastage of material in drop casting. However, the downside is that the thickness of the film is limited up to the micron range. Drop size and dilution of material in solvent decides the film thickness. It has limitations over large area coverage and poor film uniformity. On the other hand, pinhole-free and uniform film can be easily achieved in the spin coating technique. Figure 3.10 shows the drop casting technique applied for fabricating VOFET devices in patterned source electrodes.

3.5 Precursor to Pentacene Conversion

Organic material like pentacene is normally deposited by thermal evaporation for fabricating electronic devices. In solution processed devices, pentacene is used in the form of precursors. Some functional groups are attached to the pentacene molecules to make it soluble in organic solvents which can be evaporated out by thermal treatment. Pentacene is insoluble in organic solvents used for fabrication in organic electronics. To make pentacene amenable for processing in solutions, functional groups are attached to the rings of pentacene molecules. This method helps in dissolving pentacene in organic solvents for fabricating OFETs [85].

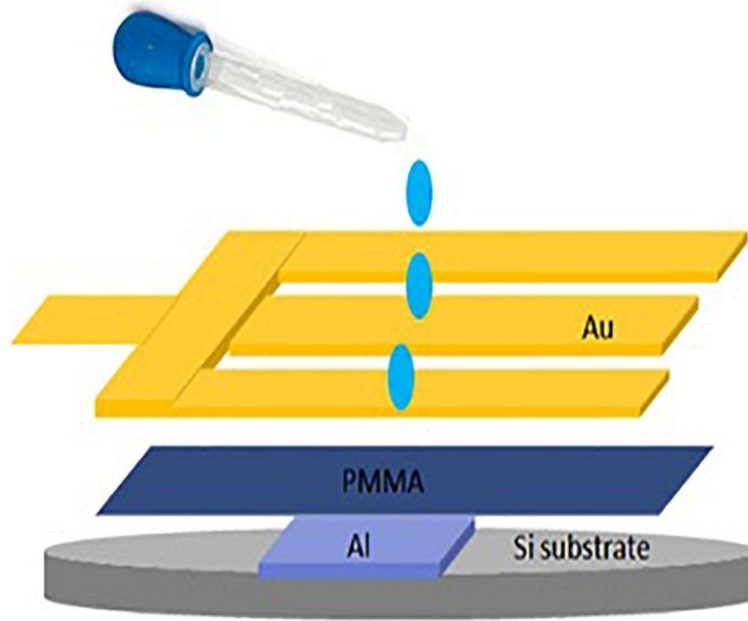


Figure 3.10 Drop casting deposition method where diluted pentacene precursor is dropped over patterned source.

The soluble pentacene precursor 13,6-Nsulfanylacetamidopentacene 97% (NSFAAP) is an excellent choice available to get pentacene material for fabricating OFETs by the solution process. The precursor to pentacene conversion process is easy, quick and low cost [86]. The thin film deposition of a pentacene by thermal evaporator requires high vacuum conditions, whereas the deposition by solution route is quiet, fast, and low cost to get uniform high quality film.

3.5.1 Solution Preparation

In solution preparation, the soluble pentacene precursor 13,6-Nsulfanylacetamidopentacene 97% (NSFAAP) is dissolved into dichlorobenzene (15mg/ml) and stirred properly overnight to make a uniform solution. The next step is to spin coat the dispensed solution at 3000 rpm speed. Thereafter, a one minute thermal treatment is required for precursor to pentacene conversion. As already mentioned, conversion process is better known as the reverse Diels-Alder process. In the next step, the wafer is treated thermally over a preheated hot

plate at 200°C/1 minute. Then, the wafer from the hot plate is allowed to stay at room temperature. After two minutes, a fine, smooth, and uniform pentacene thin film is obtained. The conversion process and chemistry involved is shown in Figure 3.11.

3.5.2 Time Temperature Optimization

Time-temperature balance optimization is an important parameter which contributes to the performance of a solution processable OFET. The precursor to pentacene conversion is governed by the reverse Diels-Alder process, in which the side chain is evaporated out of the pentacene ring during thermal treatment. To achieve the semiconducting behavior of pentacene, the side group is removed in gaseous form. Usually, a uniform but disordered thin film of pentacene is obtained after the thermal treatment.

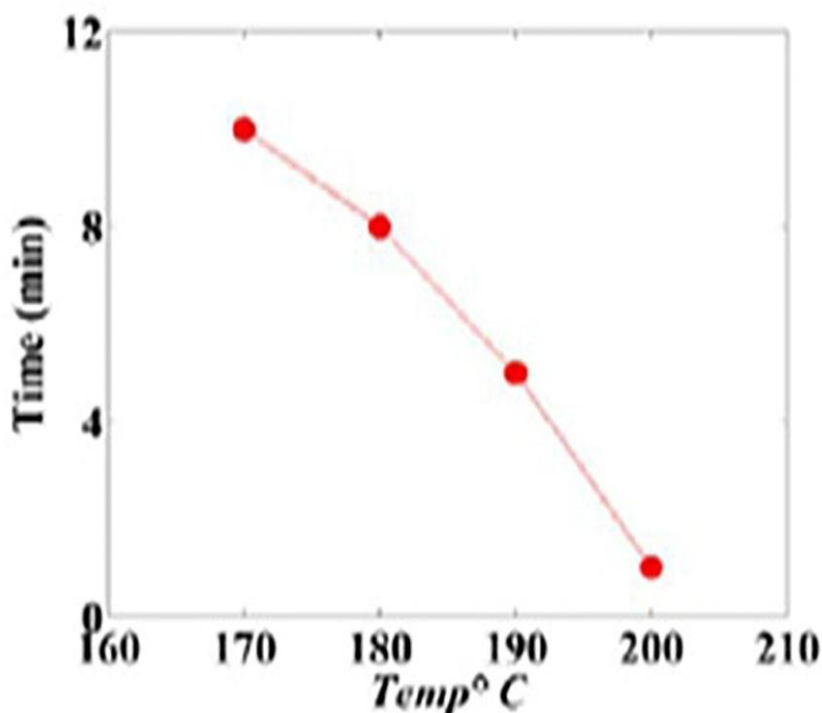


Figure 3.11 Time-temperature optimization curve for precursor to pentacene conversion process.

The conversion process optimization and spin coating rate determine the crystallinity of the pentacene film and device performance [87]. In a conversion process, time-temperature plot for a soluble pentacene precursor is recorded at different temperatures as shown in Figure 3.11. The conversion efficiency is reduced at a lower temperature, resulting in poor semiconducting quality of pentacene. Therefore, it is advisable to optimize between $180^{\circ}\text{C}/2\text{min}$ to $200^{\circ}\text{C}/1\text{min}$. The degradation of pentacene film starts at elevated temperatures beyond 220°C .

3.6 Masking and Geometry Optimization

In vertical organic device fabrication, it is very important to maintain the separation between interfacing material layers. Masking is applied in standard Micro Electro Mechanical System (MEMS) fabrication through the conventional method of photoresist into a highly ultra clean environment. In the MEMS device fabrication process, a higher number of stacking layers in a device means higher cost and design complexities. The solvents applied for etching in MEMS fabrication are unfriendly with organic materials. Thus, applying these micro fabrication solvents is undesirable in organic devices. To overcome this challenge, a novel low cost masking process is evolved for fabricating the VOFET device. Polyimide Kapton masking is selected for the separation of stacked layers. 3-M Kapton polyimide tape has excellent chemical, electrical and thermal properties. The DuPont Company made it first for NASA space missions. It's excellent thermal stability, ranging from -270°C to $+400^{\circ}\text{C}$, made it good for a wide range of extreme temperature applications.

3.6.1 Polyimide Masking for Electrode Protection

Kapton masking is applied at multiple steps during device fabrication. Kapton polyimide masking is employed at the following levels during fabrication.

- Masking for the separation of stacked and interfacing material layers.

- Shadow masks are made out of Kapton polyimide tape.
- Kapton polyimide tape is used as a flexible substrate for supporting the VOFET device.

Thermal properties of polyimide are utilized to support the thermal stability of device materials, as all the fabrication materials are selected around the glass transition temperature (T_g) of 200°C-300°C. The polyimide Kapton being thermally stable is also chemically very supportive for masking at various steps and levels of device fabrication.

3.6.2 Polyimide Shadow Masking in Metal Deposition

Kapton polyimide tape is also employed for shadow masks in the e-beam evaporation chamber for depositing the metal electrodes like gate, source, and drain. All shadow masks are made out of polyimide cuttings and designed in the lab.



Figure 3.12 Various shadow masking designs made out of polyimide Kapton tape.

Figure 3.12 shows the handmade shadow mask in various types of patterned metal electrodes. In the first step, the double layered polyimide substrate is made by joining the sticking surfaces together in order to minimize their interference. Then, shadow masking of polyimide is made to deposit the Au electrode. Step edge resolution is not that important in vertical device design.

CHAPTER 4: VOFET DEVICE CHARACTERIZATION

Solution processed vertical OFETs are fabricated using low cost techniques such as spin coating and drop casting. Fabricated devices are tested for electrical, metrological, and radiation characterizations.

4.1 Electrical Characterization

In order to verify the device performance, fabricated VOFET devices are tested at various electrical characterization standards. The basic tests performed are as follows:

- I-V Characterization
- C-V Characterization
- Transient Time Analysis
- Four Probe Resistivity

Electrical characterizations are recorded on a HP4145B semiconductor parameter analyzer at non-ambient room temperature conditions. Two types of low cost methods are adopted for VOFET fabrication:

- Spin coating method
- Drop casting method

For characterization and testing purposes, fabricated devices are classified into two categories. Devices fabricated with the spin coating method are Type I and with drop casting method are named Type II devices. Step geometry is adopted to fabricate Type I devices whereas perforated geometry (bottom digitated source electrode) is adopted for Type II devices.

In the first step, VOFET devices are tested electrically to confirm their I-V curves. Basic testing connections are made by partially removing the polyimide masking from respective electrodes.

4.1.1 Current-Voltage Characteristics

Current-voltage characteristics are plotted by sweeping the drain-to-source V_{DS} voltage for a fixed gate-to-source V_{GS} voltage. Different V_{GS} voltage values are set for each drain-to-source sweep and corresponding output current I_{DS} are recorded. The plot lines shown in Figure 4.1 illustrate the increase in output current with increasing drain-to-source voltage. Both V_{GS} and V_{DS} are negatively biased. Increase in I_{DS} at each increased V_{GS} voltage value indicates p channel (holes charge carriers, i.e. positive charge) accumulation type OFET. It is observed that the VOFET is operating in the linear region which is influenced under short channel effects. The output characteristic curves do not follow the normal trends analogous in lateral OFET transistors. The curves are unable to achieve the saturation and follow the linear trend. The presence of non-idealities, short channel SCLC effects cause the device to operate in non-saturated mode of operation. Device parameters are difficult to extract since the short channel effects are dominating at the interfaces of metal/semiconductor, thus affecting the charge injection process. The SCLC effect will be discussed in detail in Chapter 5.

Deviation from gradual channel approximation and lack of current saturation can be observed in the output characteristics during V_{DS} sweep [88]. In a normal practice for a long channel lateral OFET, the gate electric field is perpendicular to the drain field and much stronger. This results in gradual channel approximation and thus curves attained saturation. But in short channel OFETs, the space charge limited bulk current prevents the curves attaining saturation and the device operation mode is linear [89]. To achieve saturation in short channel

devices, the dielectric should be thin enough to meet the channel length condition as $L > 10 d_{dielectric}$ [90].

The transfer characteristic is plotted by sweeping V_{GS} and the corresponding I_{DS} are recorded for a fixed V_{DS} voltage. The current-voltage characteristic plots are more or less different from conventional lateral type OFET devices because of the vertical design and the presence of short channel effects. The unconventional trends in the I-V plots of VOFETs are on the expected line in vertical geometry [54, 55, 91, 92].

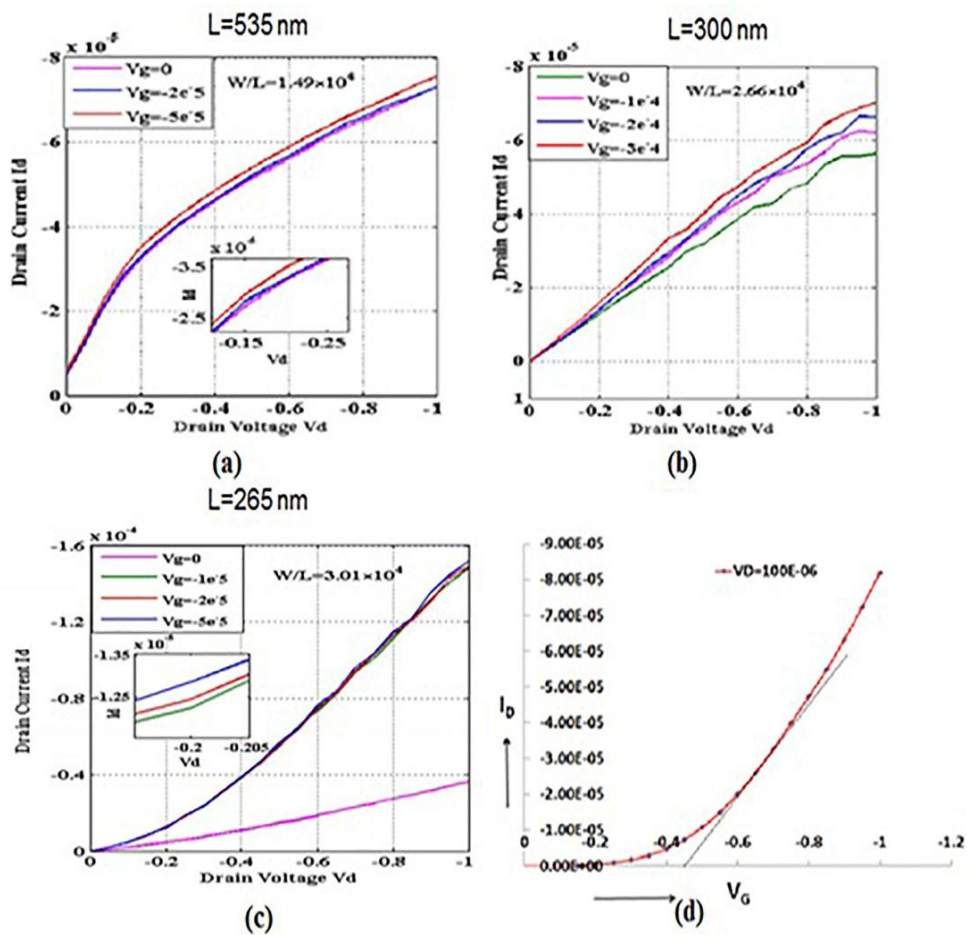


Figure 4.1 Current-voltage (I-V) output characteristic plots at various channel lengths. (a)-(c) at $L=535$ nm, 300nm and 265nm and (d) transfer characteristic curve.

The closely placed plot lines show the weak effect of the gate field and inability of the device to operate in a gradual channel approximation mode. The channel formation occurs only near the step edge of the source electrode, as shown in Figure 4.1(a). Non-uniformity and the weak strength of gate field could be one of the reasons behind the closely placed curves because the gate is more near to the source than the drain electrode. In addition, the shielding effect offered by the source electrode could also be responsible for low gate field effects.

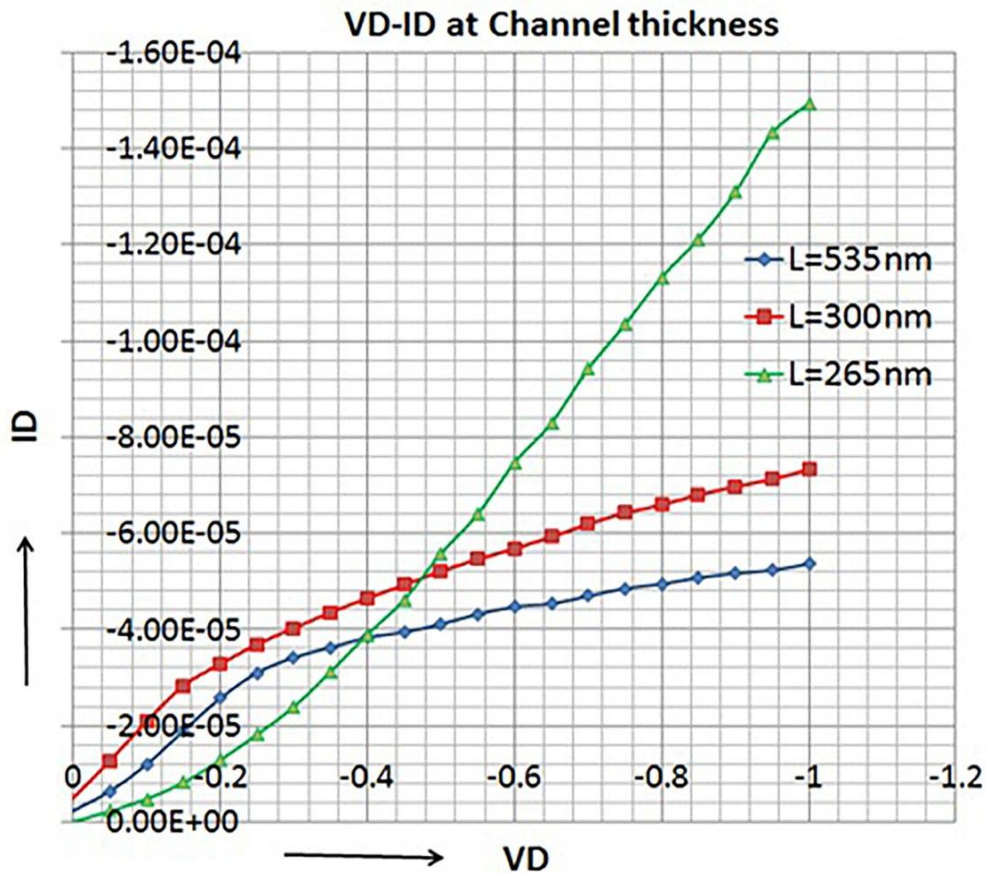


Figure 4.2 Output characteristic plots at three different channel lengths elicited short channel at L=265nm (green line).

The gate field is more effective at the edge of the source electrode where the charge injection/extraction occurs, referred to as the ON region, and the shielded part of the active layer

sandwiched between S/D is referred to as the OFF (leakage) region of the device [93]. Charge accumulation takes place near the step edge, which is extracted by vertical drain field, thus contributing towards the vertical channel formation.

In device parameter optimization, channel length is an important design consideration in VOFET that predominantly influences the operation and characteristics of the device. To study the effect of channel length on the I-V plot, three channel lengths are selected, i.e. $L=535\text{nm}$, $L=300\text{nm}$ and $L=265\text{nm}$. The output characteristics are recorded for each channel length, as shown in Figure 4.1. The bending of the curves (towards more linearity) is observed (with the reduction in channel length) as moving from $L=535\text{nm}$ to $L=265\text{nm}$. The effect of channel length on the device characteristics can be clearly observed from the output plot. The factors involved in bending of curves will be discussed in Chapter 5. To further optimize the VOFET device structure, I-V characteristic plots are recorded for Type I (spin coated method) and Type II (drop cast method) devices separately.

Table 4.1 Device parameters of two types of devices fabricated by spin coating and drop casting techniques.

Device	Type I	Type II
Geometry	Step structure	Patterned electrode
Method	Spin coating	Drop casting
Insulator	SU-8	PMMA
Channel Length	265nm	$2\mu\text{m}$

Efforts are made to design, fabricate and test the devices for patterned (perforated source electrode) and unpatterned (step geometry source electrodes). The spin coating deposition technique is adopted for step type geometry (Type I), whereas the drop casting technique is adopted for patterned (Type II) devices. Figure 4.3 shows the geometries and deposition methods adopted for device fabrication. The method discussed so far is related to the Type I device fabrication process (with spin coating technique), whereas step geometry is adopted to design the source electrode. Figure 4.3 (d) shows the transfer characteristic curve of the VOFET device.

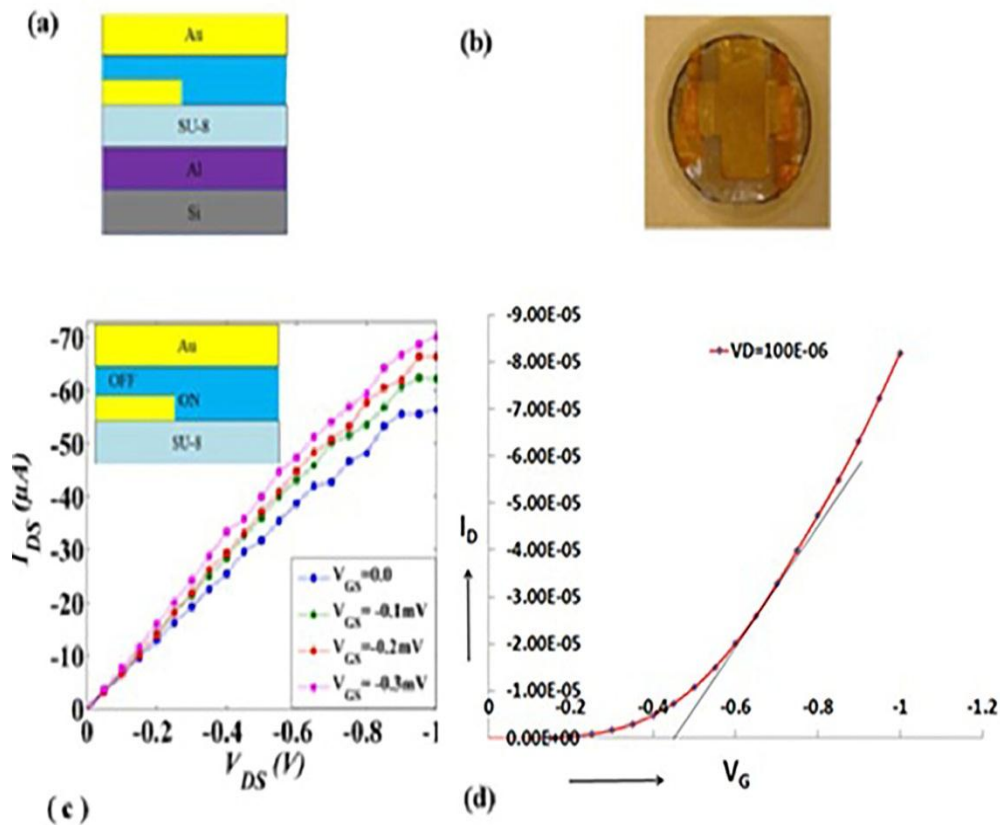


Figure 4.3 Type I devices (a) device layout (b) picture (c) I-V plot at $L=300\text{nm}$ and (d) transfer characteristic curve.

In order to study the effect of source geometry, Type II devices (drop casting method), are fabricated with the patterned source electrode. In Type II devices, perforation in the source electrode is introduced to get the complete field effect from the bottom side. To compensate the short channel effect and to get the effective gate field, two methods are employed in Type II devices.

Perforation geometry of the source electrode is used to get the bottom gate field effect and drop casting is used to reduce the SCLC effect by depositing thick films.

Width/Length (W/L) ratio is an important device parameter, which is directly related to the output current. In a perforated source electrode, both length and width of the source electrode extends and hence the W/L ratio increases. The source electrode perforation thus reduces the SCLC effect and curves show little separation and bending.

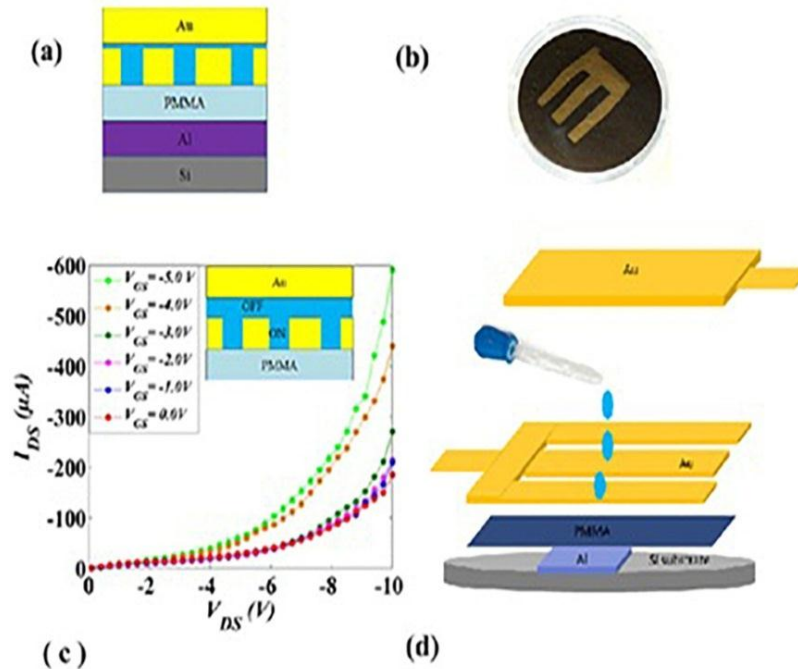


Figure 4.4 Type II devices (a) device layout (b) perforated source electrode (c) I-V plot at $L=2\mu m$, and (d) drop casting process.

As discussed earlier, in order to reduce the short channel effects, the drop casting technique has been introduced. The channel length measured for Type II devices is $L=2\mu\text{m}$. The output characteristics recorded for Type II devices clearly demonstrates the effect of the gate field, as shown in Figure 4.4. The role of the patterned electrode is also an important dimension in understanding VOFET operation. As the perforated source electrode is influenced under the combined effects of drain and gate fields, so the change in design of the source electrode reduces the shielding effect and consequently the output current, as depicted in Figure 4.4.

To confirm the SCLC effect, current densities are plotted against the normalized V_{DS} field. An increase in current density observed at lower channel length, i.e. $L=265\text{nm}$, confirms the presence of the SCLC effect. In the SCLC equation (inset), the power of V_{DS} for $n>2$ is calculated for lower channel devices [94]. The space charge limited current effect is dominating at the nanoscale channel length. The SCLC effect not only affects I-V plots and drives the devices towards non saturation, but also affects device performance. Consequently, devices are influenced under SCLC effects and are confirmed, as shown in Figure 4.5.

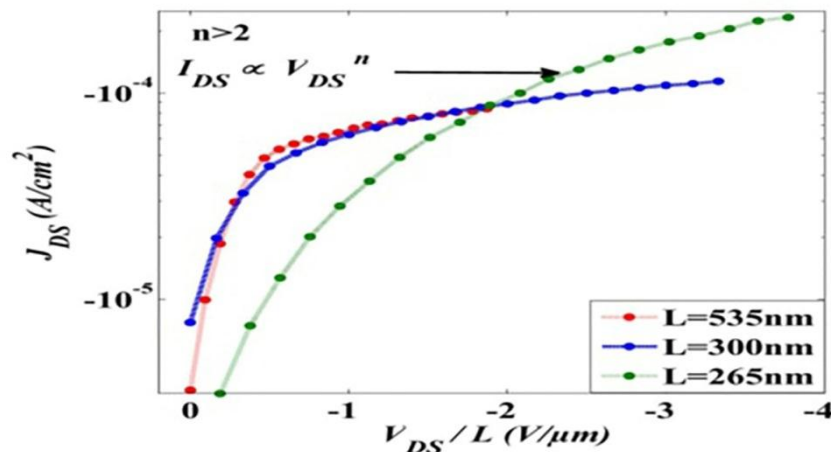


Figure 4.5 Current density Vs V_{DS} plot for $L=265\text{nm}$ channel length depicts SCLC effect at $n>2$.

4.1.2 Capacitance-Voltage Characteristics

Capacitance-voltage characteristic tests are performed to understand the inbuilt device capacitance during fabrication. VOFETs are tested to measure device capacitance and the width of depletion layer at the insulator/semiconductor interface by varying the bias voltage from -3V to +3V. Traps and defects are very common in organic semiconductors. At every step of bias reversal, the charging and discharging of traps takes place. The charging of traps and localized states, changes the device capacitance. Capacitance dependence on frequency reveals the localized states of pentacene and also helps in calculating charge carrier concentration and the width of depletion layer. In the accumulation region, study of capacitance dependence on frequency can be helpful to extract the device parameters, such as mobility, contact resistance and carrier concentration [95]. Quasi-static capacitance-voltage (C-V) measurements are made on a HP4284A LCR precision meter for experimentally estimating the intrinsic capacitance and charge carrier concentration. Au/pentacene contacts exhibits the Schottky barrier, which constitutes the depletion region near the interface. The capacitance-voltage plot reveals that a depletion region exists at the organic/insulator interface and width of depletion changes with a sweep from -3V to +3V. It has been observed that the capacitance is larger at the negative bias end due to the presence of initial interface charges. Capacitance reduces with forward bias due to charge neutralization and increases further with the charging of traps.

Figure 4.6 shows the C-V plot at various frequencies ranging from 100Hz to 60 KHz. A Mott-Schottky plot, i.e. $1/C^2$ -V, is used to extract the trap carrier concentration [96].

$$\frac{1}{C^2} = \frac{2(V_{diff} - V)}{A^2 q \epsilon_0 \epsilon_p NA} \quad (1)$$

where C is the capacitance, A is the geometrical area, q is the electronic charge, NA is the carrier concentration, ϵ_p is the relative dielectric constant of pentacene ($\epsilon_p=3$), and V_{diff} is the diffusion potential, which is extracted from the extrapolated intercept of the $1/C^2$ - V plot. From the slope of $1/C^2$ Vs V , V_{diff} is calculated, i.e. $V_{diff}=1.15$ volts. NA is calculated using eq (1), which comes out to be $NA=3.1 \times 10^{21} \text{ cm}^{-3}$. The width of the depletion layer w is calculated by using the following expression

$$w = \sqrt{\frac{2\epsilon_0\epsilon(V_{diff} - V)}{qNA}} \quad (2)$$

By substituting NA and V_{diff} , the value of w is calculated to be $w=55\text{nm}$ at zero gate bias.

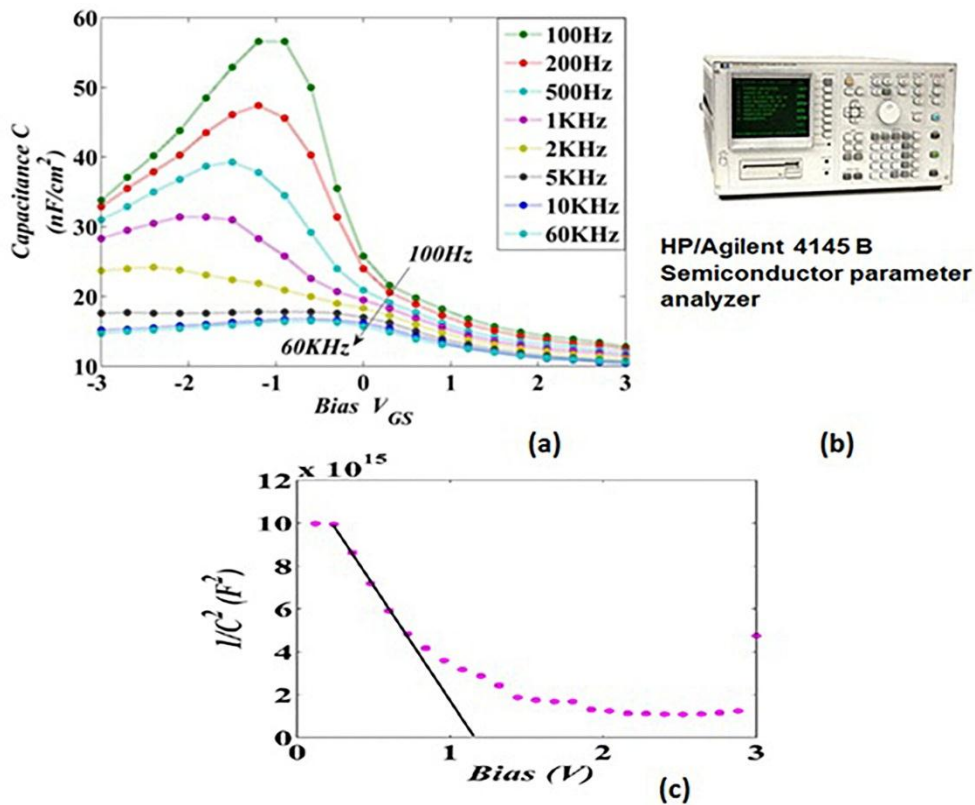


Figure 4.6 C-V plot of VOFET device (a) at frequencies ranging from 100Hz to 60 KHz (b) spectrum analyzer (c) Mott-Schottky plot i.e. $1/C^2$ - V .

4.1.2.1 C-V Analysis

The capacitance-voltage plot of the MIS structure is usually studied for analyzing semiconductor surface, interface, and bulk material behavior. The Quasi static (low frequency) capacitance of the layered device structure is measured by sweeping from +ve to -ve bias. In another device design where PMMA is used as an insulator, C-V plots are recorded, as shown in Figure 4.7. Capacitance-voltage plots show the accumulation to depletion profiles. Internal device capacitance increases as the biasing trends changes from negative to positive.

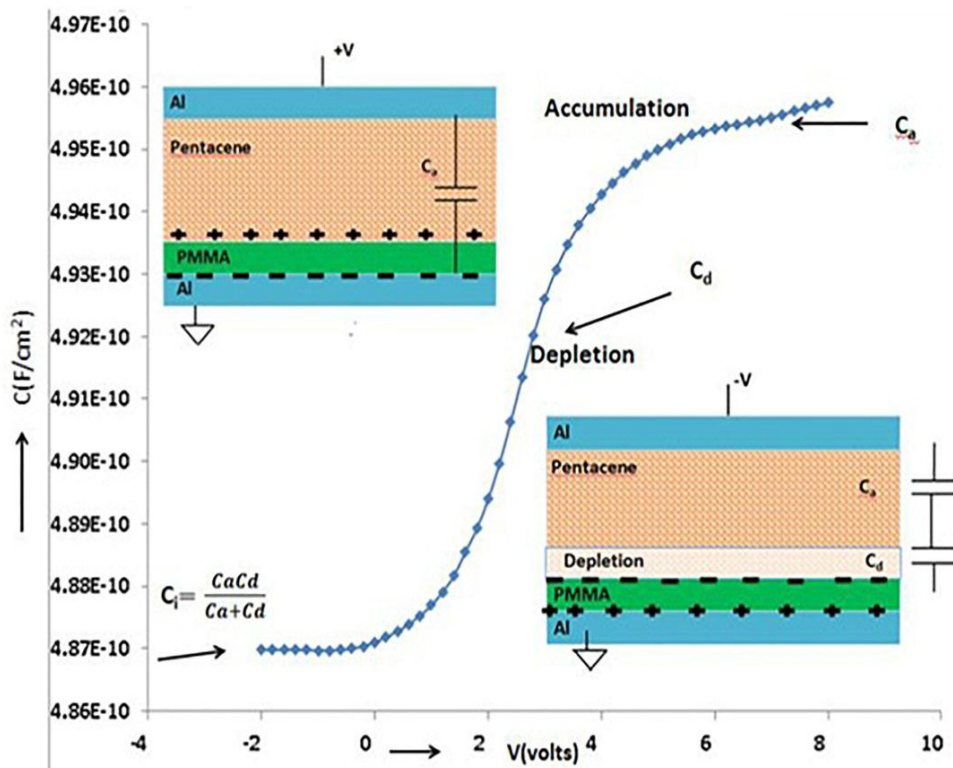


Figure 4.7 Quasi-static C-V plot of Type I device elicited the accumulation and depletion regions.

When the positive voltage is applied, the charge carriers start accumulating at the PMMA/pentacene interface resulting in accumulation capacitance (C_a). As the biasing reverses from +ve to -ve, the charges start building at the PMMA/pentacene interface. The accumulated

charge depletes the pentacene and introduces an additional depletion capacitance (C_d), which results in a series with the total device capacitance. Thus, total series capacitance (C_i) reduces due to series depletion and accumulation capacitance, as shown in Figure 4.7. Flat band voltage V_{FB} and threshold voltage V_T can be extracted from the C-V plot.

4.1.3 Transient Time Analysis

In high frequency applications of OFET, an important switching parameter is the transient behavior of charge carriers, which helps to understand the charge propagation through the channel. Switching speed of the device is expected to increase when the channel length is reduced, as shown in equation (3). The time of flight (TOF) experimental technique is employed to study the carrier's propagation through a 350nm channel length OFET. In a vertical device, time of propagation is studied as a function of applied voltage.

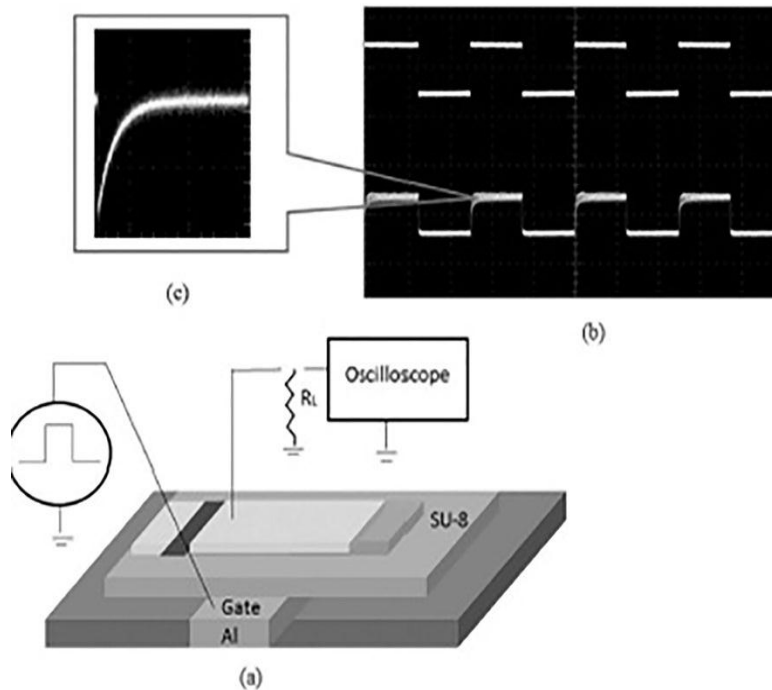


Figure 4.8 Time of flight (TOF) experiment setup (a) circuit layout (b) applied input pulse (up) and recorded output (below) (c) pulse delay.

The transient analysis experiment is designed and performed by supplying a square pulse of 1volt amplitude/1 KHz to the gate electrode and the corresponding drain current is measured, as shown in Figure 4.8. The rise time (including 90% of response) is calculated, i.e. rise time=36ms. Thus, transient time is calculated from the expression given in the equation below as

$$t_r = \frac{L^2}{2\mu(V_{GS} - V_T)} \quad (3)$$

where V_{GS} and V_T are gate-source and threshold voltages, respectively. By substituting the device parameters, in equation (3), transient time is calculated, i.e. $t_r = 12\mu s$. Material transport properties and contact resistances are the factors contributing towards transient time.

4.1.4 Resistivity Measurements

In short channel devices, the contact resistance dominates the channel resistance and contributes towards SCLC currents. The influence of interface resistance plays a dominant role in OFET performance.

Since the width is larger than the channel length, the total resistance is normalized with the width and can be expressed by the following equation as

$$R_{ON} W = R_c W + R_{sheet} L \quad (4)$$

where R_C is contact resistance and R_{ON} is the total ON resistance, which is calculated from the linear region by dividing V_{DS} with I_{DS} at different V_{GS} values.

The four-probe resistivity method is employed to measure sheet resistivity, as shown in Figure 4.9. To extract the channel (sheet) resistance, the four-point probe technique is used for measuring R_{sheet} , which is calculated as $R_{sheet} = 6.79k\Omega/sq$.

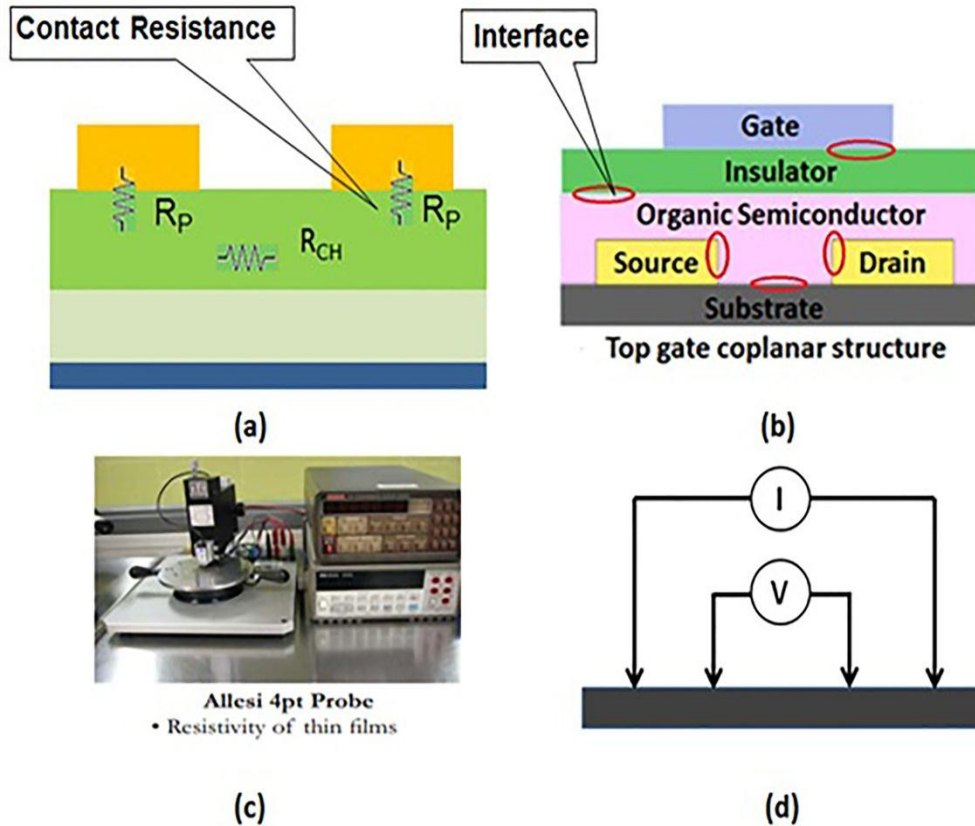


Figure 4.9 Contact resistance (a)-(b) parasitic and channel resistance (c)-(d) four probe set up and circuit connections.

The contact resistance R_C is calculated as $R_C=15.99k\Omega$. The sheet resistivity can be expressed in terms of mobility of charge carriers.

4.2 Surface Metrological Characterization

At the nanoscale level, surface roughness and mismatch interfaces play an important role in an estimation of device parameters. In a multilayer device such as a VOFET, charge transport is affected predominantly by the surface roughness and non-uniform interfaces. Interface engineering is normally seen in practice for minimizing surface effects. In the VOFET fabrication process, an intermediate phase of surface metrology characterization has been introduced before the final device fabrication. The main idea behind this is to test for pentacene material after the conversion process. The basic surface morphological tests are performed at the

precursor to pentacene conversion stage. This is named as phase II of the device fabrication stage which is created to confirm the conversion process. At this stage, multiple surface metrology tests are performed before moving forward to the final stage of device fabrication. In metrology characterizations, three basic levels of testing are performed, most notably at the surface level, molecular level, and atomic level. The tests performed at this stage are as follows:

- Transmission Electron Microscopy (TEM)
- Atomic Force Microscopy (AFM)
- Scanning Electron Microscopy (SEM)
- Raman Spectroscopy
- X-RD

4.2.1 Transmission Electron Microscopy

In the transmission electron microscopy technique, a beam of high energy electrons is exposed and allowed to transmit through the sample. The interacted and transmitted electrons form an image of the exposed area.

The TEM technique is employed to confirm the crystal formation of pentacene material immediately after thermal treatment. Samples for the TEM tests are separately prepared from the actual VOFET device. A chemical solution of pentacene precursor is prepared and dropped over the TEM sample holding mesh. The sample holding mesh is shifted over the preheated hot plate (200°C) and treated thermally for 1 minute. Then, the copper mesh holder is removed after heating the sample at $200^{\circ}\text{C}/1\text{min}$. The sample holder micromesh is cooled down and handled very carefully before processing for TEM imaging. The scanned TEM image of pentacene material is taken immediate after the annealing process. The TEM image confirms the formation of pentacene crystals, as shown in Figure 4.10.

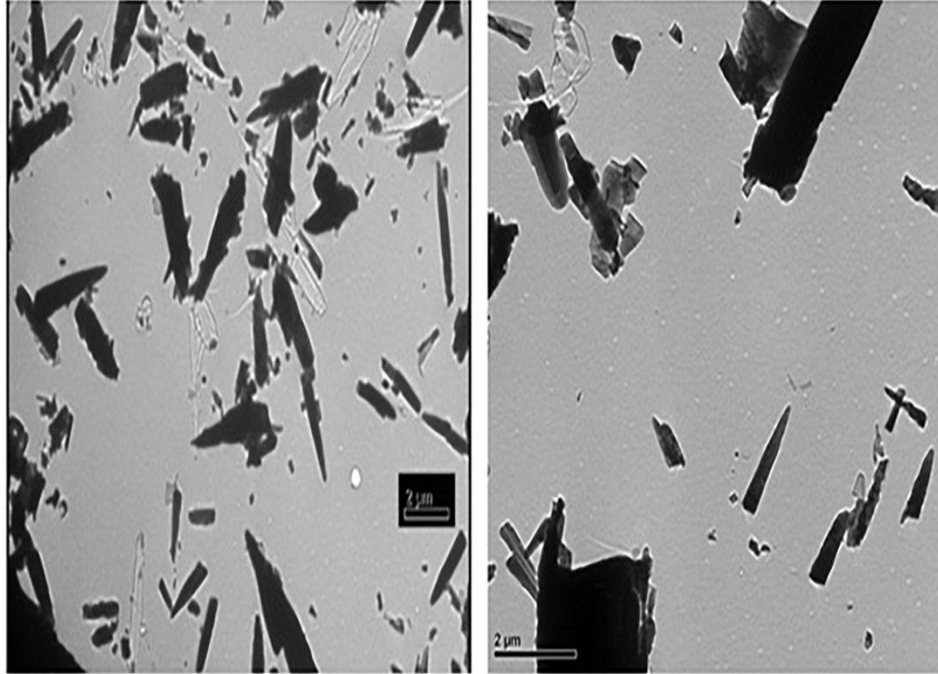


Figure 4.10 TEM images reveal formation of pentacene crystal size and grain boundaries.

4.2.2 Atomic Force Microscopy

Atomic Force Microscopy (AFM) is a scanning microscopy technique used to image and manipulate the matter at the nanoscale level. The AFM probe tip senses the atomic forces of the material surface at the nanoscale and generates the image accordingly. AFM scans are performed over a thermally treated pentacene precursor to confirm pentacene conversion, surface roughness, and grain boundary formations.

The performance of an OFET depends on the surface roughness, as the charge transport is confined to the first few mono layers of the organic channel. It is observed from the scan that the pentacene growth is disordered for roughness more than 0.3nm. In normal practice for a solution-processed pentacene, dendritic growth with less uniformity has been observed [97]. Figure 4.11 shows 3D AFM images which are scanned over a $4\mu\text{m} \times 4\mu\text{m}$ area that shows root mean square (rms) roughness of 67.3nm and a mean image roughness of 55nm.

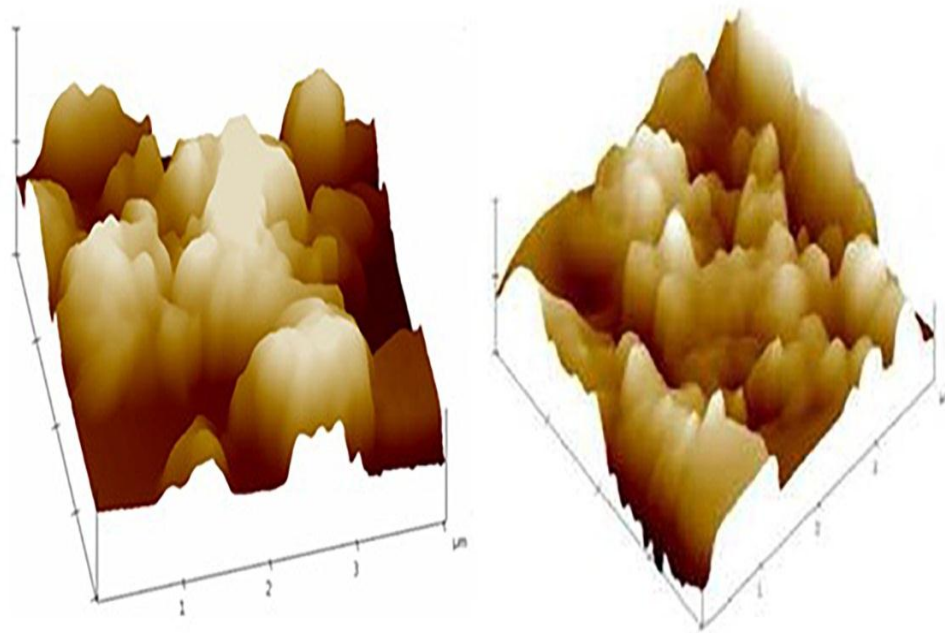


Figure 4.11 AFM image (left) dendritic growth after precursor annealing (right) fully converted pentacene.

In lateral charge movement, it's challenging to compensate the surface roughness, whereas in vertical charge movement, vertical thin channel compensates for the non-uniformity and roughness of film. AFM images are scanned for two different thermally treated samples at $200^{\circ}\text{C}/1\text{ min}$ and $170^{\circ}\text{C}/10\text{min}$. as shown in Figure 4.11.

The Phase image of AFM is used to map the two different materials present in the sample. It monitors the phase lag between the oscillating signal and output signal and creates a phase image. AFM phase images are scanned to confirm the pentacene material and the substrate material, as shown in Figure 4.12. Optimization of time-temperature balance in the thermal treatment plays an important role in deciding grain size of pentacene and its nanostructure. The grain size area measurement of ordered grain (in red) and the average grain (in black) are demonstrated in the AFM grain scan, as shown in Figure 4.13.

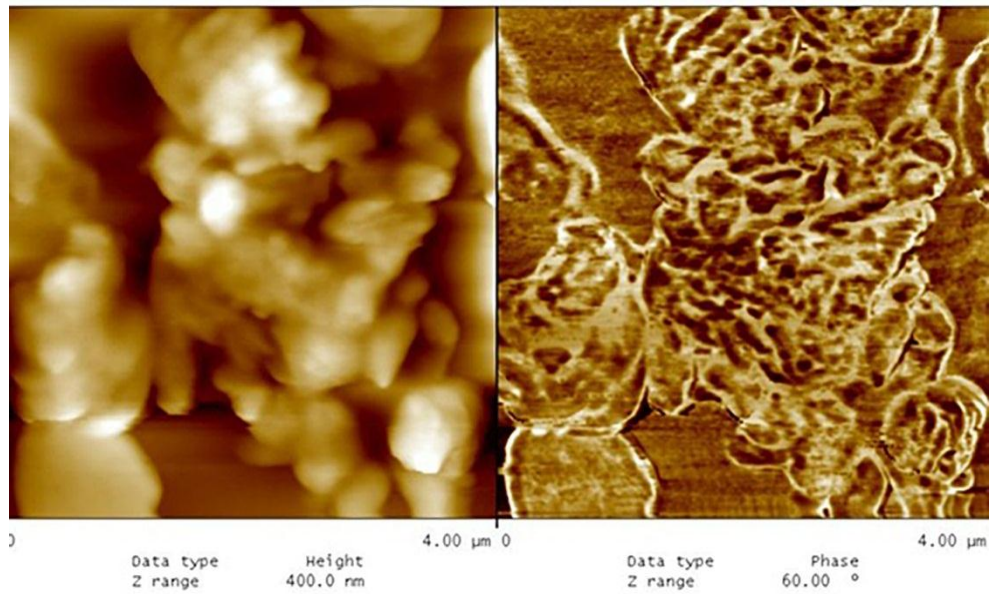


Figure 4.12 AFM height (left) and phase (right) images of pentacene after thermal treatment.

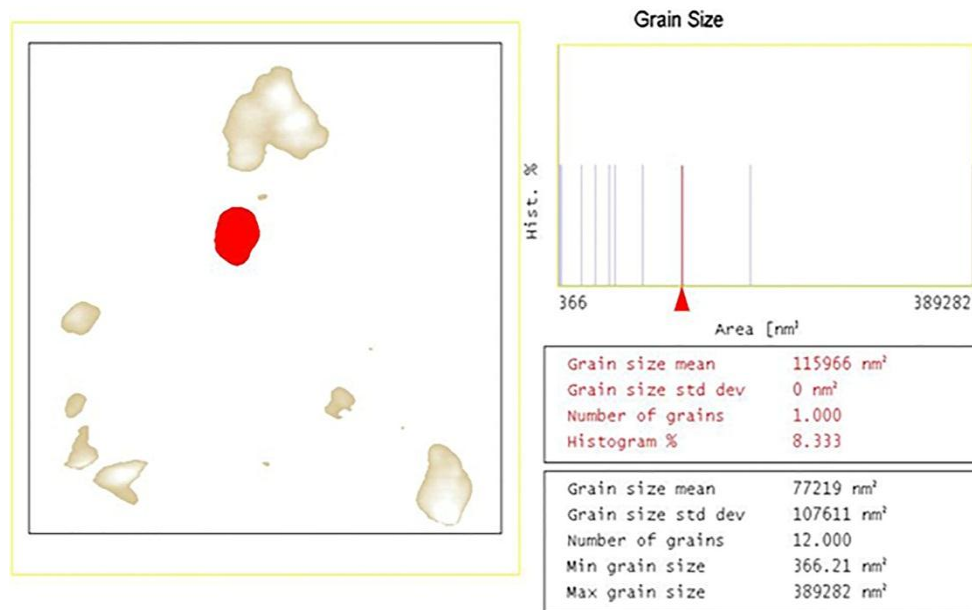


Figure 4.13 Mean (red) and average (black) grain size of pentacene recorded after conversion in AFM surface analysis.

4.2.3 Scanning Electron Microscopy

Scanning electron microscopy is a technique used to analyze the surface morphology by exposing a focused beam of electrons that interact with the atoms present inside the material. The beam of electrons interacts and received back to the detector, creates the image of the sample topography. For a VOFET device, the SEM image is scanned to confirm the deposited material layers. The sample under test for SEM analysis is diced at an angle and mounted as slanted to scan a side view. The focused electron beam is exposed on the side of the device edges. The layered VOFET device under test for SEM is a half-complete device up to the source (Au) electrode layer. Figure 4.14 shows the SEM image of stacked material layers in a VOFET device where SU-8 is deposited under the Au material.

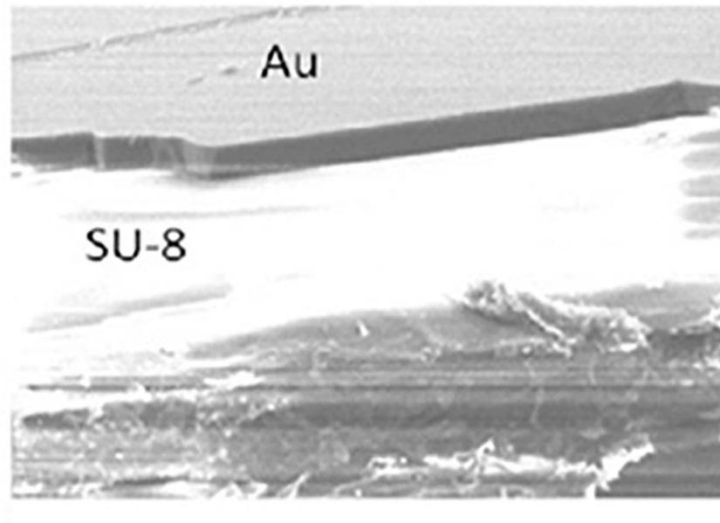


Figure 4.14 SEM image of deposited material layers elicited SU-8 insulating layer under the Au metal electrode.

4.2.4 Raman Spectroscopy

Raman spectroscopy provides unique structural information about the material. In Raman spectroscopy, the incident laser light and the scattered light shifts in a frequency which is proportionally to the structure of material. The Raman spectrograph provides this shift

information which is unique for every material. The molecular structure is an important factor in determining material property, which controls the charge carrier mobility and device performance in electronic devices. In solution processed OFETs, the interfacing between the active material uniformity with dielectric material layer results in molecular orientations. Raman spectroscopy is an important molecular mapping technique to analyze at the molecular level. This technique is useful to map local arrangement backbone orientations in the case of solution processed pentacene devices.

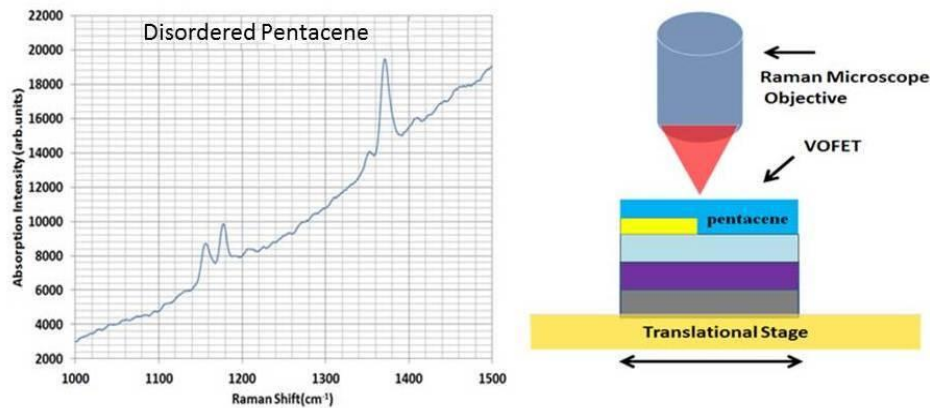


Figure 4.15 Raman spectroscopy measurement (left) and schematic representation of a Raman spectra (right).

The Raman technique is non-destructive, compared to other structural analysis methods like FT-IR and X-RD. It has the advantage of no prior sample preparation and in-situ measurements. In VOFET fabrication and molecular level pentacene confirmation, Raman spectroscopy is performed on the thermally treated pentacene layer after the conversion process, as shown in Figure 4.15. The characteristic peaks are recorded and observed to confirm the pentacene at the molecular level. The scheme adopted for Raman spectroscopy and device exposure is also depicted in the same figure.

A Raman shift is recorded over a less ordered pentacene microstructural thin film [98]. Raman shift is a powerful tool to confirm the microstructural changes in pentacene film. Some researchers reported improvement in device performance after hours of operation, owing to the source-drain electric field, which makes irreversible structural modifications confirmed after Raman measurements [99].

4.2.5 X-Ray Diffraction

The X-RD method is a very useful tool to identify the atomic and the molecular structure of a material. By measuring the angles and intensities of a diffracted beam, the three dimensional picture of a material and the corresponding electron densities can be identified. The X-RD method is used to confirm the pentacene material conversion at the atomic level by detecting the characteristic peaks.

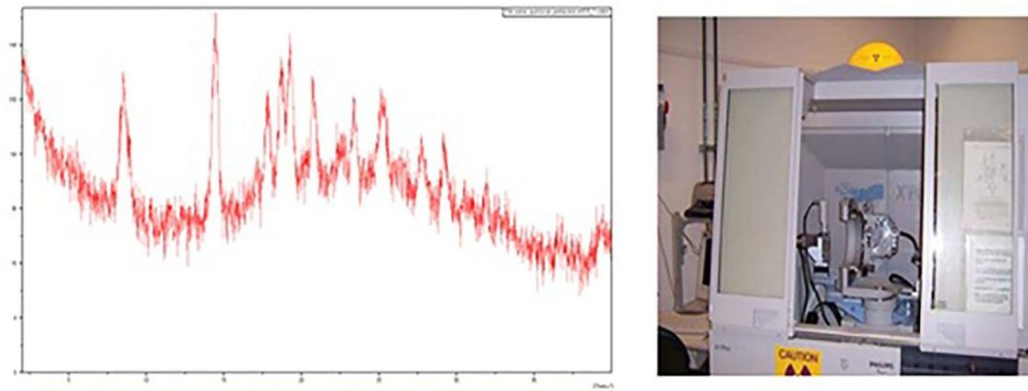


Figure 4.16 X-RD measurement (left) X-RD plot (right) diffraction system facility.

Sample for X-RD tests are prepared particularly to test the pentacene confirmation immediately after thermal treatment. A thin film of precursor is spin coated on a glass slide and treated thermally at 200°C/1 min. The sample is removed from the hot plate and then tested for X-RD characterization. Unlike Raman spectroscopy, which is used to test material at the molecular level, the X-RD technique is used to confirm material at the atomic level. Figure 4.16

shows the X-RD image of the pentacene material scanned after thermal treatment. The peaks in the plot are confirmed in the literature for the pentacene material [100].

4.3 Radiation Sensor Test

In biomedical implants, any electronic device which is considered for biological signal recordings has to prove the biocompatibility and radiation test. Keeping this in view, the VOFET devices are exposed and tested under radiation. Pentacene-based organic VOFET devices are fabricated and tested as radiation sensors by exposing them under low dose radiations. VOFET I-V characteristics are recorded after each level of irradiated doses. Three incremental steps of calibrated radiation doses (each of 5 Gy increment) are set to irradiate over the set of devices. The change in I_{DS} current is recorded after each exposure. A decrease in output current is observed with the increase in radiation dose, as shown in Figure 4.17.

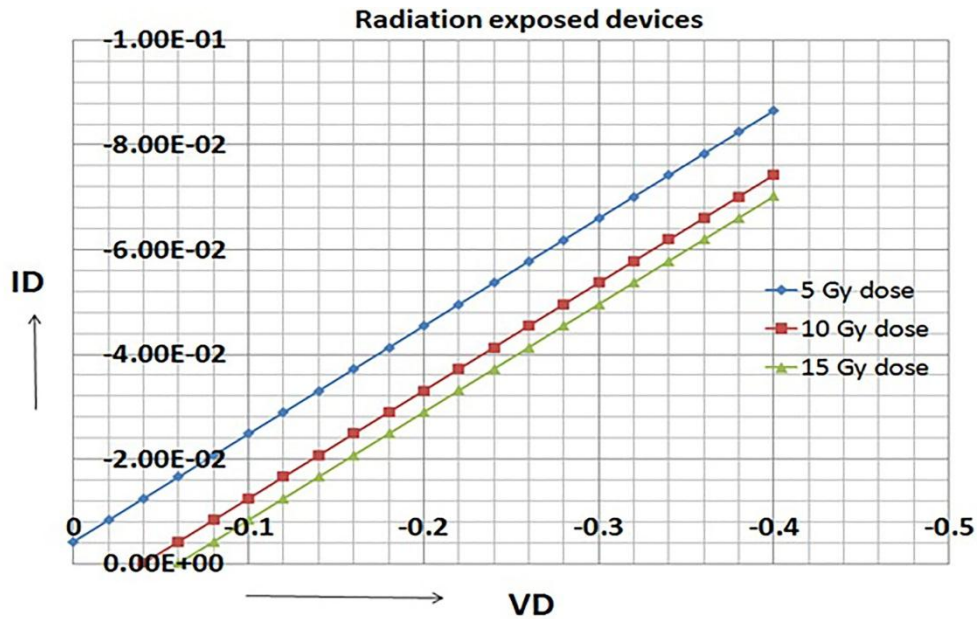


Figure 4.17 I-V plot of a VOFET resistive radiation sensor. Radiation absorption shifts elicited at every 5Gy dose increment.

In this experiment, VOFET is used as a two terminal resistive element, thus no gate voltage is supplied. Considerable changes in current are observed after exposure.

Characteristics are measured after each step of exposure, since there is no in situ facility available to record the I-V characteristics immediately after the exposure.

The characteristic feature of the VOFET system and geometry allows its application to biomedical fields. The interface of biological systems with electrical or optical sensors is highly viable. In cardiac sensor applications, the coupling of a VOFET with a flexible substrate allows for advanced detection and identification of cardiac signals with precision. For optical sensing and measurements, such as in digital pathology, the imaging and processing of cancer detection allows for advanced imaging applications. In the following sections a description is provided in each of the biomedical areas.

4.4 Flexible Cardiac Sensor

The heart is a sophisticated organ in the human body that works continuously to pump pure blood into various parts of the body. Irregular heartbeats or arrhythmias are the most common cause of sudden death in athletes [101]. Cardiac Resynchronization Therapy (CRT), evolving from pacemakers and development of ICD, has been adopted as a non-pharmacological treatment of important therapeutic value for cardiac patients. The design of the conventional ICD device is very robust and consists of a metallic case and a lead system. The overall structure and operational criteria for pacemakers and ICDs has not been changed much. Whereas significant changes have occurred in the commercially available CRT defibrillator with advancement on both the clinical and technical side, the design side still needs a lot of improvement.

4.4.1 Implantable Cardioverter Defibrillator

The ICD is a biomedical device implanted inside high risk cardiac patients to deliver the stimulation or defibrillation pulse at the onset of arrhythmia. Commercially available cardiac

resynchronization therapy-defibrillation units (CRT-Ds) are very bulky in size. The ICD device consists of a palm-sized metallic case and a set of leads that are inserted into atrial and ventricular chambers of the heart. The metallic case of the ICD is comprised of two parts, namely pulse generator and the device battery. The ICD leads consist of silicone flexible rubber with polyurethane to identify arrhythmia, i.e. the detection of bradycardia (slow beat) and/or tachycardia (fast heartbeat). The lead system in an ICD primarily serves as a source to detect arrhythmia.

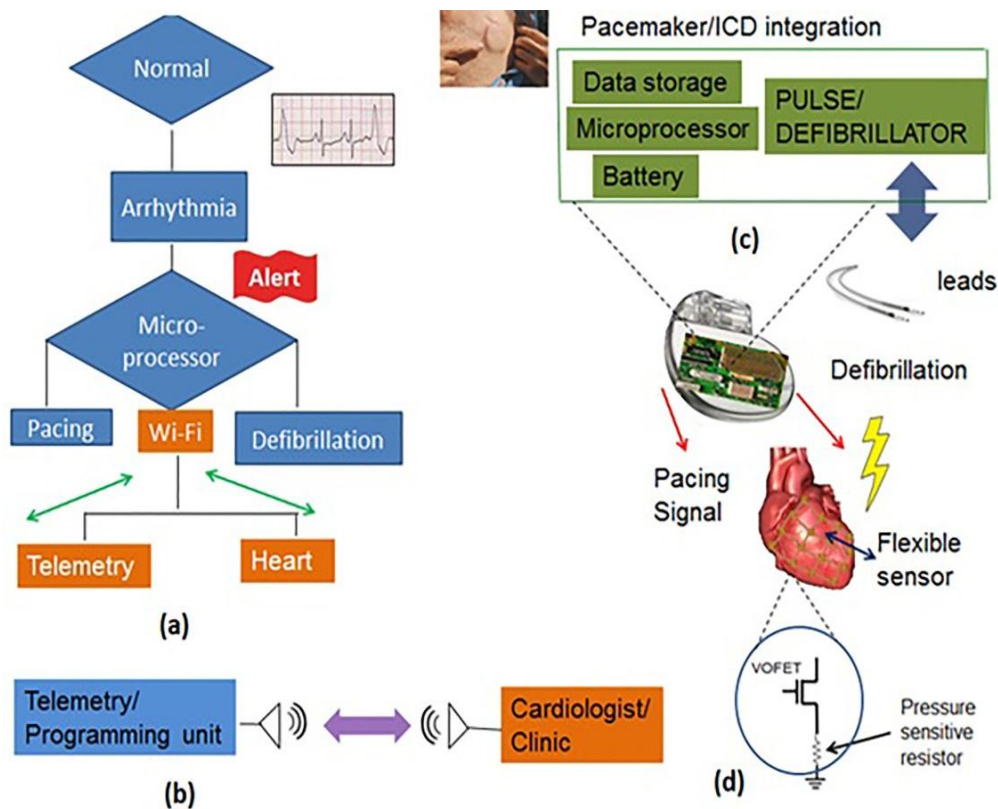


Figure 4.18 Schematic representation of OFET flexible sensor integration. (a)-(b) algorithm flow chart and ECG monitoring (c) internal architecture of ICD (d) flexible sensor.

The microprocessor collects abnormal heartbeat information in a localized manner from atrial and ventricular chambers. However, the information collected from the lead system does

not provide specific detail about the site of arrhythmia with high resolution. Therefore, there is a requirement for precision in arrhythmia detection and defibrillation. The proposed idea is for flexible wireless sensors to be incorporated into the ICD device. This approach would be a step forward towards a new generation of ICDs with complete information of arrhythmia and real time ECG monitoring.

For measuring cardiac signals from the outer surface of the heart, integration of a flexible sensor within the conventional ICD device has been proposed, as shown in Figure 4.18. In the proposed idea, arrhythmia detection and defibrillation are the focus areas. There could be a dual route for pulse delivery, either through ICD leads or through a sensor array based on the site of the arrhythmic activity. This novel idea of integration of a flexible sensor array with current ICDs would allow for a stretchable bio-electronics interfacing system.

Figure 4.18(a) shows the complete working concept to integrate signal detection and processing to allow defibrillation or pacemaker activity utilizing the flexible sensor technology. As shown in the algorithm, the arrhythmia signal will be detected by the flexible sensor at the surface of the heart, and this information will be relayed to the ICD microprocessor for analysis and identification of the arrhythmic event for delivery of pulse. The smart algorithm of the microprocessor decides whether it is a pacing or defibrillation problem. Figure 4.18(b) shows the proposed real time monitoring of the ECG pattern of high risk patients and at the same time this information is transmitted to health providers. Figure 4.18(c) describes the internal architecture of ICD which includes battery and pulse generator (hardware and electronics). ICDs are bulky in size because more than 50% of the space is occupied by the battery. Reduction in battery size would be another addition towards device miniaturization. Figure 4.18(d) shows the OFET sensor network wrapped around the heart to sense the arrhythmia and for the delivery of

defibrillation pulses. The sensor network is made up of OFETs, as shown in the zoom part of the sensor array. The flexible sensors could be designed out of stretchable materials on flexible substrates.

4.5 Imager for Digital Pathology in Breast Cancer Analysis

In clinical practice, Nottingham grading is the standard scoring system for tumors. Assessment is based, in part, on irregular nuclear pleomorphic features like shape, size, color, and intensity of individual cells. Computationally differentiated and classified nuclei enhance the assessment of diagnosis and grading. Cancer cell detection and separation is important for the accurate scoring of malignancy. Automated image analysis and scoring can deliver accurate results. Grading of cancer cells from a highly resolute histopathological image can minimize the chances of error for scoring, and thus, a better prognosis. The Artificial Neural Network (ANN) classifier's constant learning ability and nonlinear parallel processing can more accurately predict prognosis in cancer. ANN classifier is tested for optimal combinations of training, validation and testing data set with hidden neuron numbers. In a new generation of healthcare solutions for assisting pathologists, a new approach is proposed in diagnostic pathology which is parallel in nature and highly automated to deliver accurate decision.

Breast cancer malignancy scoring is influenced by complex image structure analysis and features extraction techniques. The nuclear micro texture features extraction and delineation, which is a tedious task, in spite of the detailed tumor information availability from high resolution digital whole slide images [102]. Breast cancer is a morphologically heterogeneous disease for which the grading is assessed by a characteristic trait of polymorphic nuclear and molecular features [103]. Nuclear pleomorphism assesses the mutation in nuclear geometrical features like shape and size with regard to normal epithelial/tumor cell nuclei. Pleomorphic

changes due to activation of oncogene and spatial reorganization of chromatin in cancer nuclei leads to abnormal cell production and tumor malignancy. Tumor malignancy is highly dependable on pleomorphic features of nuclei and further on morphological features for neoplasm aggressiveness and heterogeneity in the physical microenvironment (PME) [104]. The Nottingham grading system (NGS) is a grading system highly used worldwide which scores tumors on the basis of prognostic information [105]. The evaluation of NGS is based on morphological features such as (a) degree of tubule, (b) nuclear pleomorphic features (such as shape and size), and (c) mitotic count. Therefore, a better understanding of diagnostically important factors such as nuclei shape distortion, size irregularity, and heterogeneity can help the pathologist to determine better therapeutic strategies, survival rate estimation, and histopathological characteristics like vascular invasion, gene expression, and precise tumor grading.

A pathologist visually examines hundreds of slides per day under the microscope within the limitation of a human eye (differentiate between hue and intensity in the image) to detect nuclear level changes. Nuclei segmentation is the most challenging task today which requires a highly skilled workforce, and clustering algorithms like K-means, fuzzy C-means, neural networks, and Gaussian mixture models [106]. Imaging informatics, computational segmentation, classification (through automated analysis and machine learning), and grading of pleomorphic nuclei into a high spatial resolution histopathological image eliminates the chances of errors. The Nottingham grading system faces difficulties of lack of precision and agreement among pathologists because of reproducibility of less than 75% accuracy and with limited uses in core biopsies. Therefore, computational analysis is emerging as a second opinion and a reliable tool in assisting the pathologist.

4.5.1 Nuclear Pleomorphism

Changes in the shape and size of the cellular nucleus are referred to as nuclear pleomorphism. In cancer cells, the roundness of the nuclei starts deteriorating with changes in their shape. The degree of disturbance of nuclear features decides the level of malignancy in the cancer tumors. By performing a detailed analysis of the cellular nucleus, the grading of cancer cells is achieved. The Nottingham score is a well-established microscopic grading of breast cancer and is associated with survival of patients, however several groups contend that pathological evaluation alone does not provide enough information to be a reliable prognostic indicator. In order to produce a more accurate prediction of prognosis and response to therapy, there is a need to develop a more quantifiable method for automated image analysis and breast cancer scoring [100, 107].

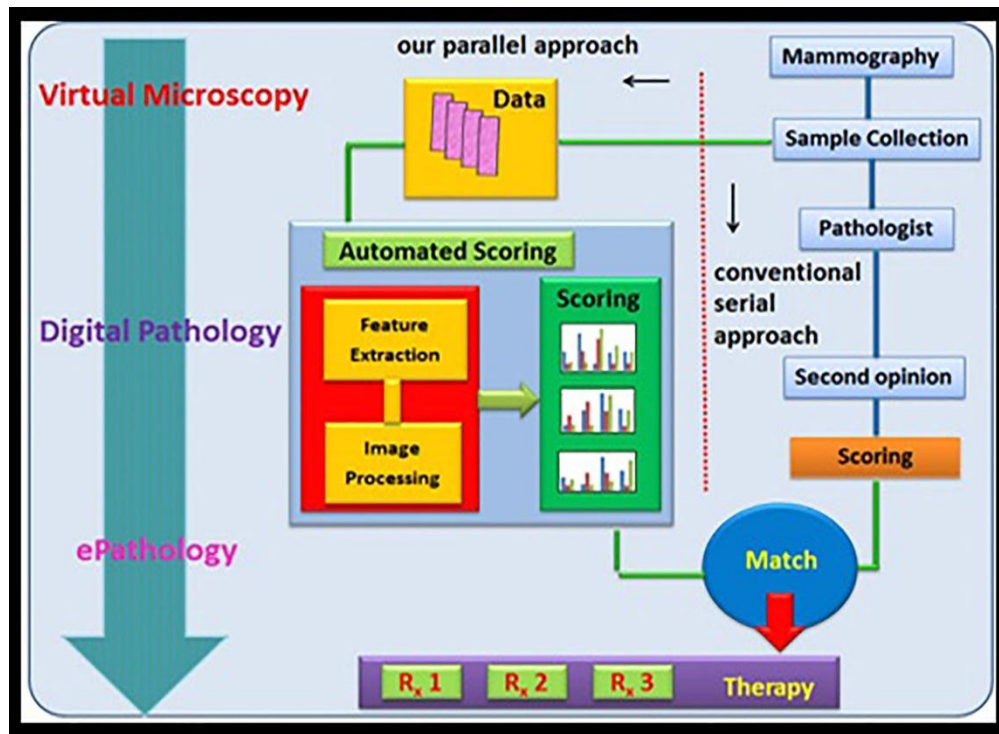


Figure 4.19 Proposed scheme of digital pathology for automated breast cancer scoring system.

A pathologist inspects visually all hematoxylin and eosin (H&E) stained histology slides, which are still considered as the gold standard for cancer diagnosis and grading of malignancy. In the Nottingham Bloom Richardson grading system, tubularity, pleomorphism and mitotic count are evaluated and graded for malignancy. In pleomorphic nuclei grading, the nuclear features like shape, size, roundness, concavity, and area are taken into account while deciding the tumor grading. Pleomorphic features of nuclei are judged as small uniform regular shape, moderate, and marked nuclear variation basis. Irregular boundaries and moderate intensity are the factors causing errors in deciding grade II tumors. The main challenges in diagnosis are the lack of agreement among pathologists and reproducibility in grade II level malignancy.

According to the Nottingham grading system [108], pathologists score nuclear pleomorphism as follows:

- Small nuclei with very little increase in size are graded as type I tumors.
- Cell size larger than normal are graded as type II tumors.
- Significant variation in size and shape, are graded as type III tumors.

The Nottingham Bloom Richardson (NGS) system, in moderate nuclei, i.e. in grade II tumors, with low reproducibility is the source of error which depends on a pathologist's experience and eye interpretation [109]. A machine learning based automated scoring system can reduce chances of errors, save time, and provide a second opinion.

An artificial neural network is an algorithm based on a neural network system to implement the designed mathematical model. It learns from its past experience and errors in a non-linear parallel processing manner. The most popular algorithm is feed forward back propagation (FFBP) [110]. The breast cancer prognostic tools can be designed based on ANN's powerful learning and processing features in a probabilistic and noisy environment. The neuron

is the basic calculating entity, which computes from a number of inputs and delivers one output comparing with threshold value and thus turned on (fired). The computational processing is done by an internal structural arrangement consisting of hidden layers which utilize the back propagation and feed forward mechanism to deliver an output close to accuracy. The learning is based on reinforcement (supervised) and unsupervised (no target) type. The unsupervised mimics the biological neuron pattern of learning. The proposed scheme of digital pathology for an automated breast cancer scoring system is shown in Figure 4.19 .

4.5.2 Experiment Design for Classifier Optimization

Two experiments are designed and performed on MATLAB and NeuroSolutions Inc. Using pattern recognition and a classification tool for breast cancer data analysis, two target values, i.e. benign and malignant tumors, are studied. The data set is pre-loaded under the cancer inputs tab, which represents 9x699 matrix for 699 patients having 9 attributes based on uniformity of cell size, clump thickness, etc. The database is categorical in nature, with dependent variables as predictors for the benign or malignant tumor class.

Experiment I is performed for data classification to test various combinations of hidden neuron numbers by varying training data, validation and out-of-sample testing data percentage. Figure 4.20 shows the optimal results of 97.25 % of accurately classified mean (%) with standard deviation (SD) of 0.478486 at fixed 70% training, 15% validation and 15% out-of-sample independent testing at 15 hidden neurons. The total run is 51 (each) for every set of testing.

Experiment II is performed with a similar number of experimental iterations (runs) by setting two variables, such as the validation (%) and testing (%) data sets. The training (%) data set is kept fixed at 70 % for each 10, 15 and 20 hidden neurons, respectively. The best results

are seen at 97.249%, whose accurately classified mean (%) is in agreement with the pathologist's view about benign and malignant tumors.

MATLAB results from two experiments show that as the training data increases, the classifier accuracy increases along with an increase in the number of hidden neurons from 10 to 15, but it falls slightly as the neuron number changes to 20. The same increasing trend shows at even fixed training (%) data as changed from 10 to 15 neuron, but falls again into 15 to 20 segments. At a fixed neuron number, the Gaussian trend appears as we move from the 60% training data set to 80%, with a peak at 70%.

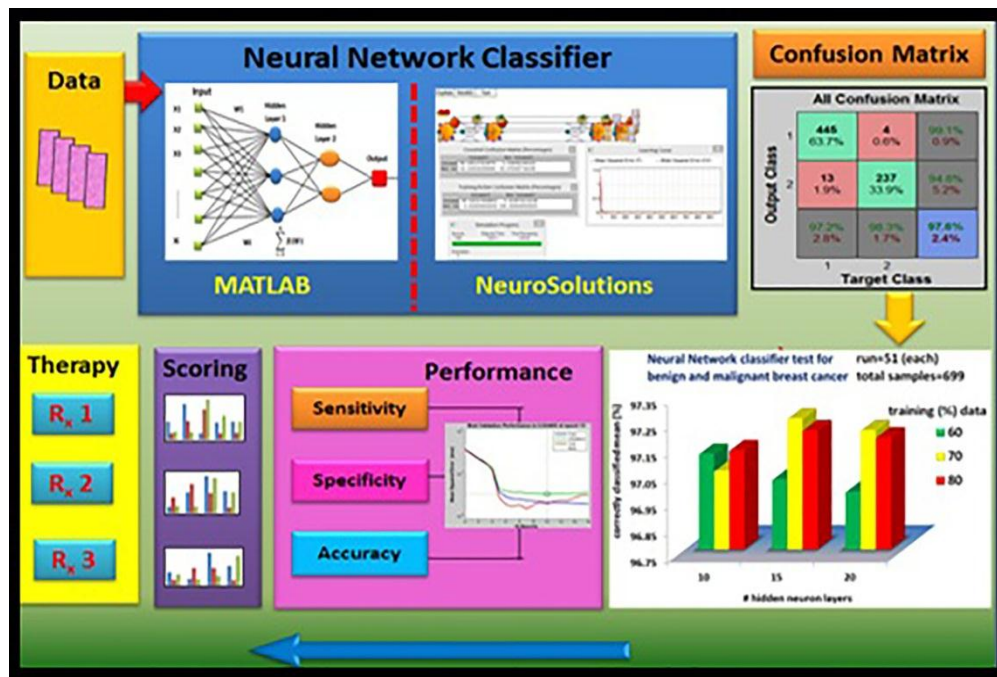


Figure 4.20 Breast cancer data classification results from MATLAB and NeuroSolutions classifier.

An independent test is performed on the NeuroSolutions classifier simulation platform for a different set of parameters. In the NeuroSolutions classifier, data fragmentation of 60% as training, 20% as cross validation check, and 20% out of sample testing are distributed. Under

classifier run for 1000 epochs at an elapsed time of 16 seconds, the results are very encouraging, correctly classified as 99.1 % benign and 100% as malignant on training/active confusion matrix, agreeing very closely with pathologist scoring. On cross-validation window, 98.1 % data is correctly classified as a benign tumor.

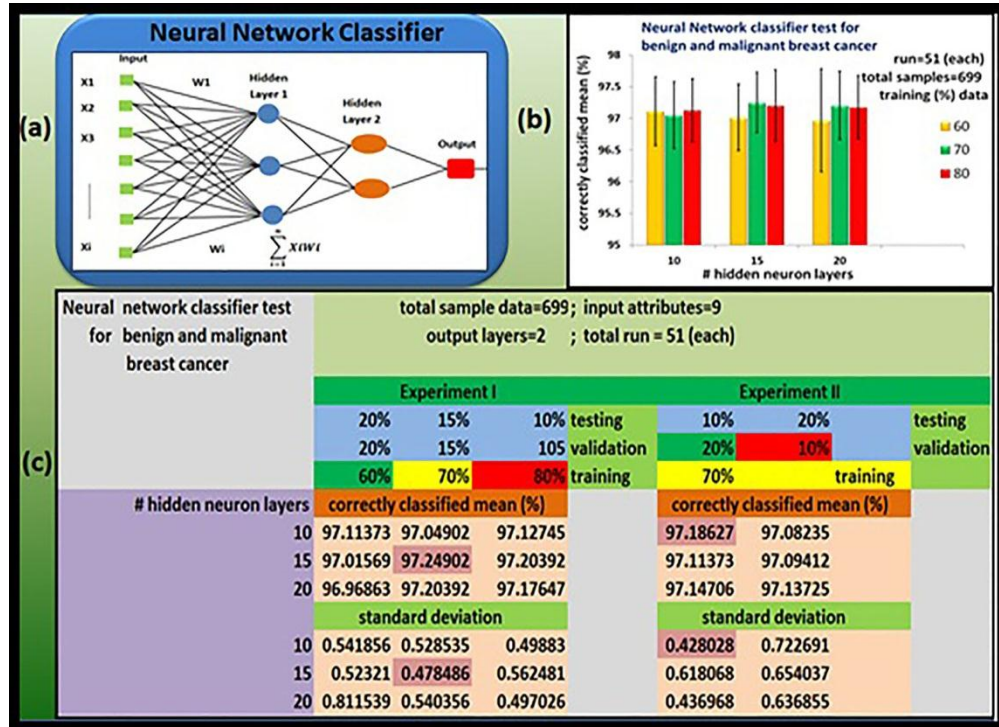


Figure 4.21 Artificial Neural Network classifier result (a)-(c) data for 699 breast cancer patients.

MATLAB and the NeuroSolutions network classifier are tested as a pilot study for breast cancer data classification. The performance of classified results is shown as confusion matrices for training, validation, and testing. Our hypothesis is to use the scoring system which may then be activated to display scoring on the basis of Nottingham Grading System (NGS), which will further be checked in parallel for a match with the pathologist score. In the conventional breast cancer diagnostics and treatment, the approach is highly serial in nature and time consuming.

The accurate diagnosis and scoring depends on a pathologist's experience and skills. Replacing the present analogue system with fully-automated digital healthcare solutions for electronic file sharing is highly demanding. Physical transportation of slides for a second opinion and collaboration is a challenge. This includes handling, packaging, logistics, and high chances of contamination, which leads to a loss of information. In solutions, digitally scanned slides are transported electronically on web based software for real time viewing, expert opinion and efficient timely health care solutions. Virtual microscopy is making this process more rapid and accurate with the use of technology.

CHAPTER 5: CONCLUSIONS, APPLICATIONS AND FUTURE WORK

5.1 Conclusions

In conclusion, the VOFET fabrication process has been developed and explored. In order to fabricate VOFET, a novel solution processable low cost fabrication process has been evolved. The design and the main framework to build a low cost and low voltage organic transistor are outlined. The cost to fabricate nano scale vertical transistors in a standard photolithographic environment is very high. In the present study, spin coating and drop casting methods are employed to fabricate a VOFET device. The main advantage of spin coating is the ease of deposition, where nanoscale film thickness can be attained. By utilizing this approach, two major issues are resolved. First, nanoscale channel length is achieved without the use of any photolithography process. The Second achievement is low operational voltage because of nanoscale channel length. Maintaining low cost and to complement the processing temperature, Kapton polyimide masking is adopted for the partition of stacking layers.

The organic material is deposited through a wet conversion process. The conversion process is an additional novelty of the device fabrication. The fabricated devices are tested under a series of standard characterization processes such as electrical, metrological, and radiation tests. Short channel effects are observed in VOFET devices during I-V electrical characterization. To overcome this SCLC effect, the drop casting method is adopted to deposit a thick organic channel. The vertical organic field effect transistor is emerging as a new type of organic transistor with several advantages, such as its low operational voltage, high current

density, and high frequency. Although lateral and vertical transistors look almost similar in design, the working principle of vertical transistors is different in many ways. The modification in the geometry provides the opportunities to reduce the fabrication cost. The main advantage of VOFET fabrication is solution processability and ease of scaling down the channel length in nanoscale.

The working of VOFET is mainly influenced by the SCLC effect, which is discussed in the following sections.

5.1.1 Influence of SCLC Effect

VOFET operation is governed by the electric field inside the channel of the device. The working of the device is largely influenced by drain-source and gate-source fields, which acts in parallel to each other unlike in a lateral device where they act normally. The electric field directions and charge movement inside the VOFET are shown in Figure 5.1 (b).

In the circuit operation, the source terminal is common with respect to the gate and drain. This is a p-type VOFET, thus negative biasing is applied at the gate and drain terminals. The organic transistor works in charge injection mode, i.e. the charge carriers, are injected into the organic material from outside the source electrode. Initially at zero gate bias, drain-to-source voltage is supplied, which allows the charge carriers (holes) to fill the traps and form a current below the threshold level.

As the source drain biasing level crosses the threshold value, a noticeable drain current starts flowing into the device at a zero gate value. According to the MTR mobility model, the injected charge carriers fill the traps and are then released to reach at drain terminal to constitute the output current. Inside the organic material, charge carriers follow the hopping mechanism to propagate through the active channel. As the gate biasing is increased, the channel starts

building and widening (accumulation) near the edge of the source electrode and facilitates the drain current. Output current modulation is noticeable (not substantial) due to asymmetric placement of the gate terminal from the source and drain, as shown in Figure 5.1 (b).

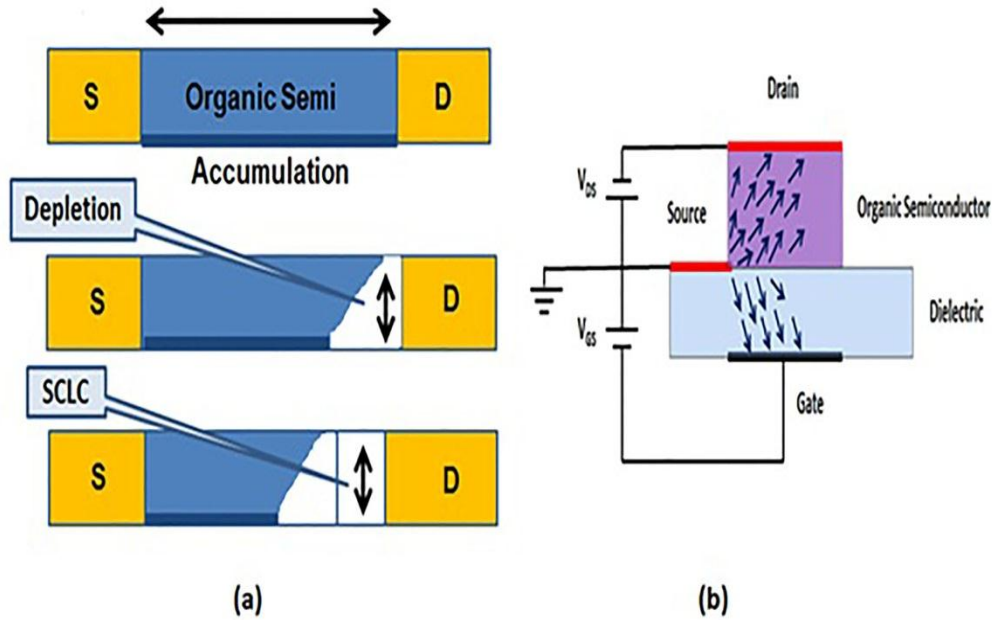


Figure 5.1 Short channel effects (a) the SCLC region formation and (b) the circuit operation.

This results in a poor ON/OFF ratio, thus, the vertical organic transistors operate in either the ON or OFF state [111]. The SCLC effect originates from the combined effect of the short channel length of device and contact effects. The rate of injection is more than the rate of diffusion, which is explained by the drift diffusion model for charge transportation [112]. The excess injected charge starts accumulating near the electrode. At this stage, more charge carriers are available inside the organic semiconductor, creating a high current density. This makes VOFET a high current device at the low drain field. As previously shown in Figure 4.5, the dependence of output current I_{DS} on V_{DS} is now reduced, with a power factor of $n > 2$ of drain-source voltage for a device of short channel length, i.e. $L=265\text{nm}$ channel length. This SCLC

effect is demonstrated with a depletion region and is shown in Figure 5.1 (a). The geometrical shape and design of the source electrode also contributes towards shielding and transporting the gate field. Apart from the structural dissimilarity of a VOFET from a lateral OFET, the main factors which influence the VOFET performance are the gate field and the physical location of the gate terminal.

5.1.2 Facts, Factors and Findings in Solution Processable VOFET

Efforts have been made to study and explore the facts and factors involved in a solution-processed VOFET fabrication. The two prominent features of VOFET are:

- Solution processed
- Vertical geometry

In addition to this, low cost and ease of fabrication are the promising advantages of VOFET. Thus, the following structural parameters and the facts about VOFET fabrication which should be carefully kept in view are:

- Source electrode design (step or perforated) which plays a crucial role in VOFET device performance.
- Stacked overlapping layers which could increase the internal device capacitance.
- Bottom gate electrode should be carefully designed to get the field effect.

The above mentioned facts and factors involved in solution processable VOFET devices are illustrated in Figure 5.2. These parameters are mainly on structural/geometrical design and electrical characterization basis. The factors are collected from experimental observations which are experienced and observed during fabrication. Materials used for device fabrication play an important role in the process development, such as maintenance of critical glass transition temperature.

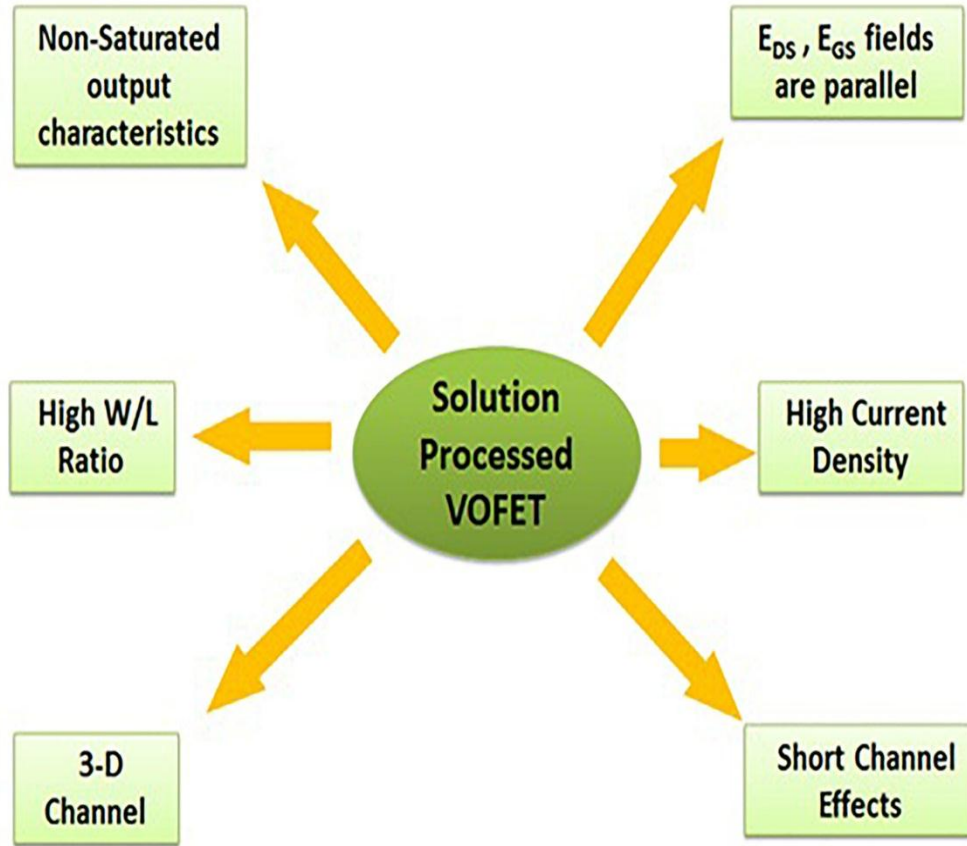


Figure 5.2 Facts and findings about solution processed VOFET device.

Apart from structural parameters, there are some other important factors which should be carefully considered and calculated while designing and estimating the performance of a solution processable VOFET.

The main factors are as follows:

- Charge carrier distribution and profile inside the organic channel.
- Electric field profile of both E_{DS} and E_{GS} .
- Contact resistances, SCLC and short channel effects.
- Surface engineering is required to minimize the contact effects and parasitic series resistances.

The VOFET device is designed, and fabricated using the low cost solution-processable method. Figure 5.3 shows the research problems which are addressed and proposed based on the potential application areas.

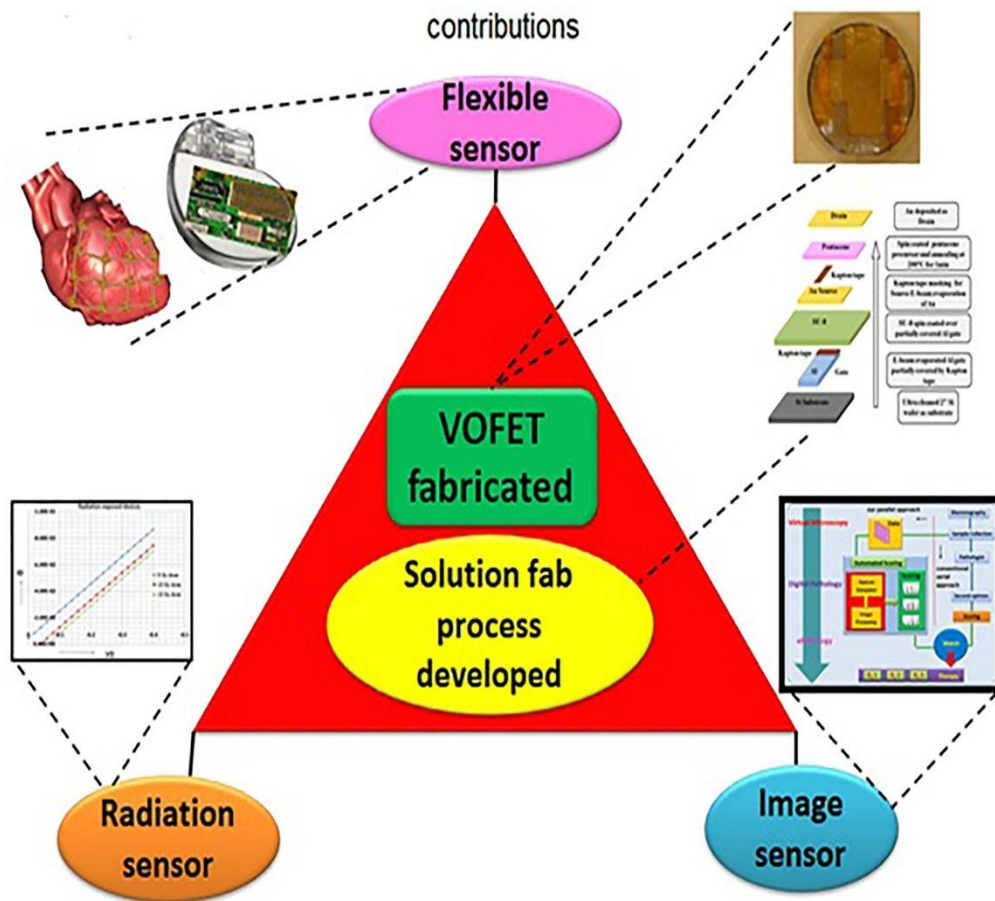


Figure 5.3 Summary of research problems addressed and proposed.

The main research problems addressed and proposed are as follows:

- VOFET solution processed devices are fabricated and a novel fabrication process evolved.
- A flexible array of VOFET is proposed as cardiac arrhythmia sensors for integration into ICD and pacemaker devices.

- VOFETs are tested for radiation sensors.
- VOFETs are proposed for imaging applications to detect and analyze the benign and malignant nuclear features of tumors.

5.2 Applications

The proposed application areas are mainly in biomedical domains. VOFETs are low power high current devices, thus they could be used for biomedical implants to record biologically important information inside the human body. It is required for implants to consume less power and last longer. The main role of VOFETs has been proposed as sensors and stimulation electrodes.

Flexible organic electronics is a fast emerging field of technology for applications in large area electronics [75]. OLED displays are already in the market in flexible mobile phone monitors and large area foldable displays. OFET is the basic building block in flexible electronics such as in OLED displays, plastic TFT, E-book and wearable flexible electronics. Due to low mobility of organic materials, OFETs are consuming high voltage. To overcome this problem, vertical organic FETs are emerging as an alternative and the first choice of researchers and industry as low cost, low voltage, and high current devices.

In bio-electronic applications, organic materials have the natural advantage of interfacing with biological systems. Organics materials have an inclination for the biological environment because of their weak molecular forces and low temperature processing. The exchange of ions between organic materials and the biological milieu makes it obvious to use them for biosensor applications. The biomedical area is VOFETs are more suitable for biology and electronics interfacing, such as in brain-machine interface [113]. Flexible biomedical implants are an extended application in BCI to record in-vivo brain activity using a flexible array of sensors

[114]. Organic materials have the ability to conduct electrons, holes, and ions. Overall, VOFETs are excellent candidates for biomedical interfacing electronics.

Neuroprosthetics is a fast developing area in therapeutics which utilizes the selective electrical stimulation of a tissue to restore lost neural functions. The disorders of a nervous system can be restored back by selective stimulation of signal pathways. It could be done by implanting microelectrode arrays for stimulation/deactivation of neural activity [115]. In a brain-machine interface, the penetrating microelectrodes record neural activity and motor signals to interfaces with the machines [116]. Organic Electrochemical Transistors (OECT) hold great potential for adhesion of biological cells to grow over the electrolyte of an OECT transistor. These new types of organic transistors have been successfully employed for biological and chemical sensor applications [117]. As known, flexible organic electronics have the natural advantage to interface with tissue to record and stimulate the neural activity inside the brain. Flexible organic electronics can bend and stretch with the tissue movement into an aqueous milieu. Large area organic electronics are expected to expand the scope of their application and prospects beyond sensors and actuators to the human-machine interface because of their ability to bend and stretch.

The VOFET devices are proposed for a new generation of biomedical applications like flexible cardiac sensors and imagers in cancer applications. The use of VOFETs as flexible cardiac sensors could be a forward step towards a new generation of cardiac implants for observing real time ECG patterns in high risk patients. This could be time saving and helpful to reduce surgery cost. In imaging application for breast cancer patients, a parallel approach is proposed to assist pathologists in grading benign and malignant tumors. This approach will be a step towards digital pathology. The idea is to share patient data with the pathologist for timely

diagnosis and therapy recommendation. This will be helpful for patients in developing countries where the patient/pathologist ratio is very less.

5.2.1 Novel Neuroprosthetics Using Flexible Organic Electronics

Neuroprosthetics are therapeutics used for restoring sensory pathways for selective electric stimulation to restore lost neural functions. In many diseases due to some underlying processes the sensory pathways become dysfunctional, which leads to impaired activity. The microelectrodes are implanted to sense those signals directly from the motor cortex and decode the neural activity to a prosthetic arm or limb. The basic point behind this activity is a good electrical interface between biology and electronics. Thus, flexible organic electronics are interfaced with tissue to record the neural activity. Flexible electronics could be a good candidate to establish an intact electrical contact between the tissue and electronics. The conventional approach of using Utah and Michigan micro electrodes is an invasive technique that harms the tissue with a loss of electrical contact due to formation of glial sheath at the site of rupture [118, 119]. This approach could result in poor signal to noise ratio. Non-invasive pressure sensitive monitoring arrays have been demonstrated [120]. The use of flexible organic VOFETs can have an advantageous edge not only to differentiate between actual signal and noise, but can also be helpful in on-site signal amplification. Thus, the use of VOFETs is proposed for sensing and stimulation in advanced neuroprosthetics applications [121, 122]. Figure 5.4(a) shows the interface of a VOFET with an enzymatic reaction system. Changes in enzymatic reaction can alter the VOFET device current, which could be recorded for sensor applications. The interface of VOFET electronics with reaction center could provide an opportunity to directly record changes in biological systems at the microorganism level. Good electrical contact and selective signal sensing would be helpful in reduction of noise and in

providing an amplified signal for processing. The action potential of a neuron can artificially be triggered by a VOFET device current as shown in Figure 5.4(b), which could be exploited for the neural stimulation purpose. A VOFET can initiate a biological reaction by providing an external trigger. To propagate an action potential, VOFET could control the minimum trigger by stimulating the neural tissue. This approach can be very helpful in Parkinson's or epilepsy diseases to deactivate the hyperactive neural activity or to initiate a neural activity in a basal ganglia for the release of dopamine. The idea of novel neural prosthetics is shown in Figure 5.4.

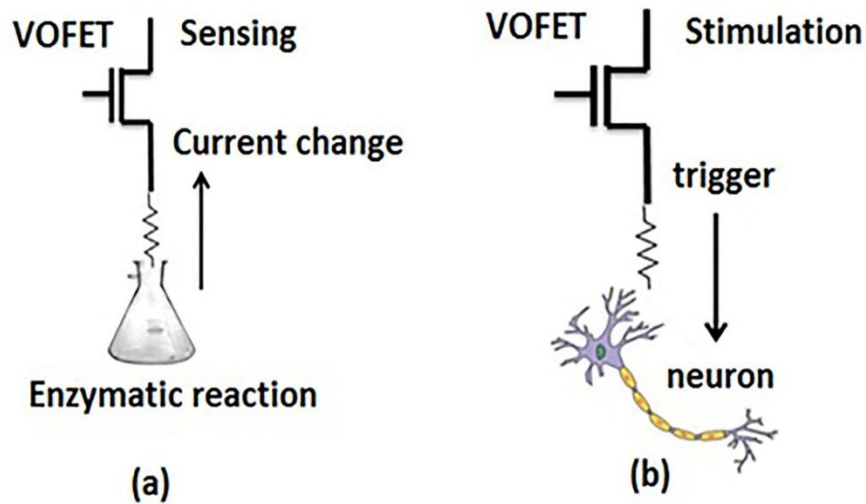


Figure 5.4 VOFET used in neuroprosthetics (a) sensor application (b) neural stimulation.

5.2.2 Flexible Stimulating Probes

In neuroprosthetics applications, the conventional approach of penetrating a Utah and Michigan type microelectrode array for recording signals from a 3D irregular shaped tissue is not sufficient. In retinal and Electrocorticography (ECoG) implants, there is always a demanding need for a high resolution output picture [123]. As shown in previous reports, state of the art retinal implants use only 100 channel microelectrodes for creating a checkerboard type of image

for a patient suffering from visual disorders and diseases. By using a dense array of curvilinear electrodes, it is possible to cover a large tissue area in the case of ECoG implants in neuroprosthetics or epilepsy [124, 125]. For a high resolution recording, the integration approach needs wires and access lines. The wiring problem can be minimized by using an array or flexible grid of VOFETs. Thus, the integration of VOFETs solves a wiring problem, helpful in on-site signal amplification, and provides a high signal-to-noise ratio. Figure 5.5 shows the flexible VOFET array integration for covering the larger tissue area.

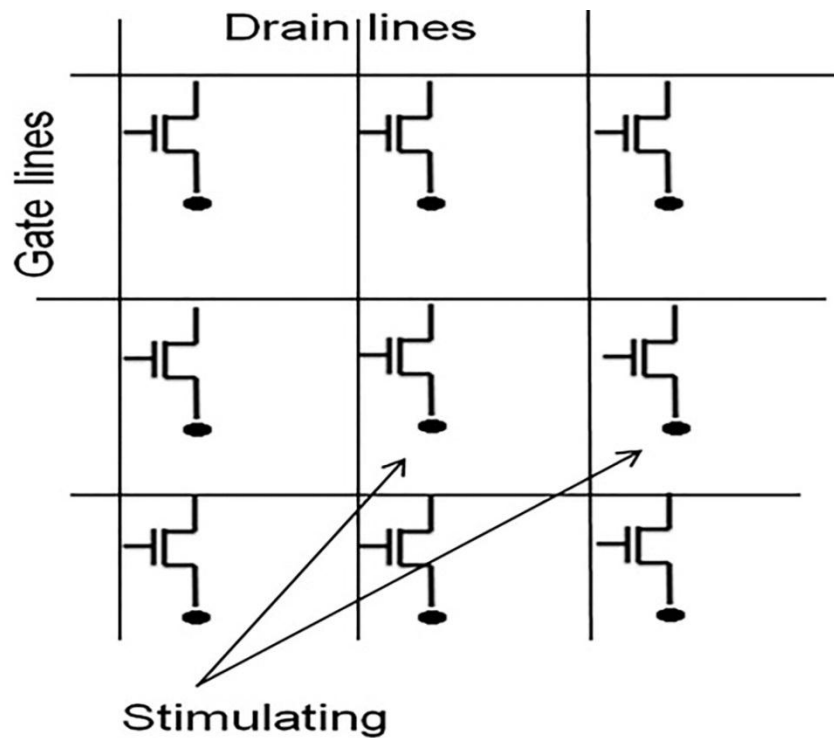


Figure 5.5 VOFET integration into large area stimulation electrodes for novel neuroprosthetics applications.

5.3 Future Work

Vertical organic transistors have been recognized as low cost and low power electronic elements for future biomedical applications. The organic materials have an inherent ability to

conduct both charge carriers (electrons and holes) and exchange ions in a natural biological environment. In addition, organic materials are low cost and easily processable at room temperature. Biocompatibility of organic materials makes them a suitable candidate for green and environmentally friendly technologies. Integration of organic materials in vertical transistors can be explored for a new generation of bio-electronic applications. Thus, convergence of all these areas could be exploited for future translational technologies.

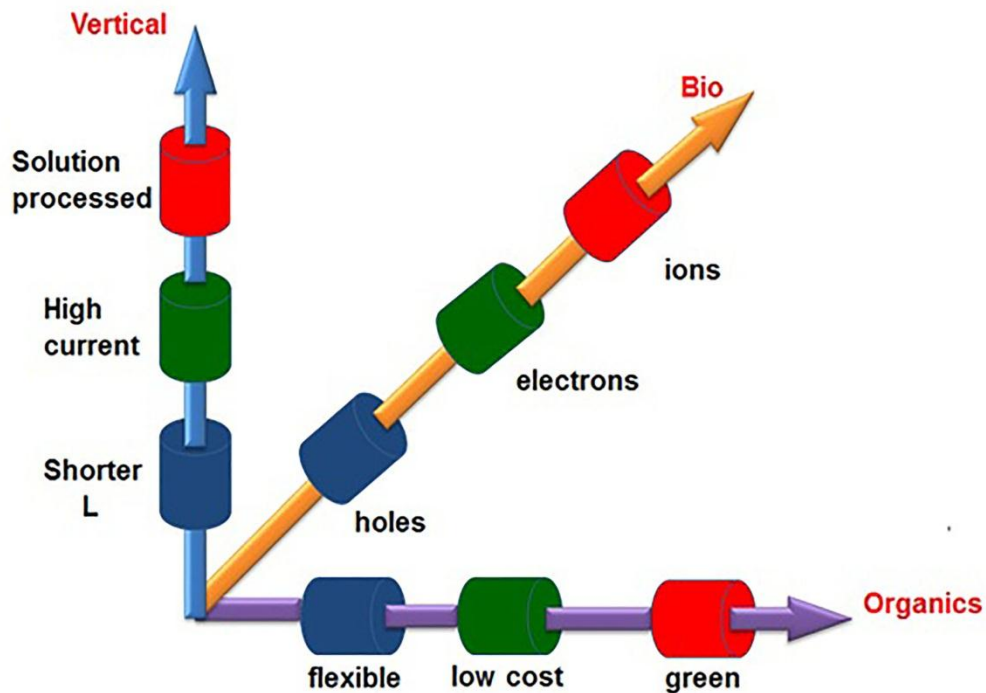


Figure 5.6 Integration of organic materials for new generation bio-electronic applications using VOFET transistors.

REFERENCES

- [1] T. Someya, Y. Kato, T. Sekitani, S. Iba, Y. Noguchi, Y. Murase, H. Kawaguchi, and T. Sakurai, "Conformable, flexible, large-area networks of pressure and thermal sensors with organic transistor active matrixes," *Proc Natl Acad Sci U S A*, vol. 102, no. 35, pp. 12321-5, Aug, 2005.
- [2] T. Someya, A. Dodabalapur, J. Huang, K. C. See, and H. E. Katz, "Chemical and physical sensing by organic field-effect transistors and related devices," *Adv Mater*, vol. 22, no. 34, pp. 3799-811, Sep, 2010.
- [3] N. T. Tien, S. Jeon, D. I. Kim, T. Q. Trung, M. Jang, B. U. Hwang, K. E. Byun, J. Bae, E. Lee, J. B. Tok, Z. Bao, N. E. Lee, and J. J. Park, "A flexible bimodal sensor array for simultaneous sensing of pressure and temperature," *Adv Mater*, vol. 26, no. 5, pp. 796-804, Feb, 2014.
- [4] H.-W. Zan, Y.-H. Hsu, H.-F. Meng, C.-H. Huang, Y.-T. Tao, and W.-W. Tsai, "High output current in vertical polymer space-charge-limited transistor induced by self-assembled monolayer," *Applied Physics Letters*, vol. 101, no. 9, pp. 093307, 2012.
- [5] C. D. Dimitrakopoulos, and P. R. L. Malenfant, "Organic Thin Film Transistors for Large Area Electronics," *Advanced Materials*, vol. 14, no. 2, pp. 99-117, 2002.
- [6] M. Irimia-Vladu, P. A. Troshin, M. Reisinger, L. Shmygleva, Y. Kanbur, G. Schwabegger, M. Bodea, R. Schwödauer, A. Mumyatov, J. W. Fergus, V. F. Razumov, H. Sitter, N. S. Sariciftci, and S. Bauer, "Biocompatible and Biodegradable Materials for Organic Field-Effect Transistors," *Advanced Functional Materials*, vol. 20, no. 23, pp. 4069-4076, 2010.
- [7] L. Torsi, M. Magliulo, K. Manoli, and G. Palazzo, "Organic field-effect transistor sensors: a tutorial review," *Chem Soc Rev*, vol. 42, no. 22, pp. 8612-28, Nov, 2013.
- [8] J. J. Van Gompel, G. A. Worrell, M. L. Bell, T. A. Patrick, G. D. Cascino, C. Raffel, W. R. Marsh, and F. B. Meyer, "Intracranial electroencephalography with subdural grid electrodes: techniques, complications, and outcomes," *Neurosurgery*, vol. 63, no. 3, pp. 498-506, Sep, 2008.

- [9] G. Schalk, and E. C. Leuthardt, "Brain-computer interfaces using electrocorticographic signals," *IEEE Rev Biomed Eng*, vol. 4, pp. 140-54, 2011.
- [10] K. Myny, S. Van Winckel, S. Steudel, P. Vicca, S. De Jonge, M. J. Beenhakkers, C. W. Sele, N. A. J. M. Van Aerle, G. H. Gelinck, J. Genoe, and P. Heremans, "An Inductively-Coupled 64b Organic RFID Tag Operating at 13.56MHz with a Data Rate of 787b/s," *Solid-State Circuits Conference*, pp. 290, 2008.
- [11] Y. Noguchi, T. Sekitani, and T. Someya, "Organic-transistor-based flexible pressure sensors using ink-jet-printed electrodes and gate dielectric layers," *Applied Physics Letters*, vol. 89, no. 25, 2006.
- [12] D. T. Simon, S. Kurup, K. C. Larsson, R. Hori, K. Tybrandt, M. Goiny, E. W. Jager, M. Berggren, B. Canlon, and A. Richter-Dahlfors, "Organic electronics for precise delivery of neurotransmitters to modulate mammalian sensory function," *Nat Mater*, vol. 8, no. 9, pp. 742-6, Sep, 2009.
- [13] S. K. Attili, A. Lesar, A. McNeill, M. Camacho-Lopez, H. Moseley, S. Ibbotson, I. D. W. Samuel, and J. Ferguson, "An open pilot study of ambulatory photodynamic therapy using a wearable low-irradiance organic light-emitting diode light source in the treatment of nonmelanoma skin cancer," *British Journal of Dermatology* vol. 161, no. 1, pp. 170–173, 2009.
- [14] J. Rivnay, R. M. Owens, and G. G. Malliaras, "The Rise of Organic Bioelectronics," *Chemistry of Materials*, Sept, 19 2013.
- [15] A. C. Arias, J. Daniel, T. N. Ng, S. Garner, G. L. Whiting, L. Lavery, B. Russo, and B. Krusor, "Flexible printed sensor tape based on solution processed materials," *IEEE Photonic Society*, no. 2010 23rd Annual Meeting, pp. 18-19, 2010.
- [16] K. Cherenack, C. Zysset, T. Kinkeldei, N. Münzenrieder, and G. Tröster, "Woven electronic fibers with sensing and display functions for smart textiles," *Adv Mater*, vol. 22, no. 45, pp. 5178-82, Dec, 2010.
- [17] A. N. Sokolov, B. C. Tee, C. J. Bettinger, J. B. Tok, and Z. Bao, "Chemical and engineering approaches to enable organic field-effect transistors for electronic skin applications," *Acc Chem Res*, vol. 45, no. 3, pp. 361-71, Mar, 2012.
- [18] S. Xu, Y. Zhang, L. Jia, K. E. Mathewson, K. I. Jang, J. Kim, H. Fu, X. Huang, P. Chava, R. Wang, S. Bhole, L. Wang, Y. J. Na, Y. Guan, M. Flavin, Z. Han, Y. Huang, and J. A. Rogers, "Soft microfluidic assemblies of sensors, circuits, and radios for the skin," *Science*, vol. 344, no. 6179, pp. 70-4, Apr, 2014.

- [19] T. Sekitani, U. Zschieschang, H. Klauk, and T. Someya, "Flexible organic transistors and circuits with extreme bending stability," *Nat Mater*, vol. 9, no. 12, pp. 1015-22, Dec, 2010.
- [20] S. R. Forrest, "The path to ubiquitous and low-cost organic electronic appliances on plastic," *Nature*, vol. 428, no. 6986, pp. 911-8, Apr, 2004.
- [21] C. D. Dimitrakopoulos, and D. J. Masecaro, "Organic thin-film transistors: A review of recent advances," *IBM Journal of Research and Development*, vol. 45, no. 1, pp. 11-27, 2001
- [22] K. Kuribara, H. Wang, N. Uchiyama, K. Fukuda, T. Yokota, U. Zschieschang, C. Jaye, D. Fischer, H. Klauk, T. Yamamoto, K. Takimiya, M. Ikeda, H. Kuwabara, T. Sekitani, Y. L. Loo, and T. Someya, "Organic transistors with high thermal stability for medical applications," *Nat Commun*, vol. 3, pp. 723, 2012.
- [23] T. Someya, S. Iba, Y. Kato, and T. Sekitani, "A large-area, flexible, and lightweight sheet image scanner integrated with organic field-effect transistors and organic photodiodes," *Electron Devices Meeting, IEDM Technical Digest. IEEE International*. pp. 365-368, 2004.
- [24] M. Kaltenbrunner, T. Sekitani, J. Reeder, T. Yokota, K. Kuribara, T. Tokuhara, M. Drack, R. Schwödiauer, I. Graz, S. Bauer-Gogonea, S. Bauer, and T. Someya, "An ultra-lightweight design for imperceptible plastic electronics," *Nature*, vol. 499, no. 7459, pp. 458-63, Jul, 2013.
- [25] T. Sekitani, and T. Someya, "Stretchable, large-area organic electronics," *Adv Mater*, vol. 22, no. 20, pp. 2228-46, May, 2010.
- [26] M. Puri, K. C. Chapalamadugu, A. C. Miranda, S. Gelot, W. Moreno, P. C. Adithya, C. Law, and S. M. Tipparaju, "Integrated approach for smart implantable cardioverter defibrillator (ICD) device with real time ECG monitoring: use of flexible sensors for localized arrhythmia sensing and stimulation," *Front Physiol*, vol. 4, pp. 300, 2013.
- [27] P. Cosseddu, L. Basirico, A. Loi, S. Lai, P. Maiolino, E. Baglini, S. Denei, F. Mastrogiovanni, G. Cannata, and A. Bonfiglio, "Inkjet printed Organic Thin Film Transistors based tactile transducers for artificial robotic skin," *IEEE RAS/EMBS International Conference on Biomedical Robotics and Biomechatronics*, 2012.
- [28] M. Muccini, "A bright future for organic field-effect transistors," *Nat Mater*, vol. 5, no. 8, pp. 605-13, Aug, 2006.

- [29] T. Someya, Y. Kato, S. Iba, Y. Noguchi, T. Sekitani, H. Kawaguchi, and T. Sakurai, "Integration of organic FETs with organic photodiodes for a large area, flexible, and lightweight sheet image scanners," *IEEE Transactions on Electron Devices*, vol. 52, no. 11, pp. 2502-2511, 2005
- [30] A. E. Rizzardi, A. T. Johnson, R. I. Vogel, S. E. Pambuccian, J. Henriksen, A. P. Skubitz, G. J. Metzger, and S. C. Schmechel, "Quantitative comparison of immunohistochemical staining measured by digital image analysis versus pathologist visual scoring," *Diagn Pathol*, vol. 7, pp. 42, 2012.
- [31] E. A. B. Silva, J. F. Borin, P. Nicolucci, C. F. O. Graeff, T. G. Netto, and R. F. Bianchi, "Low dose ionizing radiation detection using conjugated polymers," *Applied Physics Letters*, vol. 86, no. 13, pp. 131902-3, 2005.
- [32] E. S. Bronze-Uhle, A. Batagin-Neto, F. C. Lavarda, and C. F. O. Graeff, "Ionizing radiation induced degradation of poly (2-methoxy-5-(2'-ethyl-hexyloxy) -1,4-phenylene vinylene) in solution," *Journal of Applied Physics*, vol. 110, no. 7, pp. 073510-, 2011.
- [33] H. N. Raval, and V. Ramgopal Rao, "Low-Operating-Voltage Operation and Improvement in Sensitivity With Passivated OFET Sensors for Determining Total Dose Radiation," *Electron Device Letters, IEEE*, vol. 31, no. 12, pp. 1482-1484, 2010.
- [34] J. M. Lobez, and T. M. Swager, "Radiation detection: resistivity responses in functional poly(olefin sulfone)/carbon nanotube composites," *Angew Chem Int Ed Engl*, vol. 49, no. 1, pp. 95-8, 2010.
- [35] Y. Yuan, Q. Dong, B. Yang, F. Guo, Q. Zhang, M. Han, and J. Huang, "Solution-Processed Nanoparticle Super-Float-Gated Organic Field-Effect Transistor as Un-cooled Ultraviolet and Infrared Photon Counter," *Sci Rep*, vol. 3, pp. 2707, Sep, 2013.
- [36] M. K. a. Y. Arakawa, "Pentacene-based organic field-effect transistors," *Journal of Physics: Condensed Matter*, vol. 20, no. 18, pp. 184011, 2008.
- [37] J. L. Brédas, D. Beljonne, V. Coropceanu, and J. Cornil, "Charge-transfer and energy-transfer processes in pi-conjugated oligomers and polymers: a molecular picture," *Chem Rev*, vol. 104, no. 11, pp. 4971-5004, Nov, 2004.
- [38] G. Horowitz, R. Hajlaoui, and P. Delannoy, "Temperature Dependence of the Field-Effect Mobility of Sexithiophene. Determination of the Density of Traps," *J. Phys. III France*, vol. 5, no. 4, pp. 355-371, 1995.
- [39] M. Vissenberg, and M. Matters, "Theory of the field-effect mobility in amorphous organic transistors," *Physical Review B*, vol. 57, pp. 12964, 1998.

- [40] Y. Liang, H.-C. Chang, P. Paul Ruden, and C. Daniel Frisbie, "Examination of Au, Cu, and Al contacts in organic field-effect transistors via displacement current measurements," *Journal of Applied Physics*, vol. 110, no. 6, pp. 064514-, 2011.
- [41] H. E. Katz, and Z. Bao, "The Physical Chemistry of Organic Field-Effect Transistors," *J. Phys. Chem. B*, vol. 104, no. 4, pp. 671-678, 2000.
- [42] Y. Yuan, G. Giri, A. L. Ayzner, A. P. Zoombelt, S. C. Mannsfeld, J. Chen, D. Nordlund, M. F. Toney, J. Huang, and Z. Bao, "Ultra-high mobility transparent organic thin film transistors grown by an off-centre spin-coating method," *Nat Commun*, vol. 5, pp. 3005, Jan, 2014.
- [43] T. Richards, and H. Sirringhaus, "Bias-stress induced contact and channel degradation in staggered and coplanar organic field-effect transistors," *Applied Physics Letters*, vol. 92, no. 2, pp. -, 2008.
- [44] T. J. Richards, and H. Sirringhaus, "Analysis of the contact resistance in staggered, top-gate organic field-effect transistors," *Journal of Applied Physics*, vol. 102, no. 9, pp. 094510-1-094510-6, 2007.
- [45] G. Horowitz, "Organic Field-Effect Transistors," *Advanced Materials*, vol. 10, no. 5, pp. 365-377, 1998.
- [46] A. C. Arias, J. D. MacKenzie, I. McCulloch, J. Rivnay, and A. Salleo, "Materials and applications for large area electronics: solution-based approaches," *Chemical reviews*, vol. 110, no. 1, pp. 3-24, 2010.
- [47] H.-W. Zan, Y.-H. Hsu, H.-F. Meng, C.-H. Huang, Y.-T. Tao, and W.-W. Tsai, "High output current in vertical polymer space-charge-limited transistor induced by self-assembled monolayer," *Applied Physics Letters*, vol. 101, no. 9, pp. 093307-4, 2012.
- [48] H. Sirringhaus, "Device Physics of Solution-Processed Organic Field-Effect Transistors," *Advanced Materials*, vol. 17, no. 20, pp. 2411-2425, 2005.
- [49] H. Kleemann, A. A. Günther, K. Leo, and B. Lüssem, "High-Performance Vertical Organic Transistors," *Small*, vol 9, no. 21, pp 3670–3677, Nov 11, 2013
- [50] J. Liu, L. Herlogsson, A. Sawatdee, P. Favia, M. Sandberg, X. Crispin, I. Engquist, and M. Berggren, "Vertical polyelectrolyte-gated organic field-effect transistors," *Applied Physics Letters*, vol. 97, no. 10, pp. 103307, 2010.

- [51] K. Kudo, T. Takano, H. Yamauchi, and M. Iizuka, "High-speed operation of step-edge vertical-channel organic transistors with pentacene and 6, 13-bis (triisopropylsilylethynyl) pentacene," *JJAP*, vol. 49, 2010.
- [52] T. Takano, H. Yamauchi, M. Iizuka, M. Nakamura, and K. Kudo, "High-Speed Operation of Vertical Type Organic Transistors Utilizing Step-Edge Structures," *Applied Physics Express*, vol. 2, no. 7, 2009.
- [53] M. A. McCarthy, B. Liu, and A. G. Rinzler, "High current, low voltage carbon nanotube enabled vertical organic field effect transistors," *Nano Lett*, vol. 10, no. 9, pp. 3467-72, Sep, 2010.
- [54] A. J. Ben-Sasson, Z. Chen, A. Facchetti, and N. Tessler, "Solution-processed ambipolar vertical organic field effect transistor," *Applied Physics Letters*, vol. 100, no. 26, pp. 263306, 2012.
- [55] L. Rossi, K. F. Seidel, W. S. Machado, and I. A. Hummelgen, "Low voltage vertical organic field-effect transistor with polyvinyl alcohol as gate insulator," *Journal of Applied Physics*, vol. 110, no. 9, pp. 094508, 2011.
- [56] Z. Xu, S.-H. Li, L. Ma, G. Li, and Y. Yang, "Vertical organic light emitting transistor," *Applied Physics Letters*, vol. 91, no. 9, pp. 092911-092911-3, 2007.
- [57] M. Liping, and Y. Yang, "Unique architecture and concept for high-performance organic transistors," *Appl. Phys. Lett*, vol. 85, no. 5084, 2004.
- [58] C. Yu-Chiang, M. Hsin-Fei, H. Sheng-Fu, and H. Chain-Shu, "High-performance solution-processed polymer space-charge-limited transistor," *Organic Electronics*, vol. 9, pp. 310-316, 2008.
- [59] K. Fujimoto, T. Hiroi, K. Kudo, and M. Nakamura, "High-Performance, Vertical-Type Organic Transistors with Built-In Nanotriode Arrays," *Adv. Mater*, vol. 19, pp. 525-530, 2007.
- [60] M. G. Lemaitre, E. P. Donoghue, M. A. McCarthy, B. Liu, S. Tongay, B. Gila, P. Kumar, R. K. Singh, B. R. Appleton, and A. G. Rinzler, "Improved transfer of graphene for gated Schottky-junction, vertical, organic, field-effect transistors," *ACS Nano*, vol. 6, no. 10, pp. 9095-102, Oct, 2012.
- [61] F. S. Keli, R. Lucieli, M. Q. M. Regina, and A. H. Ivo, "Vertical organic field effect transistor using sulfonated polyaniline/aluminum bilayer as intermediate electrode," *J Mater Sci*, vol. 24, no. 1052-1056, 2013.

- [62] M. Berggren, and A. Richter-Dahlfors, "Organic Bioelectronics," *Advanced Materials*, vol. 19, no. 12, pp. 3201–3213, 2007.
- [63] K. Svennersten, K. C. Larsson, M. Berggren, and A. Richter-Dahlfors, "Organic bioelectronics in nanomedicine," *Biochim Biophys Acta*, vol. 1810, no. 3, pp. 276-85, Mar, 2011.
- [64] D. Feili, M. Schuettler, and T. Stieglitz, "Matrix-addressable, active electrode arrays for neural stimulation using organic semiconductors-cytotoxicity and pilot experiments in vivo," *J Neural Eng*, vol. 5, no. 1, pp. 68-74, Mar, 2008.
- [65] D. Khodagholy, T. Doublet, P. Quilichini, M. Gurfinkel, P. Leleux, A. Ghestem, E. Ismailova, T. Hervé, S. Sanaur, C. Bernard, and G. G. Malliaras, "In vivo recordings of brain activity using organic transistors," *Nat Commun*, vol. 4, pp. 1575, 2013.
- [66] D. Khodagholy, J. Rivnay, M. Sessolo, M. Gurfinkel, P. Leleux, L. H. Jimison, E. Stavriniidou, T. Herve, S. Sanaur, R. M. Owens, and G. G. Malliaras, "High transconductance organic electrochemical transistors," *Nat Commun*, vol. 4, pp. 2133, 2013.
- [67] L. H. Jimison, S. A. Tria, D. Khodagholy, M. Gurfinkel, E. Lanzarini, A. Hama, G. G. Malliaras, and R. M. Owens, "Measurement of barrier tissue integrity with an organic electrochemical transistor," *Adv Mater*, vol. 24, no. 44, pp. 5919-23, Nov, 2012.
- [68] D. E. Johnston, K. G. Yager, C. Y. Nam, B. M. Ocko, and C. T. Black, "One-volt operation of high-current vertical channel polymer semiconductor field-effect transistors," *Nano Lett*, vol. 12, no. 8, pp. 4181-6, Aug, 2012.
- [69] B. Kang, W. H. Lee, and K. Cho, "Recent advances in organic transistor printing processes," *ACS Appl Mater Interfaces*, vol. 5, no. 7, pp. 2302-15, Apr, 2013.
- [70] L. Li, P. Gao, M. Baumgarten, K. Müllen, N. Lu, H. Fuchs, and L. Chi, "Organic Transistors: High Performance Field-Effect Ammonia Sensors Based on a Structured Ultrathin Organic Semiconductor Film (Adv. Mater. 25/2013)," *Advanced Materials*, vol. 25, no. 25, pp. 3500, Jul, 2013.

- [71] M. Uno, K. Nakayama, J. Soeda, Y. Hirose, K. Miwa, T. Uemura, A. Nakao, K. Takimiya, and J. Takeya, "High-speed flexible organic field-effect transistors with a 3D structure," *Adv Mater*, vol. 23, no. 27, pp. 3047-51, Jul, 2011.
- [72] W. Yang-Kai, H. Jian-Hao, T. Wu-Wei, C. Yung-Pin, L. Shih-Chieh, H. Yung, Z. Hsiao-Wen, M. Hsin-Fei, and L. A. Wang, "Solution-Processed Vertical Organic Transistors Fabricated by Nanoimprint Lithography," *IEEE Electron Device Letters*, vol. 34, no. 2, Feb, 2013.
- [73] S. Allard, M. Forster, B. Souharce, H. Thiem, and U. Scherf, "Organic semiconductors for solution-processable field-effect transistors (OFETs)," *Angewandte Chemie, Wiley-VCH Verlag GmbH & Co*, vol. 47, pp. 4070-4098, 2008.
- [74] N. Stutzmann, R. H. Friend, and H. Sirringhaus, "Self-aligned, vertical-channel, polymer field-effect transistors," *Science*, vol. 299, no. 5614, pp. 1881-4, Mar, 2003.
- [75] R. Parashkov, E. Becker, T. Riedl, H. Johannes, and W. Kowalsky, "Large Area Electronics Using Printing Methods," *Proceedings of the IEEE*, vol. 93, no. 7, 2005.
- [76] S. Ochiai, K. Palanisamy, S. Kannappan, and P.-K. Shin, "Pentacene Active Channel Layers Prepared by Spin-Coating and Vacuum Evaporation Using Soluble Precursors for OFET Applications," *ISRN Condensed Matter Physics*, vol. 2012, pp. 7, 2012.
- [77] C. S. Kim, S. Lee, E. D. Gomez, J. E. Anthony, and Y.-L. Loo, "Solvent-dependent electrical characteristics and stability of organic thin-film transistors with drop cast bis(triisopropylsilylethynyl) pentacene," *Applied Physics Letters*, vol. 93, no. 10, pp. 103302, 2008.
- [78] W. H. Lee, J. H. Cho, and K. Cho, "Control of mesoscale and nanoscale ordering of organic semiconductors at the gate dielectric/semiconductor interface for organic transistors," *Journal of Materials Chemistry*, vol. 20, no. 13, pp. 2549-2561, 2010.
- [79] A. Afzali, C. D. Dimitrakopoulos, and T. L. Breen, "High-performance, solution-processed organic thin film transistors from a novel pentacene precursor," *J Am Chem Soc*, vol. 124, no. 30, pp. 8812-3, Jul, 2002.
- [80] C. R. Kagan, A. Afzali, and T. O. Graham, "Operational and environmental stability of pentacene thin-film transistors," *Applied Physics Letters*, vol. 86, no. 19, pp. 193505, 2005.
- [81] J. H. Cho, D. H. Kim, Y. Jang, W. H. Lee, K. Ihm, J.-H. Han, S. Chung, and K. Cho, "Effects of metal penetration into organic semiconductors on the electrical properties of organic thin film transistors," *Applied Physics Letters*, vol. 89, no. 13, pp. 132101, 2006.

- [82] M. Puri, and S. Bhanja, "13,6-N-sulfinylacetamidopentacene based Fully Encapsulated Low Voltage Vertical Short Channel OFET," in *OSA*, pp. JWE5, 2011.
- [83] I. McCulloch, M. Heeney, C. Bailey, K. Genevicius, I. Macdonald, M. Shkunov, D. Sparrowe, S. Tierney, R. Wagner, W. Zhang, M. L. Chabinyc, R. J. Kline, M. D. McGehee, and M. F. Toney, "Liquid-crystalline semiconducting polymers with high charge-carrier mobility," *Nat Mater*, vol. 5, no. 4, pp. 328-33, Apr, 2006.
- [84] M. Zhang, H. Tsao, W. Pisula, C. Yang, A. Mishra, and K. Müllen, "Field-effect transistors based on a benzothiadiazole-cyclopentadithiophene copolymer," *American Chemical Society*, vol. 129, pp. 3472-3473, 2007.
- [85] M. M. Payne, S. R. Parkin, J. E. Anthony, C. C. Kuo, and T. N. Jackson, "Organic field-effect transistors from solution-deposited functionalized acenes with mobilities as high as $1 \text{ cm}^2/\text{V} \times \text{s}$," *J Am Chem Soc*, vol. 127, no. 14, pp. 4986-7, Apr, 2005.
- [86] E. Menard, M. A. Meitl, Y. Sun, J. U. Park, D. J. Shir, Y. S. Nam, S. Jeon, and J. A. Rogers, "Micro- and nanopatterning techniques for organic electronic and optoelectronic systems," *Chem Rev*, vol. 107, no. 4, pp. 1117-60, Apr, 2007.
- [87] S. K. Volkman, S. Molesa, B. Mattis, P. C. Chang, and V. Subramanian, "Inkjetted organic transistors using a novel pentacene precursor," *MRS Proceedings*, vol. 769, 2003.
- [88] M. L. Chabinyc, J.-P. Lu, R. A. Street, Y. Wu, P. Liu, and B. S. Ong, "Short channel effects in regioregular poly(thiophene) thin film transistors," *Journal of Applied Physics*, vol. 96, no. 4, pp. 2063-2070, 2004.
- [89] J. Zaumseil, and H. Sirringhaus, "Electron and ambipolar transport in organic field-effect transistors," *Chem Rev*, vol. 107, no. 4, pp. 1296-323, Apr, 2007.
- [90] L.-L. Chua, P. K. H. Ho, H. Sirringhaus, and R. H. Friend, "High-stability ultrathin spin-on benzocyclobutene gate dielectric for polymer field-effect transistors," *Applied Physics Letters*, vol. 84, no. 17, pp. 3400-3402, 2004.
- [91] K. Yutani, K.-i. Nakayama, and M. Yokoyama, "Fabrication of Vertical Organic Field Effect Transistor at the Edge of Patterned Photoresist," *Molecular Crystals and Liquid Crystals*, vol. 444, no. 1, pp. 197-202, 2006/02/01, 2006.
- [92] T. Hirose, T. Nagase, T. Kobayashi, R. Ueda, A. Otomo, and H. Naito, "Device characteristics of short-channel polymer field-effect transistors," *Applied Physics Letters*, vol. 97, no. 8, pp. 083301, 2010.

- [93] A. J. Ben-Sasson, and N. Tessler, "Patterned electrode vertical field effect transistor: Theory and experiment," *Journal of Applied Physics*, vol. 110, no. 4, pp. 044501, 2011.
- [94] J. N. Haddock, X. Zhang, S. Zheng, Q. Zhang, S. R. Marder, and B. Kippelen, "A comprehensive study of short channel effects in organic field-effect transistors," *Organic electronics*, vol. 7, no. 1, pp. 45-54, 2006.
- [95] B. H. Hamadani, C. A. Richter, J. S. Suehle, and D. J. Gundlach, "Insights into the characterization of polymer-based organic thin-film transistors using capacitance-voltage analysis," *Applied Physics Letters*, vol. 92, no. 20, pp. 203303, 2008.
- [96] V. S. Reddy, S. Das, S. K. Ray, and A. Dhar, "Electrical characteristics of pentacene thin film junctions," *Physics of Semiconductor Devices IEEE IWPSD*, pp. 569 - 572, 2007.
- [97] Y. Tidiishi, S. Naka, and H. Okada, "Surface Roughness of Organic Semiconductor Superlattice Using Pentacene as Semiconductor," *Japanese Journal of Applied Physics*, vol. 47, no. 1, pp. 438-440, 2008.
- [98] D. T. James, B. K. Kjellander, W. T. Smaal, G. H. Gelinck, C. Combe, I. McCulloch, R. Wilson, J. H. Burroughes, D. D. Bradley, and J. S. Kim, "Thin-film morphology of inkjet-printed single-droplet organic transistors using polarized Raman spectroscopy: effect of blending TIPS-pentacene with insulating polymer," *ACS Nano*, vol. 5, no. 12, pp. 9824-35, Dec, 2011.
- [99] H. L. Cheng, W. Y. Chou, C. W. Kuo, Y. W. Wang, Y. S. Mai, F. C. Tang, and S. W. Chu, "Influence of Electric Field on Microstructures of Pentacene Thin-Films in Field-Effect Transistors," *Advanced Functional Materials*, vol. 18, no. 2, pp. 285–293, 2008.
- [100] D. Knipp, R. Street, A. Völkel, and J. Ho, "Pentacene thin film transistors on inorganic dielectrics: Morphology, structural properties, and electronic transport," *Journal of Applied Physics*, vol. 93, no. 1, pp. 347-355, 2002.
- [101] D. Corrado, C. Basso, and G. Thiene, "Sudden cardiac death in athletes: what is the role of screening?," *Curr Opin Cardiol*, vol. 27, no. 1, pp. 41-8, Jan, 2012.
- [102] S. Petushi, F. U. Garcia, M. M. Haber, C. Katsinis, and A. Tozeren, "Large-scale computations on histology images reveal grade-differentiating parameters for breast cancer," *BMC Med Imaging*, vol. 6, pp. 14, 2006.
- [103] E. A. Rakha, S. A. O'Toole, I. O. Ellis, and P. H. Tan, "Breast pathology today: morphology and molecules," *J Clin Pathol*, vol. 66, no. 6, pp. 457, Jun, 2013.

- [104] P. Friedl, and S. Alexander, "Cancer invasion and the microenvironment: plasticity and reciprocity," *Cell*, vol. 147, no. 5, pp. 992-1009, Nov, 2011.
- [105] C. W. Elston, and I. O. Ellis, "Pathological prognostic factors in breast cancer. I. The value of histological grade in breast cancer: experience from a large study with long-term follow-up," *Histopathology*, vol. 41, no. 3A, pp. 154-61, Sep, 2002.
- [106] M. Kowal, P. Filipczuk, A. Obuchowicz, J. Korbicz, and R. Monczak, "Computer-aided diagnosis of breast cancer based on fine needle biopsy microscopic images," *Comput Biol Med*, vol. 43, no. 10, pp. 1563-72, Oct, 2013.
- [107] J. R. Dalle, W. K. Leow, D. Racoceanu, A. E. Tutac, and T. C. Putti, "Automatic breast cancer grading of histopathological images," *Conf Proc IEEE Eng Med Biol Soc*, vol. 2008, pp. 3052-5, 2008.
- [108] G. Bussolati, C. Marchiò, L. Gaetano, R. Lupo, and A. Sapino, "Pleomorphism of the nuclear envelope in breast cancer: a new approach to an old problem," *J Cell Mol Med*, vol. 12, no. 1, pp. 209-18, Jan-Feb, 2008.
- [109] B. Dunne, and J. J. Going, "Scoring nuclear pleomorphism in breast cancer," *Histopathology*, vol. 39, no. 3, pp. 259-65, Sep, 2001.
- [110] M. Dietzel, P. A. Baltzer, A. Dietzel, R. Zoubi, T. Gröschel, H. P. Burmeister, M. Bogdan, and W. A. Kaiser, "Artificial Neural Networks for differential diagnosis of breast lesions in MR-Mammography: a systematic approach addressing the influence of network architecture on diagnostic performance using a large clinical database," *Eur J Radiol*, vol. 81, no. 7, pp. 1508-13, Jul, 2012.
- [111] A. J. Ben-Sasson, and N. Tessler, "Unraveling the physics of vertical organic field effect transistors through nanoscale engineering of a self-assembled transparent electrode," *Nano Lett*, vol. 12, no. 9, pp. 4729-33, Sep, 2012.
- [112] A. Bolognesi, A. Di Carlo, and P. Lugli, "Influence of carrier mobility and contact barrier height on the electrical characteristics of organic transistors," *Applied Physics Letters*, vol. 81, no. 24, pp. 4646-4648, 2002.
- [113] R. M. Owens, and G. G. Malliaras, "Organic Electronics at the Interface with Biology," *MRS Bulletin*, vol. 35, no. 06, pp. 449-456, 2010.

- [114] J. Viventi, D. H. Kim, L. Vigeland, E. S. Frechette, J. A. Blanco, Y. S. Kim, A. E. Avrin, V. R. Tiruvadi, S. W. Hwang, A. C. Vanleer, D. F. Wulsin, K. Davis, C. E. Gelber, L. Palmer, J. Van der Spiegel, J. Wu, J. Xiao, Y. Huang, D. Contreras, J. A. Rogers, and B. Litt, "Flexible, foldable, actively multiplexed, high-density electrode array for mapping brain activity in vivo," *Nat Neurosci*, vol. 14, no. 12, pp. 1599-605, Dec, 2011.
- [115] S. Waldert, T. Pistohl, C. Braun, T. Ball, A. Aertsen, and C. Mehring, "A review on directional information in neural signals for brain-machine interfaces," *J Physiol Paris*, vol. 103, no. 3-5, pp. 244-54, 2009 Sep-Dec, 2009.
- [116] N. Jiang, L. Gizzi, N. Mrachacz-Kersting, K. Dremstrup, and D. Farina, "A brain-computer interface for single-trial detection of gait initiation from movement related cortical potentials," *Clin Neurophysiol*, May, 2014.
- [117] P. Lin, and F. Yan, "Organic Thin-Film Transistors for Chemical and Biological Sensing," *Advanced Materials*, vol. 24, no. 1, pp. 34-51, 2012.
- [118] T. H. Yoon, E. J. Hwang, D. Y. Shin, S. I. Park, S. J. Oh, S. C. Jung, H. C. Shin, and S. J. Kim, "A micromachined silicon depth probe for multichannel neural recording," *IEEE Trans Biomed Eng*, vol. 47, no. 8, pp. 1082-7, Aug, 2000.
- [119] M. HajjHassan, V. Chodavarapu, and S. Musallam, "NeuroMEMS: Neural Probe Microtechnologies" *Sensors*, vol. 8, pp. 6704-6726, 2008.
- [120] P. Cosseddu, A. Bonfiglio, R. Neelgund, and H. W. Tyrer, "Arrays of pressure sensors based on organic field effect: a new perspective for non invasive monitoring," *Conf Proc IEEE Eng Med Biol Soc*, vol. 2009, pp. 6151-4, 2009.
- [121] V. Benfenati, S. Toffanin, S. Bonetti, G. Turatti, A. Pistone, M. Chiappalone, A. Sagnella, A. Stefani, G. Generali, G. Ruani, D. Saguatti, R. Zamboni, and M. Muccini, "A transparent organic transistor structure for bidirectional stimulation and recording of primary neurons," *Nat Mater*, vol. 12, no. 7, pp. 672-80, Jul, 2013.
- [122] D. R. Kipke, W. Shain, G. Buzsáki, E. Fetz, J. M. Henderson, J. F. Hetke, and G. Schalk, "Advanced neurotechnologies for chronic neural interfaces: new horizons and clinical opportunities," *J Neurosci*, vol. 28, no. 46, pp. 11830-8, Nov, 2008.
- [123] J. D. Weiland, W. Liu, and M. S. Humayun, "Retinal prosthesis," *Annu Rev Biomed Eng*, vol. 7, pp. 361-401, 2005.
- [124] Q. Qing, S. K. Pal, B. Tian, X. Duan, B. P. Timko, T. Cohen-Karni, V. N. Murthy, and C. M. Lieber, "Nanowire transistor arrays for mapping neural circuits in acute brain slices," *Proc Natl Acad Sci U S A*, vol. 107, no. 5, pp. 1882-7, Feb, 2010.

- [125] P. Boon, R. Raedt, V. de Herdt, T. Wyckhuys, and K. Vonck, "Electrical stimulation for the treatment of epilepsy," *Neurotherapeutics*, vol. 6, no. 2, pp. 218-27, Apr, 2009.